NTIS # PB2008-

SSC-453

WELDING DISTORTION ANALYSIS OF HULL BLOCKS USING EQUIVALENT LOAD METHOD BASED ON INHERENT STRAIN

SHIP STRUCTURE COMMITTEE
2008

Ship Structure Committee

Ship
Structure
Committee

Address Correspondence to:

Executive Director
Ship Structure Committee
U.S. Coast Guard (CG-5212/SSC)
2100 2nd Street, SW
Washington, D.C. 20593-0001
Web site: http://www.shipstructure.org

SSC – 453
SR – 1450

OCTOBER 3, 2008

WELDING DISTORTION ANALYSIS OF HULL BLOCKS USING EQUIVALENT LOAD METHOD BASED ON INHERENT STRAIN

This report suggests an efficient method to predict the welding distortion of a curved double bottom block of actual ship. Due to its efficiency and accuracy, the proposed method can provide a powerful solution to predict the welding distortion of actual ship hull blocks with high complexity in structural shape.

The prediction of welding deformation of stiffened curved plates is based on the inherent strain theory combined with the finite element method. The equivalent load was determined by integrating inherent strain components which are calculated in the vicinity of heat affected zone using the highest temperature and the degree of restraint.

BRIAN M. SALERNO
Rear Admiral, U.S. Coast Guard
Chairman, Ship Structure Committee

Technical Report Documentation Page

1. Report No.	2. Government Accession No.	3. Recipient's Catalog No.
SSC – 453		

4. Title and Subtitle	5. Report Date / 6. Performing Organization Code
Welding Distortion Analysis of Hull Blocks Using Equivalent Load Method Based on Inherent Strain	5. September 11, 2007 6.
7. Author(s) C.D. Jang	8. Performing Organization Report No. SR-1450
9. Performing Organization Name and Address Seoul National University Department of Naval Architecture & Ocean Engineering San 56-1, Shillim-Dong, Gwanak-Gu Seoul 151-742 , KOREA	10. Work Unit No. (TRAIS) 11. Contract or Grant No.
12. Sponsoring Agency Name and Address Ship Structure Committee C/O Commandant (CG-5212/SSC) United States Coast Guard 2100 2nd Street, SW Washington, DC 20593-0001	13. Type of Report Final Report 14. Sponsoring Agency Code CG - 5

15. Supplementary Notes
Sponsored by the Ship Structure Committee and its member agencies

16. Abstract

This paper suggests an efficient method (Equivalent Load Method) for predicting the welding deformation of stiffened curved plates based on the inherent strain theory combined with the finite element method. The proposed method can predict the various modes of welding distortions of stiffened curved plates such as angular distortion, in-plane shrinkage, longitudinal and transverse bending deformations considering welding sequence according to the fabrication stages. The equivalent load was determined by integrating inherent strain components which are calculated in the vicinity of heat affected zone using the highest temperature and the degree of restraint. The welding distortions of curved stiffened panels under equivalent load were calculated by elastic analysis and compared with those by the experiment as well as the thermal elasto-plastic finite element analysis. The welding distortions of stiffened curved plates by the proposed method showed fairly good agreements with those by the experiment and intensive finite element analysis. It has been verified that the proposed method has a high efficiency and accuracy.

By the proposed method, it was possible to predict the welding distortion of a curved double bottom block of actual ship. Due to its efficiency and accuracy, the present method can provide a powerful solution to predict the welding distortion of actual ship hull blocks with high complexity in structural shape.

17. Key Words	18. Distribution Statement
Aluminum structure, marine structure, aluminum design, aluminum fabrication	National Technical Information Service U.S. Department of Commerce Springfield, VA 22151 Ph. (703) 487-4650 / www.ntis.gov

19. Security Classif. (of this report)	20. Security Classif. (of this page)	21. No. of Pages	22. Price
Unclassified	Unclassified		

CONVERSION FACTORS
(Approximate conversions to metric measures)

To convert from	to	Function	Value
LENGTH			
inches	meters	divide	39.3701
inches	millimeters	multiply by	25.4000
feet	meters	divide by	3.2808
VOLUME			
cubic feet	cubic meters	divide by	35.3149
cubic inches	cubic meters	divide by	61,024
SECTION MODULUS			
inches^2 feet^2	centimeters^2 meters^2	multiply by	1.9665
inches^2 feet^2	centimeters^3	multiply by	196.6448
inches^4	centimeters^3	multiply by	16.3871
MOMENT OF INERTIA			
inches^2 feet^2	centimeters^2 meters	divide by	1.6684
inches^2 feet^2	centimeters^4	multiply by	5993.73
inches^4	centimeters^4	multiply by	41.623
FORCE OR MASS			
long tons	tonne	multiply by	1.0160
long tons	kilograms	multiply by	1016.047
pounds	tonnes	divide by	2204.62
pounds	kilograms	divide by	2.2046
pounds	Newtons	multiply by	4.4482
PRESSURE OR STRESS			
pounds/inch^2	Newtons/meter^2 (Pascals)	multiply by	6894.757
kilo pounds/inch^2	mega Newtons/meter^2 (mega Pascals)	multiply by	6.8947
BENDING OR TORQUE			
foot tons	meter tons	divide by	3.2291
foot pounds	kilogram meters	divide by	7.23285
foot pounds	Newton meters	multiply by	1.35582
ENERGY			
foot pounds	Joules	multiply by	1.355826
STRESS INTENSITY			
kilo pound/inch^2 inch^{½}(ksi√in)	mega Newton MNm$^{3/2}$	multiply by	1.0998
J-INTEGRAL			
kilo pound/inch	Joules/mm^2	multiply by	0.1753
kilo pound/inch	kilo Joules/m^2	multiply by	175.3

CONTENTS

List of Figures

List of Tables

1. Introduction

1.1 Background of this study

Nowadays, most commercial and naval ships are constructed by the block building method in shipyards. The blocks which constitute the ship hull are built in a series of production process and transferred to the pre-erection area for the preparation works including the correction of distortion. The distortion of a block is inevitably induced by welding and is accumulated during the sequential fabrication process.

As the block erection step accounts for about one-third of the whole shipbuilding process, the accuracy of a block's shape and size has a close relation with the overall efficiency of production in the shipyard.

The welding distortions reduce the fabrication accuracy of ship hull blocks and decrease productivity due to lots of correction works. To increase the precision of fabrication, the welding distortion and the exact distortion margin at every fabrication stage should be estimated to meet the allowable tolerances of ship hull blocks.

The prediction and control of welding distortions at the design stage has been an essential task for most shipyards to ensure the higher quality as well as higher productivity in shipbuilding.

For the prediction of welding distortions, many studies have been done for the simple structures, however, few studies have been performed for actual ship hull blocks and they are still far from the practical application due to many difficulties such as :

- Extremely complicate stiffened curved ship hull structures
- Multiple welding passes,various welding methods and many fabrication stages
- Huge computation time and cost.

In order to overcome above difficulties, some efficient approaches to predict the welding distortion of the actual ship hull blocks are needed, but have not been well established yet.

For the development of an efficient approach to predict the welding distortion of actual ship hull blocks considering the fabrication sequences and phase transformation of steel, the analysis method should satisfy the following requirements.

- The analysis method should be capable of considering the various modes of welding distortions such as longitudinal/transverse shrinkage and longitudinal/transversal bending simultaneously.
- The analysis should reflect the change of structural stiffness according to the fabrication stages.
- The analysis should be able to consider the welding sequence.

- The analysis should reflect the change of phase transformation of steel by material properties
- The efficiency of calculation time and cost should be guaranteed considering the complexity of hull block shapes.
- The analysis method should predict the distortion of not only the stiffened flat plates but also of stiffened curved plates.

1.2 Objectives

The main purpose of this study is to propose an efficient approach to predict the welding distortions of the stiffened flat and curved plates based on the inherent strain theory combined with the finite element analysis. In order to verify the efficiency and the effectiveness of this method, some numerical simulation and experiments of welding distortions of various stiffened and curved plates with the different curvatures considering the different fabrication sequences will be performed.

2. Development of equivalent load method for welding distortion analysis based on inherent strain

2.1. Inherent strain due to welding

In the welding process, the heat input around a weld joint causes a non-uniform temperature distribution and thermal stress. As a result, the plastic strain remains around the weld bead and permanent deformation occurs after welding. The plastic strain that causes the welding deformation can be defined as the inherent strain. In general, the inherent strain induced by welding has six components according to their directions. However, in the case where a plate has a large length/thickness ratio such as a ship hull plate, only two components ε_x^* and ε_y^* are dominant. Some typical types of welding deformation due to inherent strain are shown in Fig. 1.

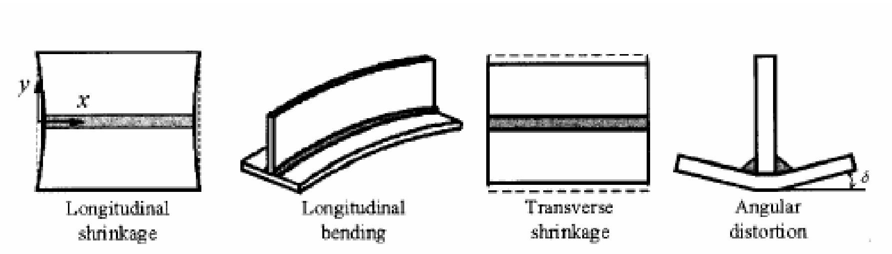

Fig. 1 Types of welding deformation

2.1.1. Calculation of the inherent strain

The inherent strain distribution can be formulated using a simplified thermal elasto-plastic analysis model as shown in Fig. 2. The welding region, where inherent strain occurs, can be modeled as a bar and a spring.

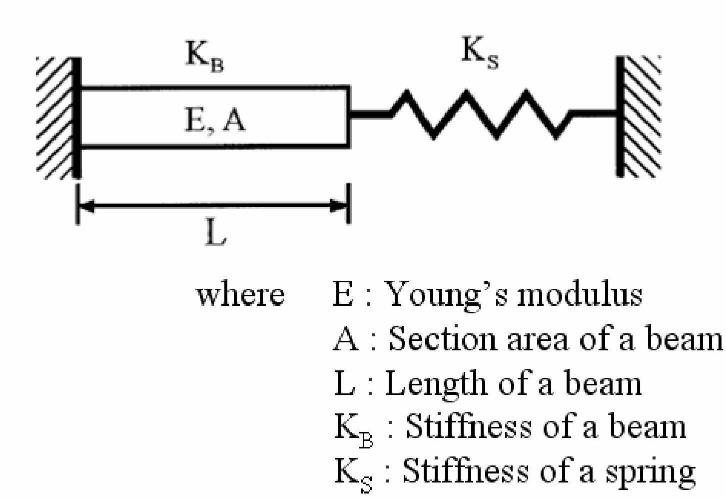

Fig. 2 Simplified thermal elasto-plastic analysis model

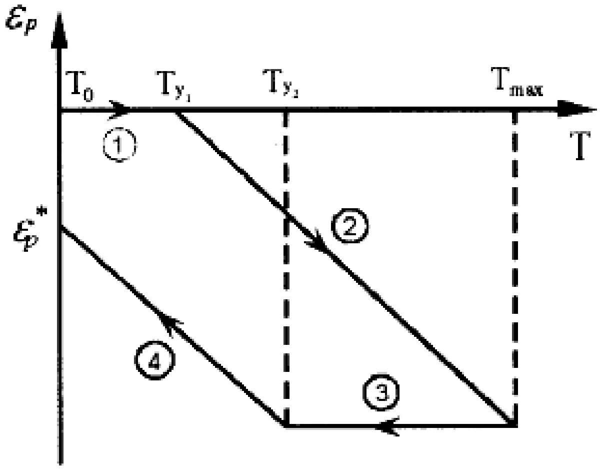

Fig. 3 Thermal history of plastic strain

The thermal history of the inherent strain according to the temperature change of a bar can be divided into four steps, as shown in Fig. 3. After all the thermal history the compressive plastic strain remains as an amount of ε_p^*. The magnitude of residual plastic strain was calculated from the total strain, the stress-strain relation and the equilibrium equation of a bar-spring system.

Total strain : $$\varepsilon = \varepsilon_{th} + \varepsilon_e + \varepsilon_p \qquad (1)$$

Stress-strain relation : $$\sigma = E\varepsilon_e \qquad (2)$$

Equilibrium equation : $$F_B = F_S \qquad (3)$$

2.1.2. Distribution of the highest temperature

The highest temperature means the maximum temperature that each point in the heat effected region experiences through whole welding time. The heat transfer analysis is conducted to calculate the temperature distribution of welded structures. The welding heat source is modeled as a normal distributed moving heat flux. Finally, the highest temperature at each node in the finite element model is calculated by the heat transfer analysis.

The temperature of bar is changed from the room temperature $T_0 \rightarrow T_{\max} \rightarrow T_0$. If the highest temperature ($T_{\max}$) is reached sufficiently high, the section is divided in 4 steps shown in Fig. 4. The section of OA, AB is elastic and plastic process during a temperature rising and the section of BC, CD is elastic and plastic process during a temperature falling.

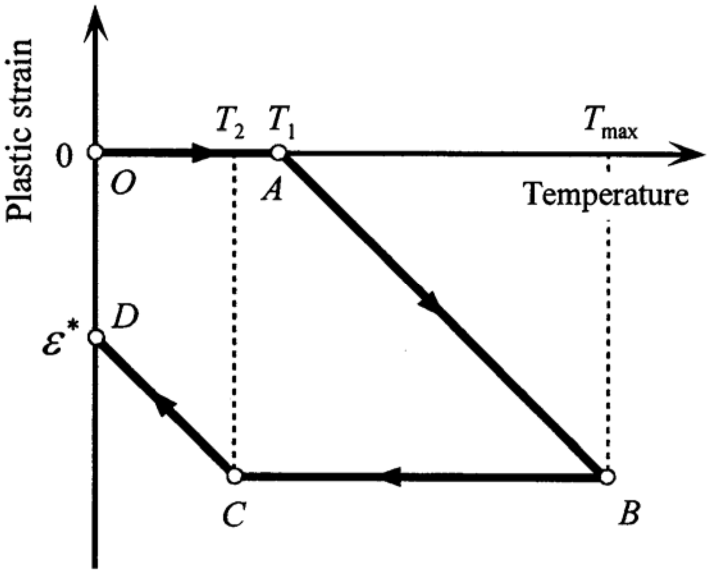

Fig. 4 Thermal history of stress

If a material nonlinearity is considered, thermal histories of stress and plastic strain are shown in Fig. 5.

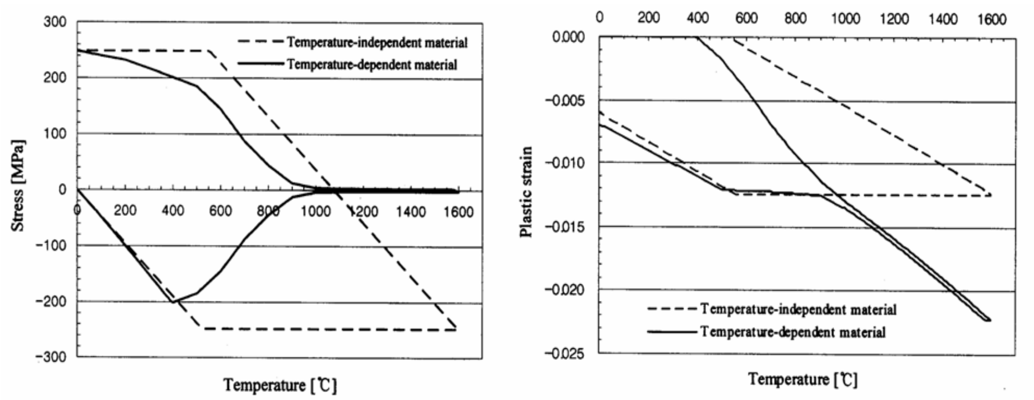

Fig. 5 Comparison of stress and plastic strain considering material nonlinearity

2.1.3. Calculation of degree of restraint

The degree of restraint represents the level of resistance against the thermal deformation of the welding region. The degree of restraint of stiffened panel is determined from the analogy of the bar-spring model and the elastic finite element analysis using unit load.

Since the fabrication process will greatly affect the welding deformation, the degree of structural restraint should be calculated considering all the fabrication sequences.

To grasp of the influence of degree of restraint, the thermal history is calculated for four cases of $\beta = 0.1, 0.2, 0.3, 0.4$.

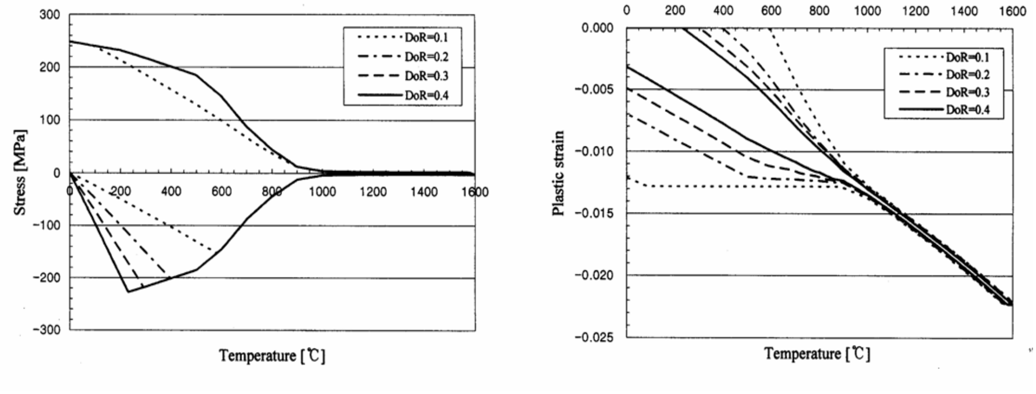

Fig. 6 Effect of the degree of restraint on stress and plastic strain

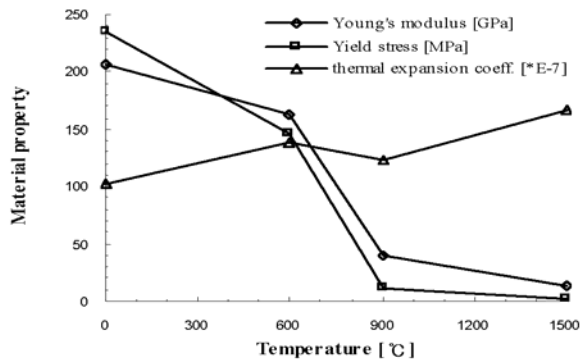

Fig. 7 Temperature dependent material properties

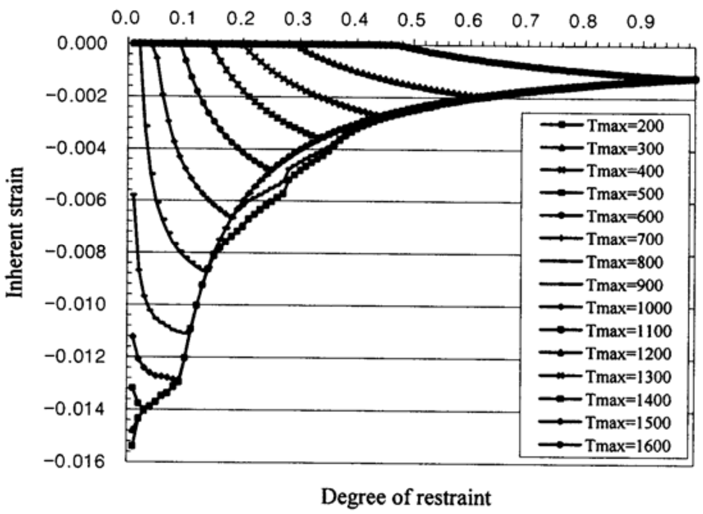

Fig. 8 Inherent strain chart of steel with temperature rising-falling cycle

In case of thermal elasto-plastic analysis, the temperature dependent material properties in Fig.7

should be incorporated in the numerical calculation. The final inherent strain after thermal cycle can be determined using the highest temperature and degree of restraints shown in Fig.8.

In this report, the highest temperature is divided by 50℃ from 0℃ to 2500℃ and the degree of restraint is divided by 0.01 intervals from 0.01 to 0.99.

2.1.4. Phase transformation by cooling rate

Heat transfer analysis is conducted to calculate the cooling rate. Phase transformation of steel was determined by cooling rate as shown in Fig. 9.

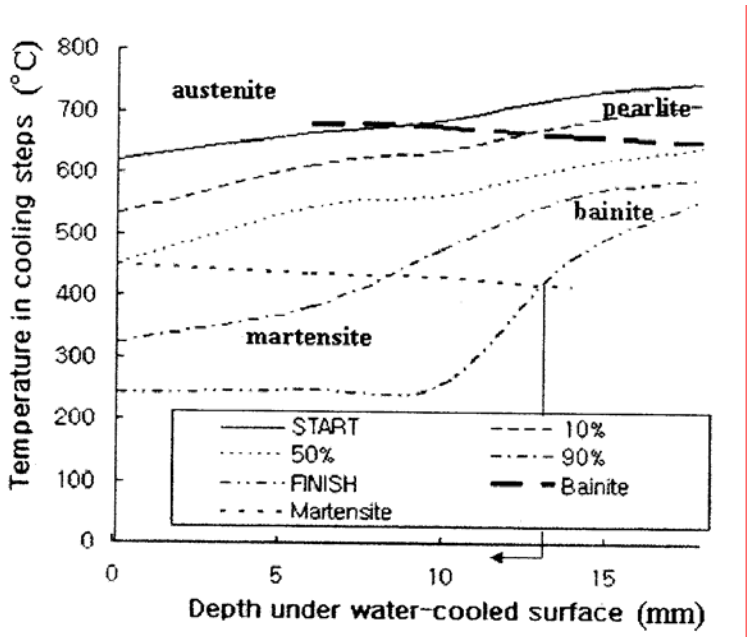

Fig. 9 CCTD(Continuous cooling transformation diagrams) at C=0.18% steel

2.2. Calculation of equivalent loads

The equivalent forces and moments are obtained by using the inherent strain. Using the obtained equivalent loads, the welding deformation can be calculated by elastic FE analysis. All types of equivalent loads are shown in Fig. 9. The shrinkage force f_i can be obtained using Eq. (4).

$$f_i = \frac{AE}{l}\sum_{j=1}^{N_i}\varepsilon_j^* l_j \quad (4)$$

The equivalent transverse forces and moments are calculated using Eq. (5) and Eq. (6), respectively.

$$f_y = \sum_{i=1}^{N} f_i \quad (5)$$

$$m_y = \sum_{i=1}^{N} f_i z_i \quad (6)$$

Also the longitudinal shrinkage force f_x and bending moment m_x can be calculated using inherent strain.

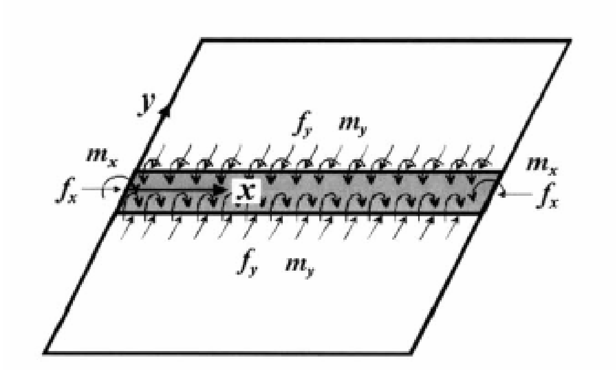

Fig. 10 Equivalent loads of inherent strain

2.3. Simulation of welding deformation

The welding deformation of curved stiffened panel blocks will be simulated using both the equivalent load method based on inherent strain and FE analysis. The simulation procedures can be summarized into three steps. The first step analyzes heat transfer to calculate temperature distribution of each welding section with the given information on welding parameters. The FE model uses heat conduction elements and considers convection on the surface. And cooling rate is calculated to determine phase transformation. The second step computes the degree of restraint by the FE analysis. The third step calculates the inherent strain components and their equivalent loads, and the welding deformation of a structure is obtained by FE analysis.

By using this equivalent load approach, the simulation for welding deformation of stiffened curved panel blocks will be performed based on the results of experiment and finite element analysis of simple curved plate models with one or two stiffeners.

3. Prediction of welding deformation of stiffened plates using thermal elasto-plastic analysis

APDL(ANSYS Parametric Design Language) is used to perform the finite element simulation. Each flat plate and curved plate has 4 kinds of analysis models.

3.1. Thermal elasto-plastic analysis of stiffened flat plates

3.1.1. Models of thermal elasto-plastic analysis of stiffened flat plates

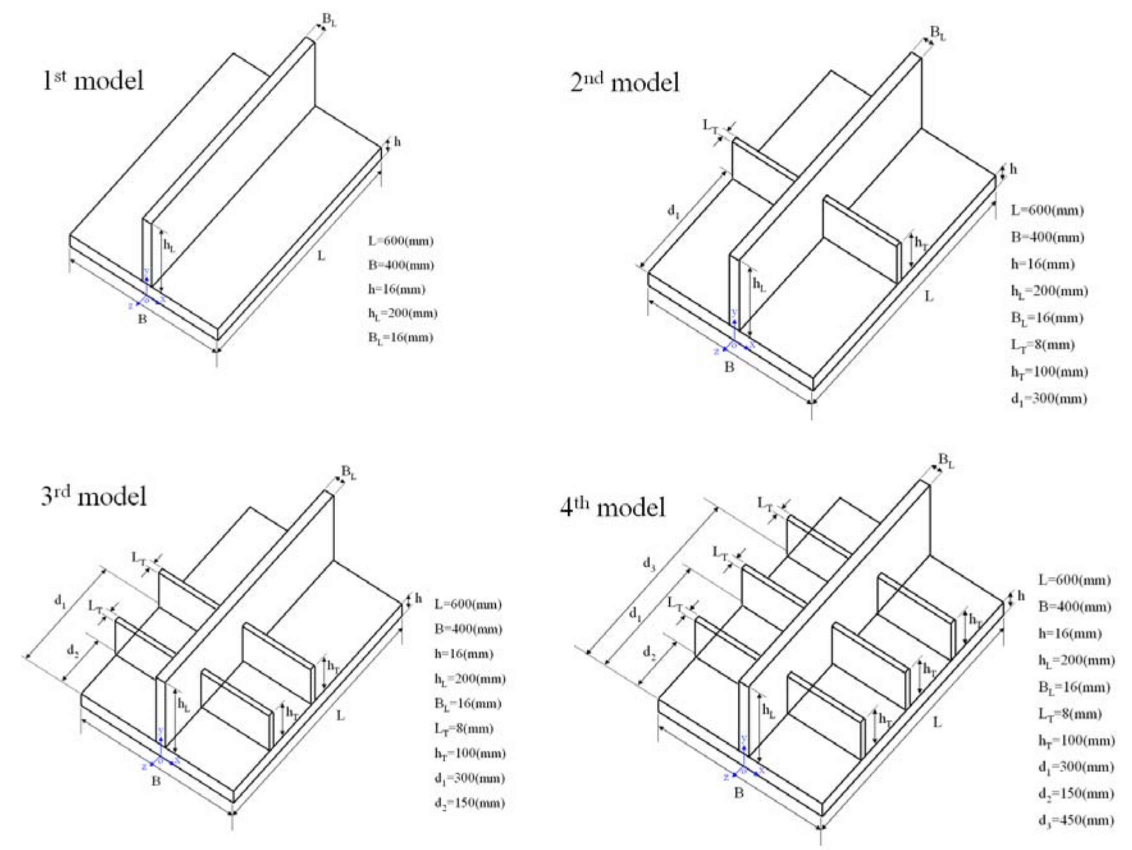

Fig. 11 Models of thermal elasto-plastic analysis of stiffened flat plates

Four kinds of analysis models of stiffened flat plate are adopted. The 1^{st} model has 1 longitudinal stiffener and no transverse stiffener. And the 2^{nd}, 3^{rd}, 4^{th} model has each 1, 2 and 3 stiffeners. Each model has a same base flat plate of L(600mm)×B(400mm)×h(16mm) and a same longitudinal stiffener of L(600mm)×B(16mm)×h(200mm). And the size of each transverse stiffener is same as L(8mm)×B(400mm)×h(100mm). The longitudinal stiffeners are equally spaced and located at $z = -150(mm)$, $z = -300(mm)$, $z = -450(mm)$ respectively.

3.1.2. Thermal elasto-plastic analysis of stiffened flat plates

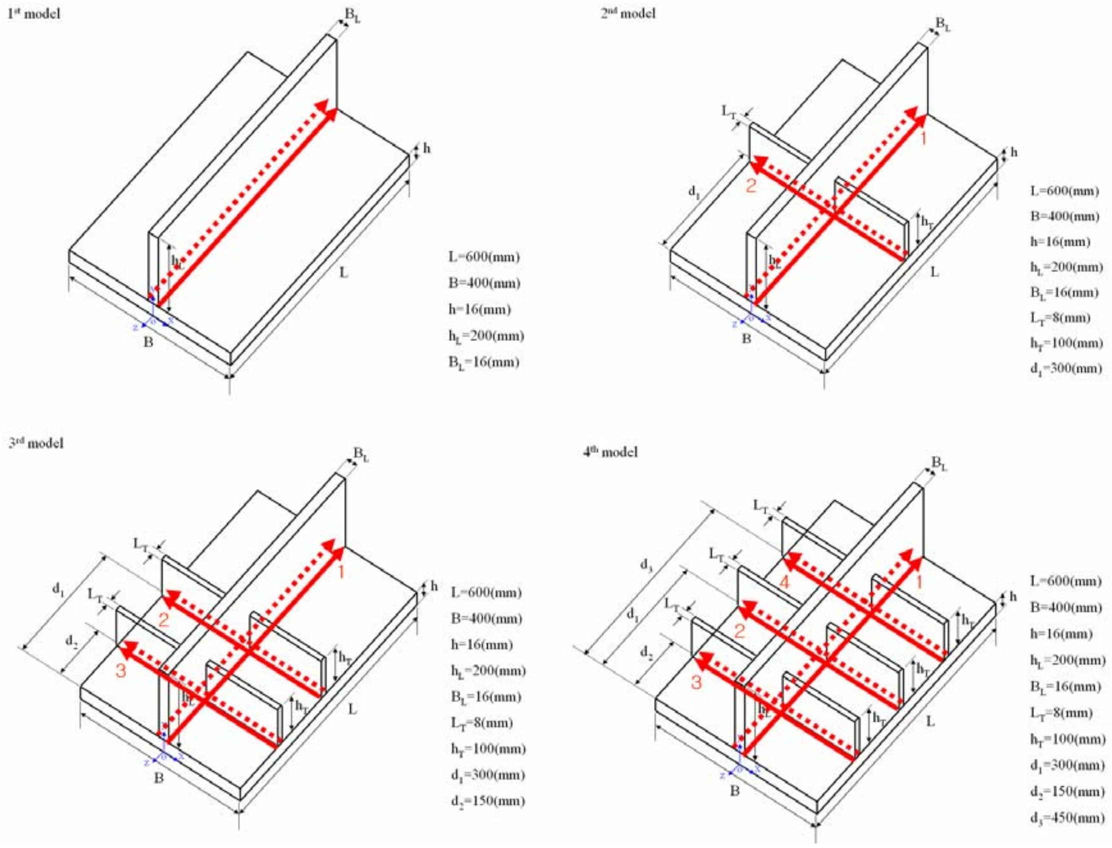

Fig. 12 Welding sequence of each model

A welding line shown in Fig. 12, all of the welding line is coupled by full line and dotted line. It means that the welding is preformed at one time along the coupled line. Welding sequence shown in Fig. 12, the longitudinal stiffener is welded at first and then the transverse stiffeners are welded in order for each model.

An arc-welding is adopted and all of the welding conditions are same as 30(V) of voltage, 300(A) of current and 5(mm/s) of welding velocity.

3.1.3. Analysis models of thermal elasto-plastic analysis of stiffened flat plates

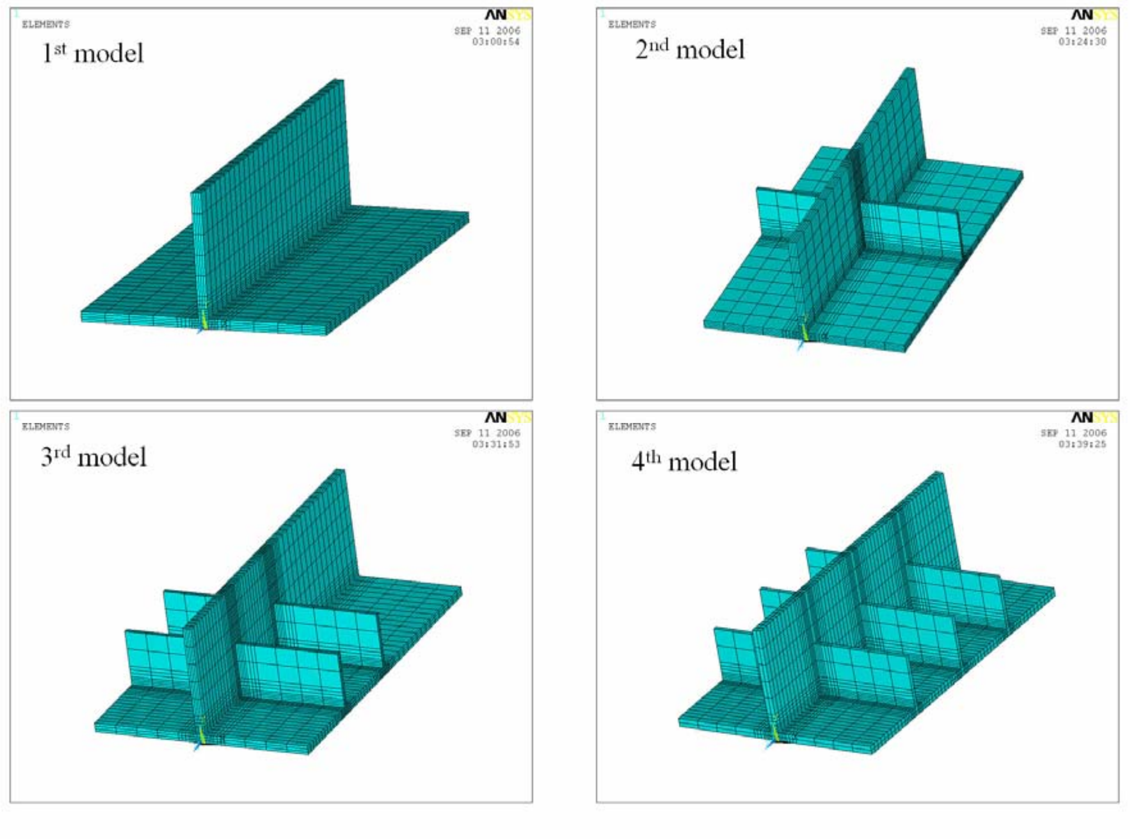

Fig. 13 Analysis models of Thermal elasto-plastic analysis of stiffened flat plates

As shown in Fig. 9 all of the shapes of element are rectangular parallelepiped. The element size is smaller as closer to the heat input area. And the four models have about 10,000 elements. For the thermal analysis all the model have surface element for reflection of thermal convection.

3.1.4. Heat transfer analysis of stiffened flat plates

(a) Element type

3-D thermal solid element and 3-D thermal surface element are used for heat transfer analysis.

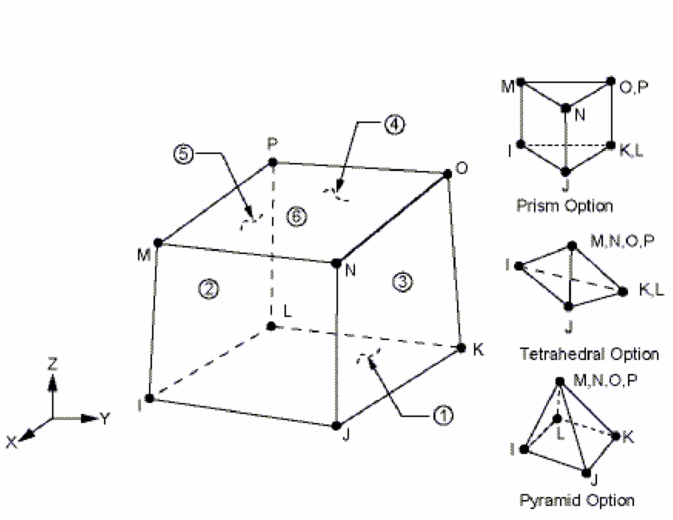

Fig. 14 3-D thermal solid element

The 3-D thermal solid element has eight nodes with a single degree of freedom, temperature, at each node. The element is applicable to a 3-D, steady-state or transient thermal analysis. The element can compensate for mass transport heat flow from a constant velocity field. The geometry, node locations and the coordinate system for this element are shown in Fig. 14.

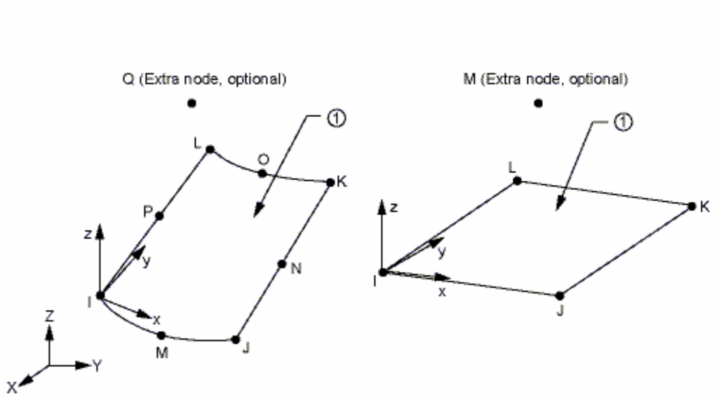

Fig. 15 3-D thermal surface element

The 3-D thermal surface element overlaid onto an area face of 3-D solid element. This element is used for reflection of thermal convection. The geometry, node location and the coordinate system for this element are shown in Fig.15. The element is defined by four to nine nodes and material properties. An extra node may be used for convection or radiation effects.

(b) Results of heat transfer analysis

All the analysis of heat input is performed by heat flux at nodes. For reflection of the line welding heat input process is divided several steps. The step size of heat input process is

100mm of welding line. So the longitudinal welding is analyzed 6 steps and the transverse welding is analyzed 4 steps.

All the cooling process has 10 steps of cooling analysis. Right after the heat input, the cooling step size should be small because the temperature gradient is large. As the temperature gradient become small, the cooling step size getting larger. At the end of the cooling step, 10th step, the temperature gradient is nearly zero.

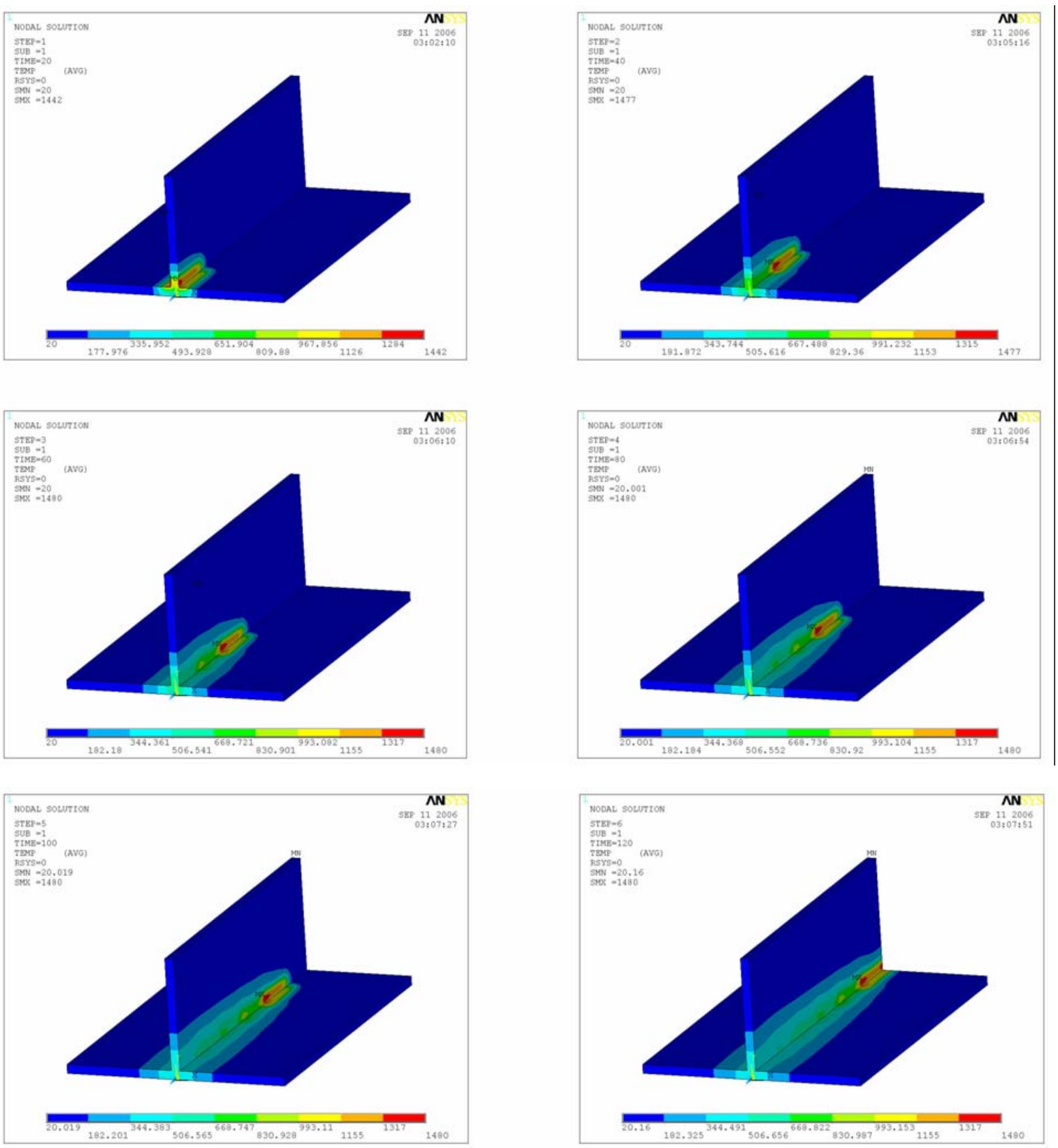

Fig. 16 Heat input process of 1st model of stiffened flat plate

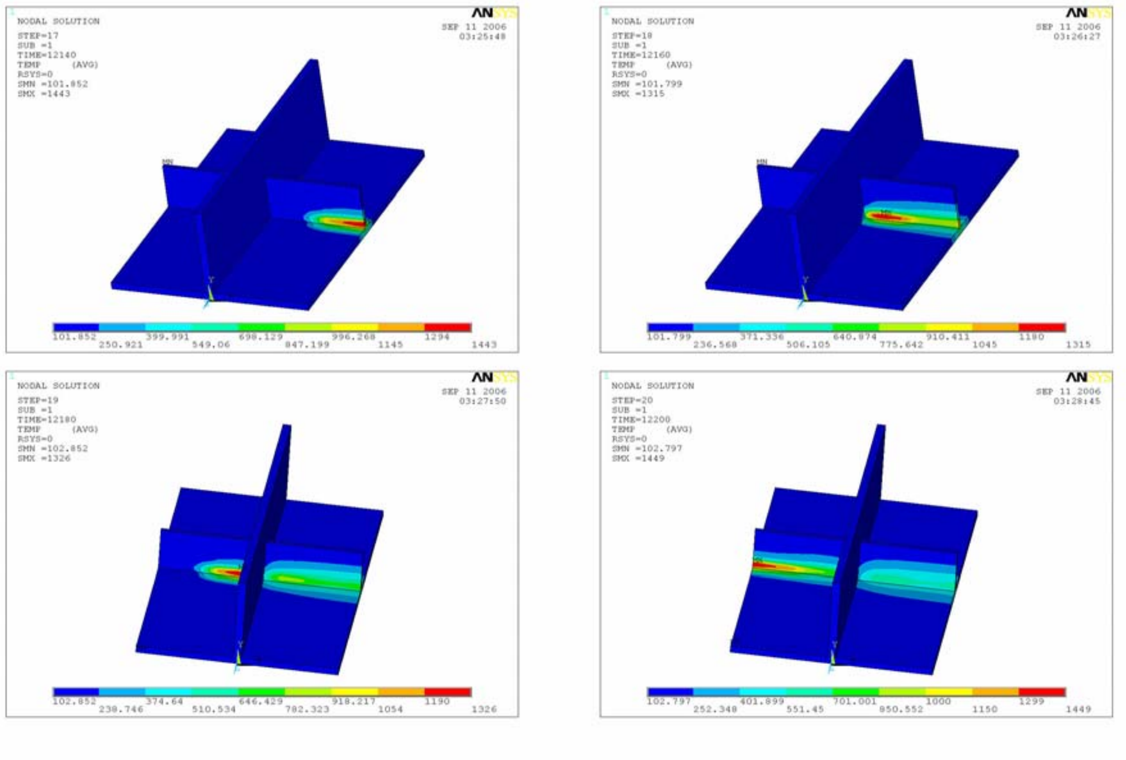

Fig. 17 Heat input process of 2nd model of stiffened flat plate

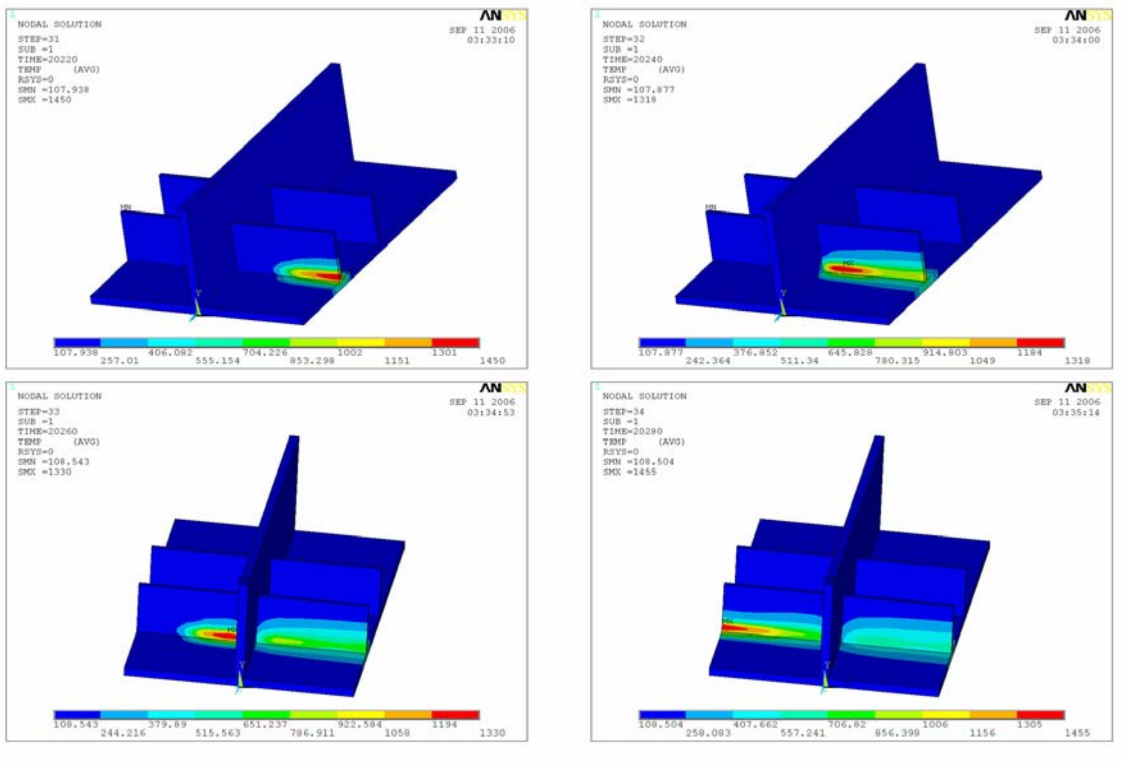

Fig. 18 Heat input process of 3rd model of stiffened flat plate

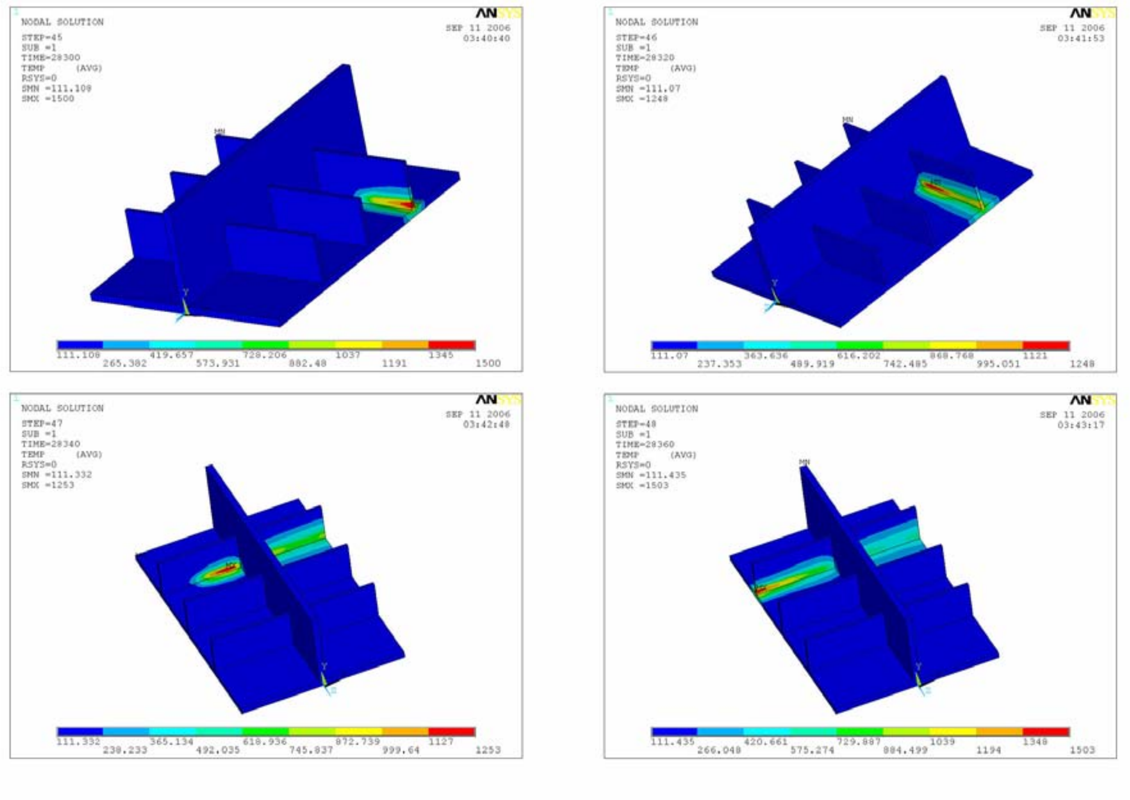

Fig. 19 Heat input process of 4th model of stiffened flat plate

3.1.5. Prediction of welding deformation of stiffened flat plates

(a) Boundary conditions

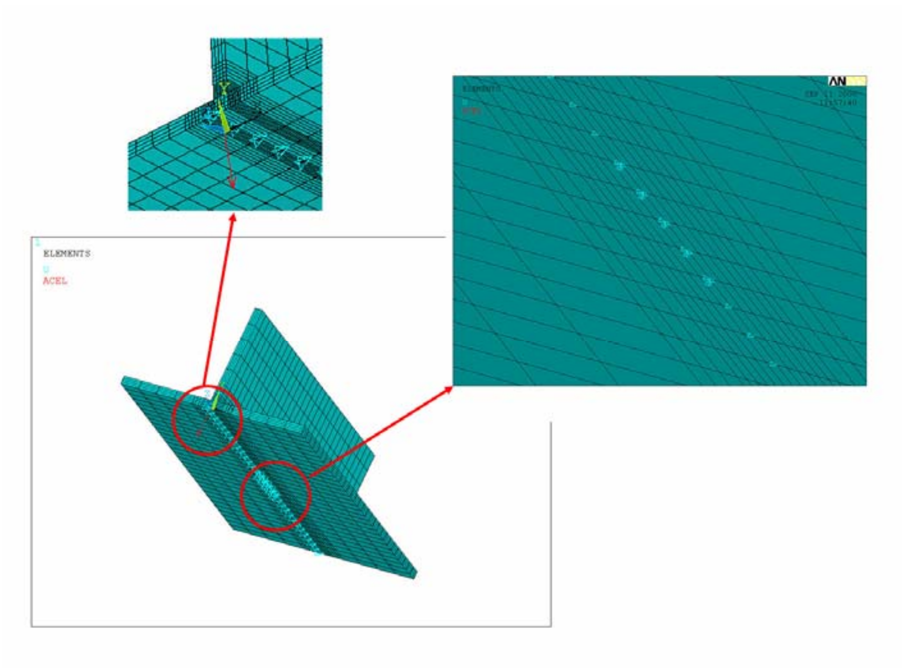

Fig. 20 Boundary conditions of stiffened flat plate

All of the boundary condition of stiffened flat plate is applied at the bottom of mail plate. As shown in Fig. 20 along the middle of the breadth direction (x=0), all of nodes are fixed to x direction. And around the middle of the length, some nodes are fixed all direction of x, y, and z.

(b) Analysis results

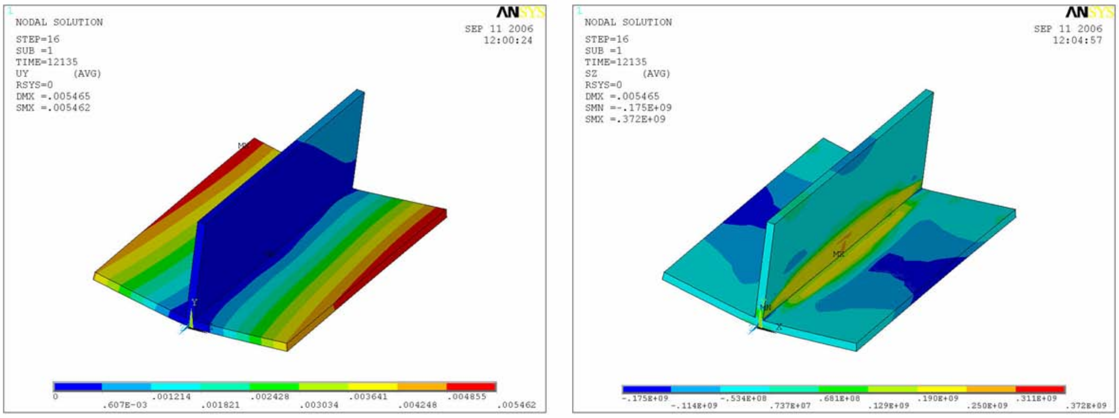

Displacement in y direction　　　　Stress in z direction

Fig. 21 Analysis result of 1st case of stiffened flat plate

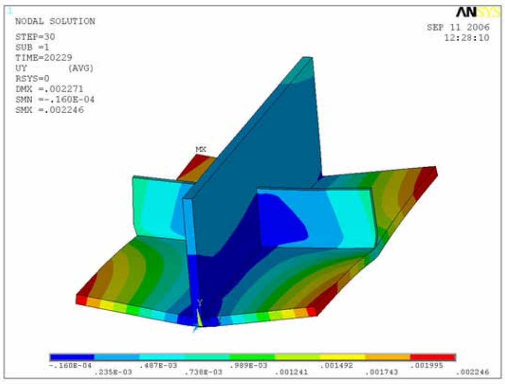

Displacement in y direction

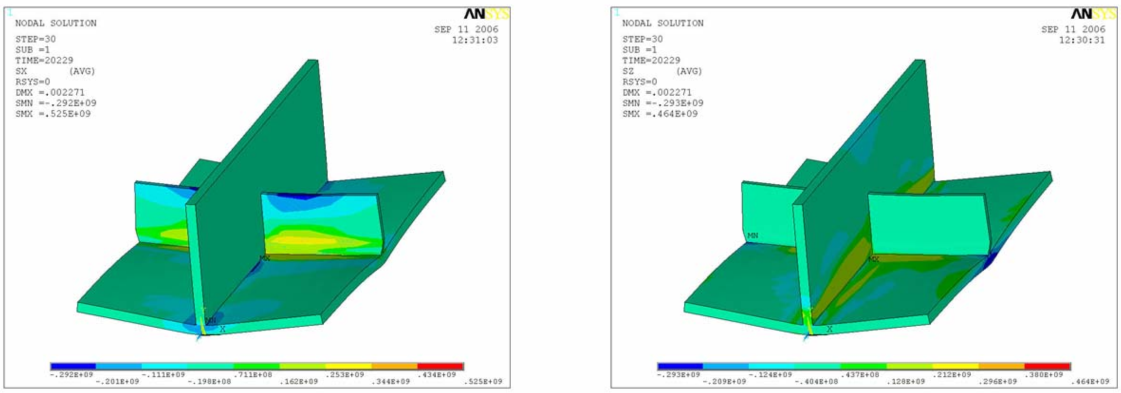

Stress in x direction　　　　Stress in z direction

Fig. 22 Analysis result of 2nd case of stiffened flat plate

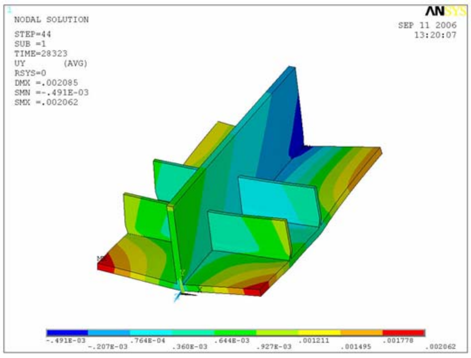

Displacement in y direction

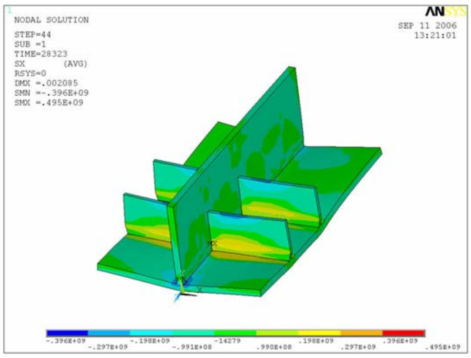

Stress in x direction

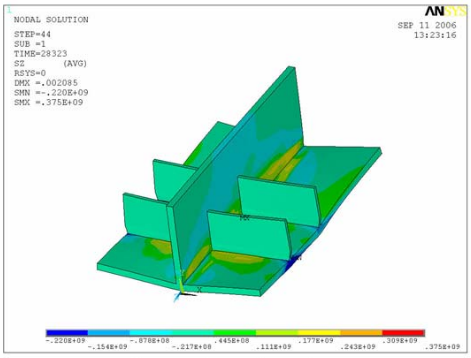

Stress in z direction

Fig. 23 Analysis result of 3rd case of stiffened flat plate

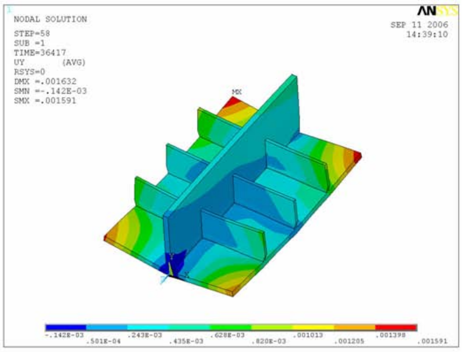

Displacement in y direction

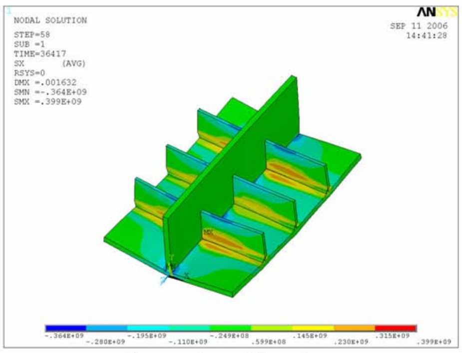

Stress in x direction

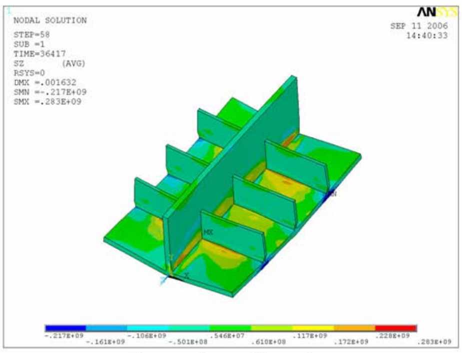

Stress in z direction

Fig. 24 Analysis result of 4th case of stiffened flat plate

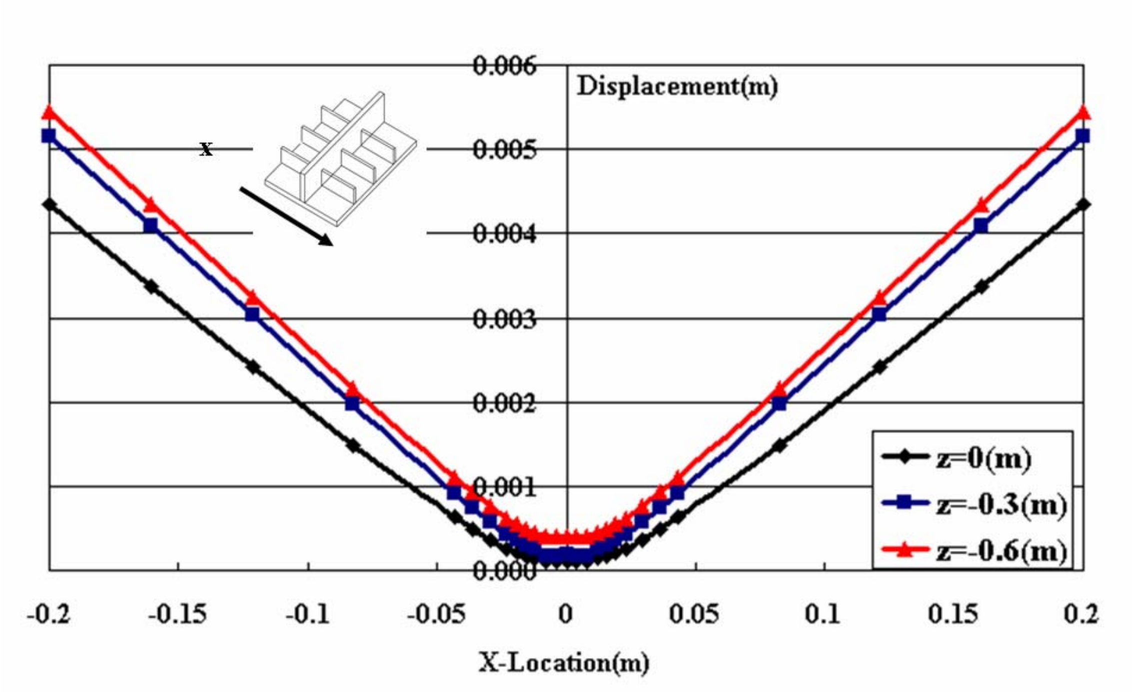

Fig. 25 Welding deformation of stiffened flat plates (Model 1)

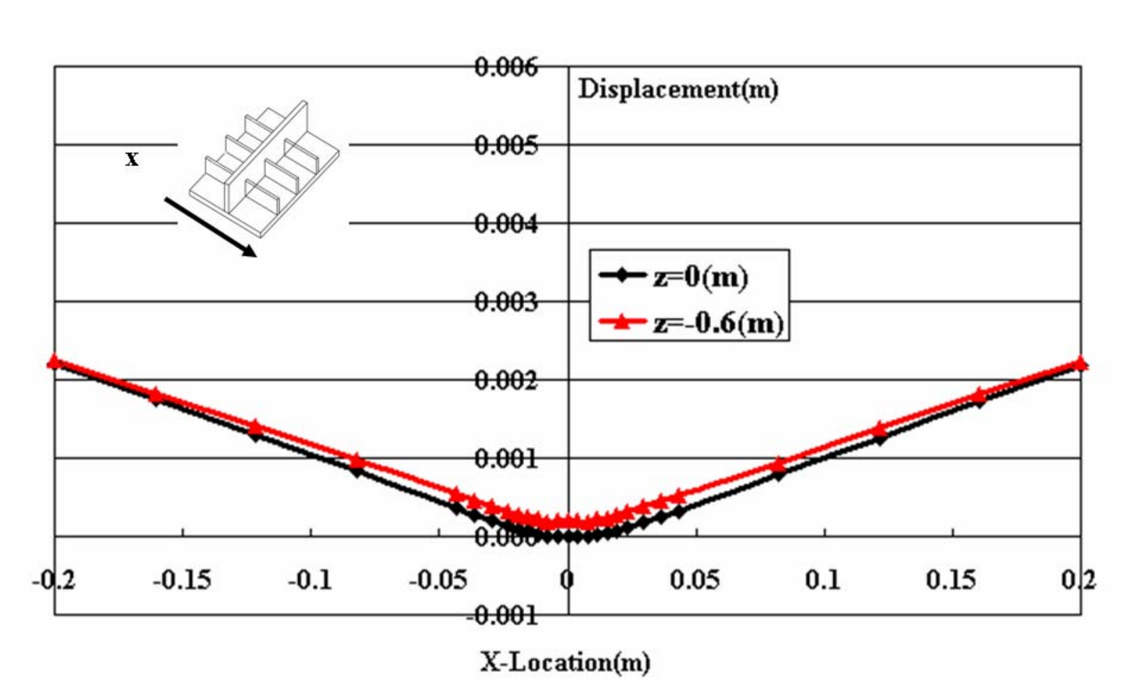

Fig. 26 Welding deformation of stiffened flat plates (Model 2)

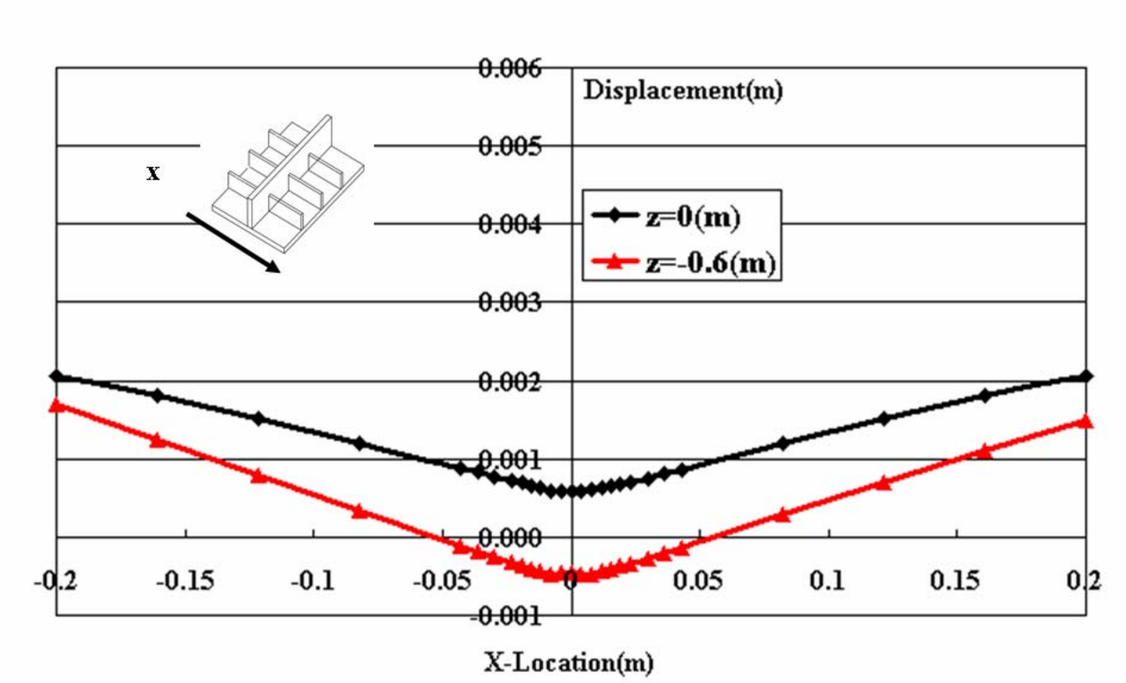

Fig. 27 Welding deformation of stiffened flat plates (Model 3)

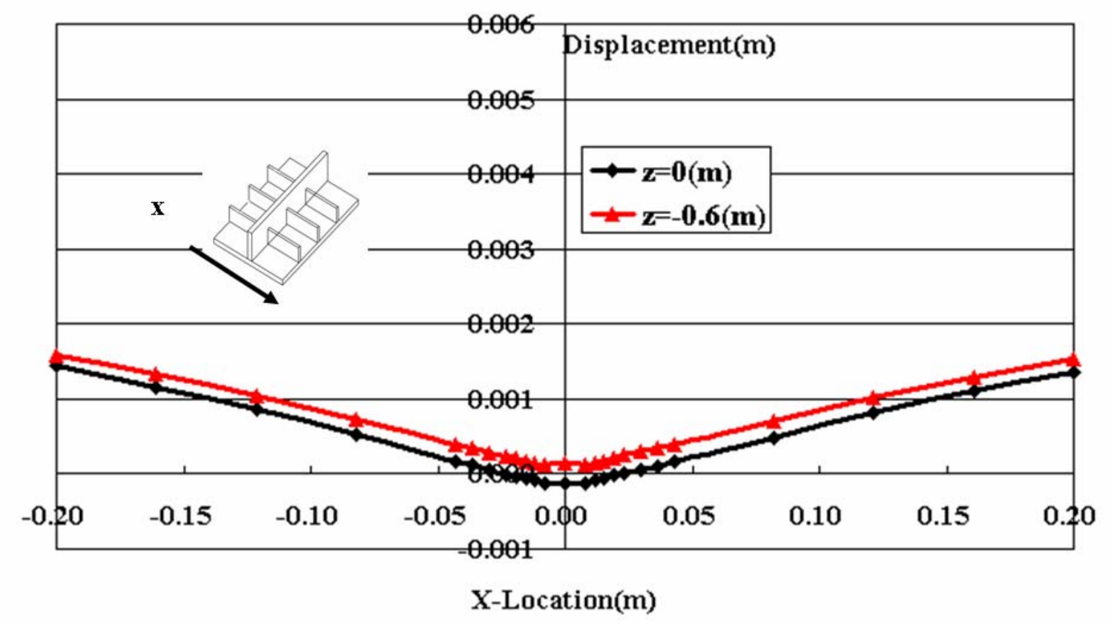

Fig. 28 Welding deformation of stiffened flat plates (Model 4)

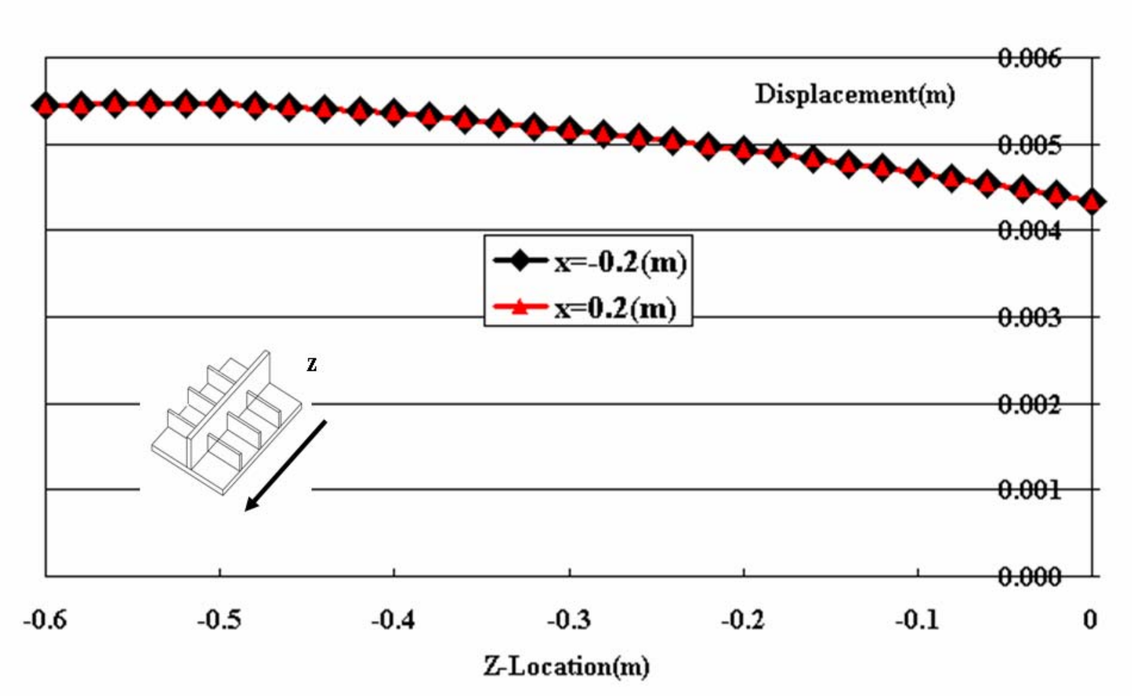

Fig. 29 Welding deformation of stiffened flat plates (Model 1)

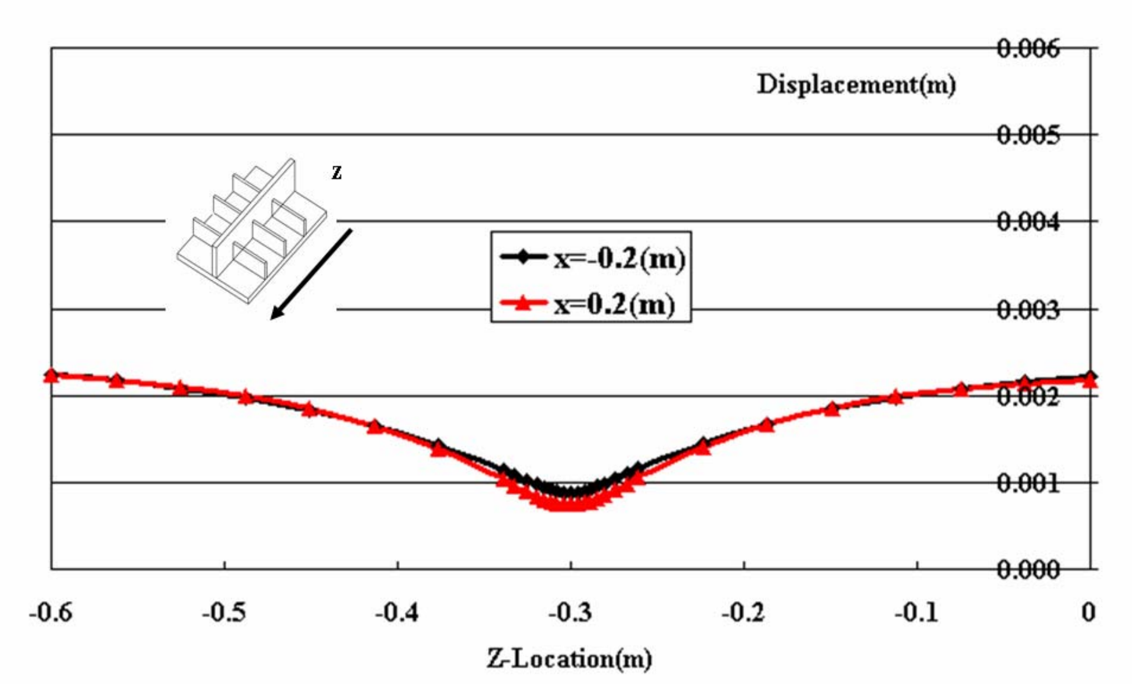

Fig. 30 Welding deformation of stiffened flat plates (Model 2)

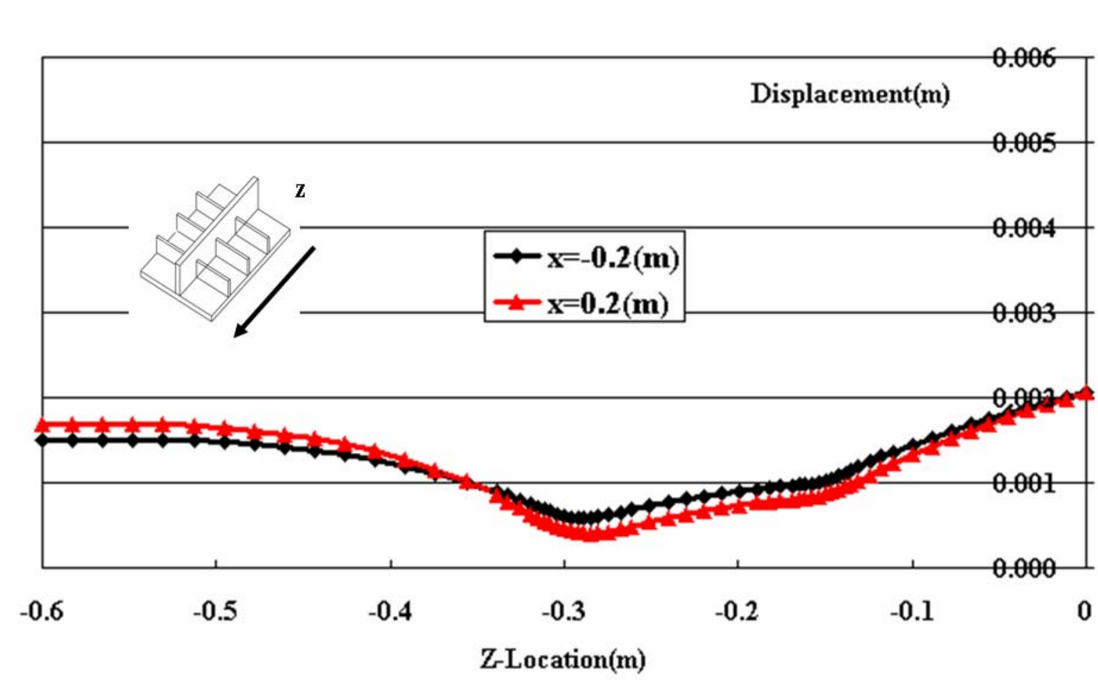

Fig. 31 Welding deformation of stiffened flat plates (Model 3)

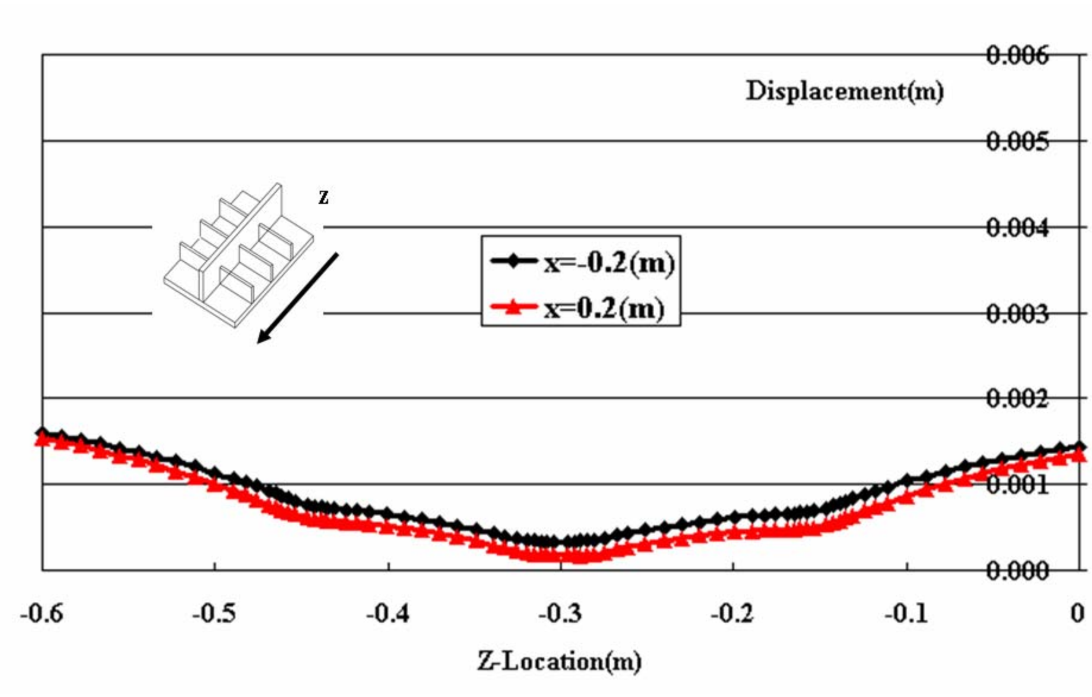

Fig. 32 Welding deformation of stiffened flat plates (Model 4)

3.2. Thermal elasto-plastic analysis of stiffened curved plates

3.2.1. Models of thermal elasto-plastic analysis of stiffened curved plates

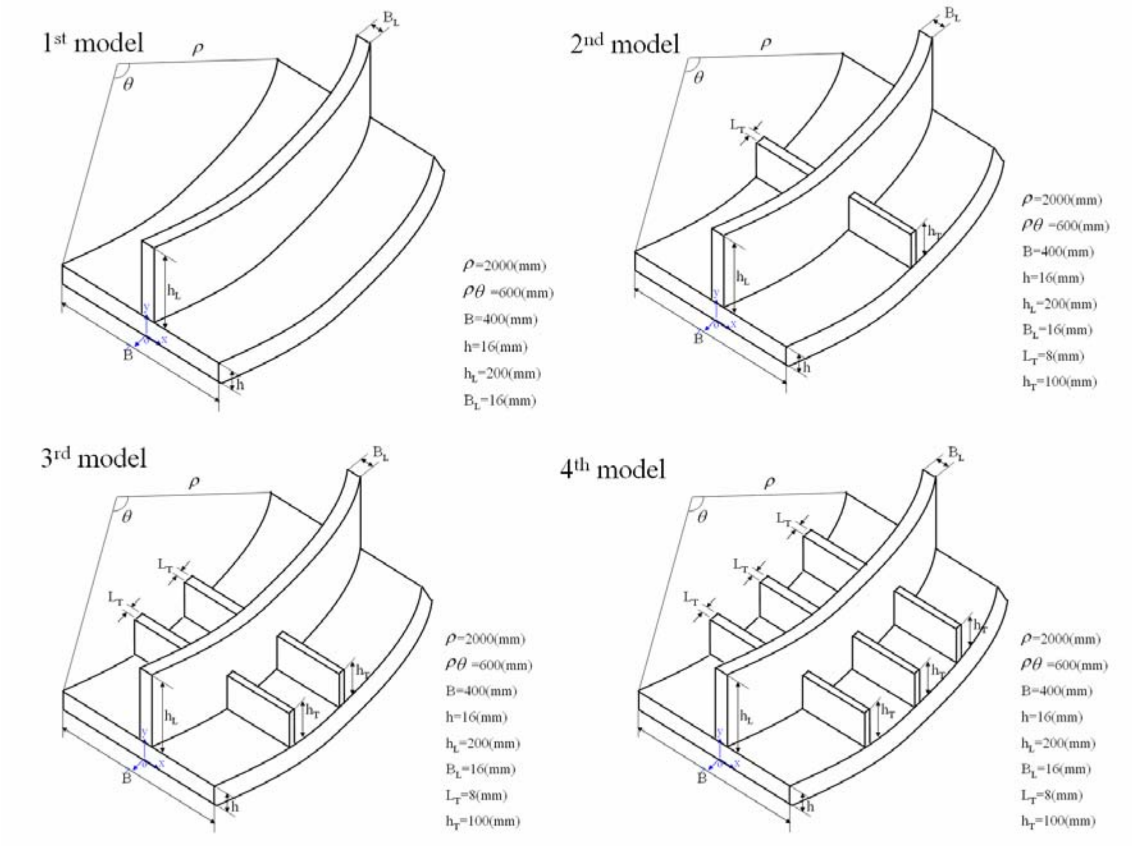

Fig. 33 Models of thermal elasto-plastic analysis of stiffened curved plates

Four kinds of analysis models of stiffened flat plate are adopted. The 1st model has 1 longitudinal stiffener and no transverse stiffener. And the 2nd, 3rd, 4th model has each 1, 2 and 3 stiffeners. Each model has a same base flat plate of L(600mm)×B(400mm)×h(16mm) and a same longitudinal stiffener of L(600mm)×B(16mm)×h(200mm). And the size of each transverse stiffener is same as L(8mm)×B(400mm)×h(100mm). The transverse stiffeners are equally spaced and located at $z = -150(mm)$, $z = -300(mm)$, $z = -450(mm)$ respectively. All of the sizes of the stiffened curved plate are same as the sizes of the stiffened flat plat.

3.2.2. Thermal elasto-plastic analysis of stiffened curved plates

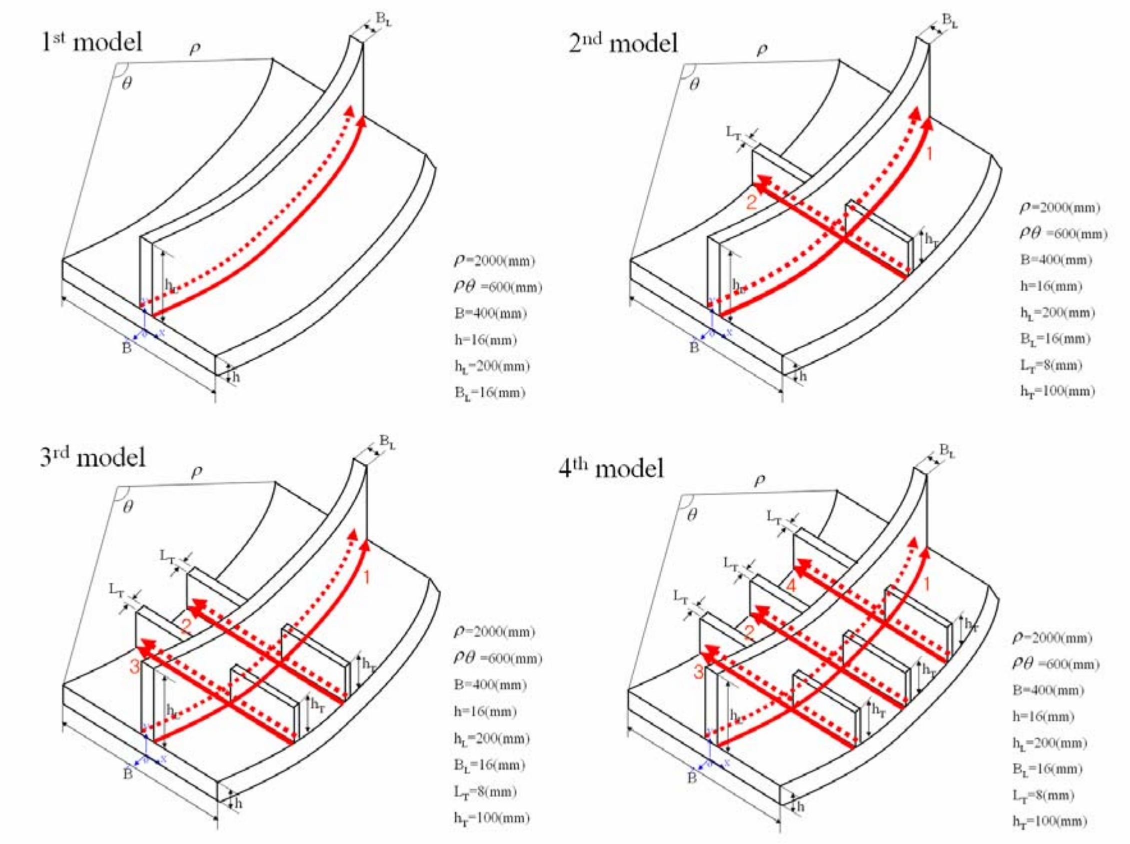

Fig. 34 Welding sequence of each model

Welding lines are shown in Fig. 34, every welding line is coupled by full line and dotted line. It means that the welding is preformed at one time along the coupled line. As shown in Fig. 34, the longitudinal stiffener is welded at first and then the transverse stiffeners are welded in order for 2nd 3rd, 4th model.

An arc-welding is adopted and all of the welding conditions are same as 30(V) of voltage, 300(A) of current and 5(mm/s) of welding velocity. All of the sequences, welding methods and welding conditions of curved plate are same as those of the stiffened flat plat cases.

3.2.3. Analysis models of Thermal elasto-plastic analysis of stiffened curved plates

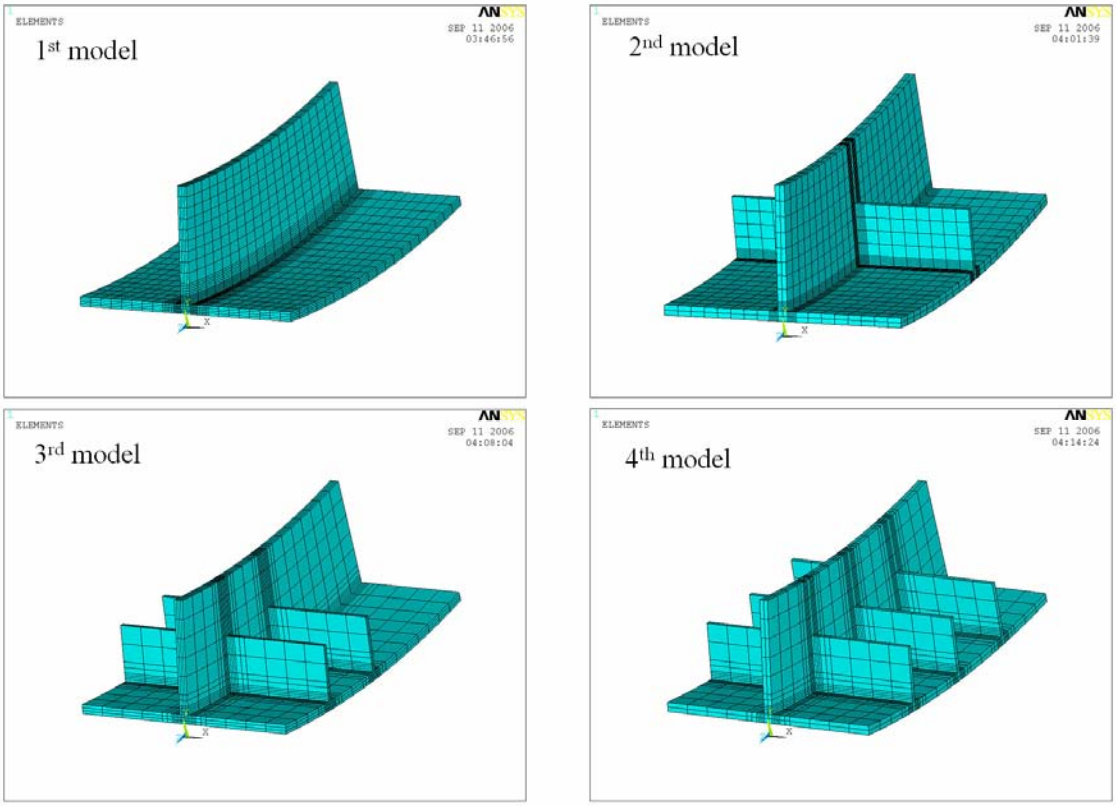

Fig. 35 Analysis models of Thermal elasto-plastic analysis of stiffened curved plates

As shown in Fig. 35 all of the shapes of element are rectangular parallelepiped. The element size is smaller as closer to the heat input area. And the four models have about 10,000 elements. For the thermal analysis all the model have surface element for reflection of thermal convection.

3.2.4. Heat transfer analysis of stiffened curved plates

In heat transfer analysis of curved plate, 3-D thermal solid element type and 3-D thermal surface element type are used same as the stiffened flat plate case.

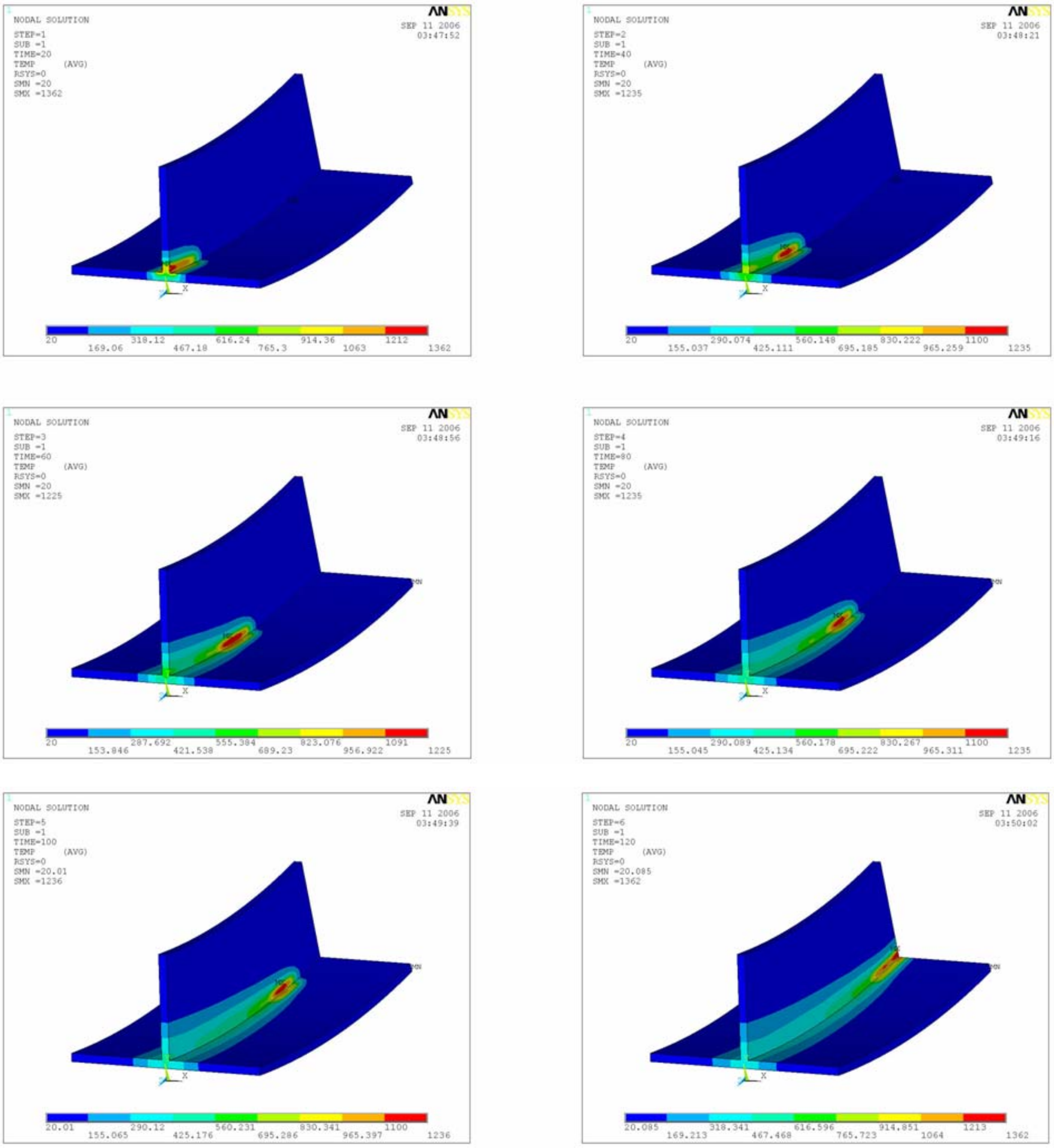

Fig. 36 Heat input process of 1st model of stiffened curved plate

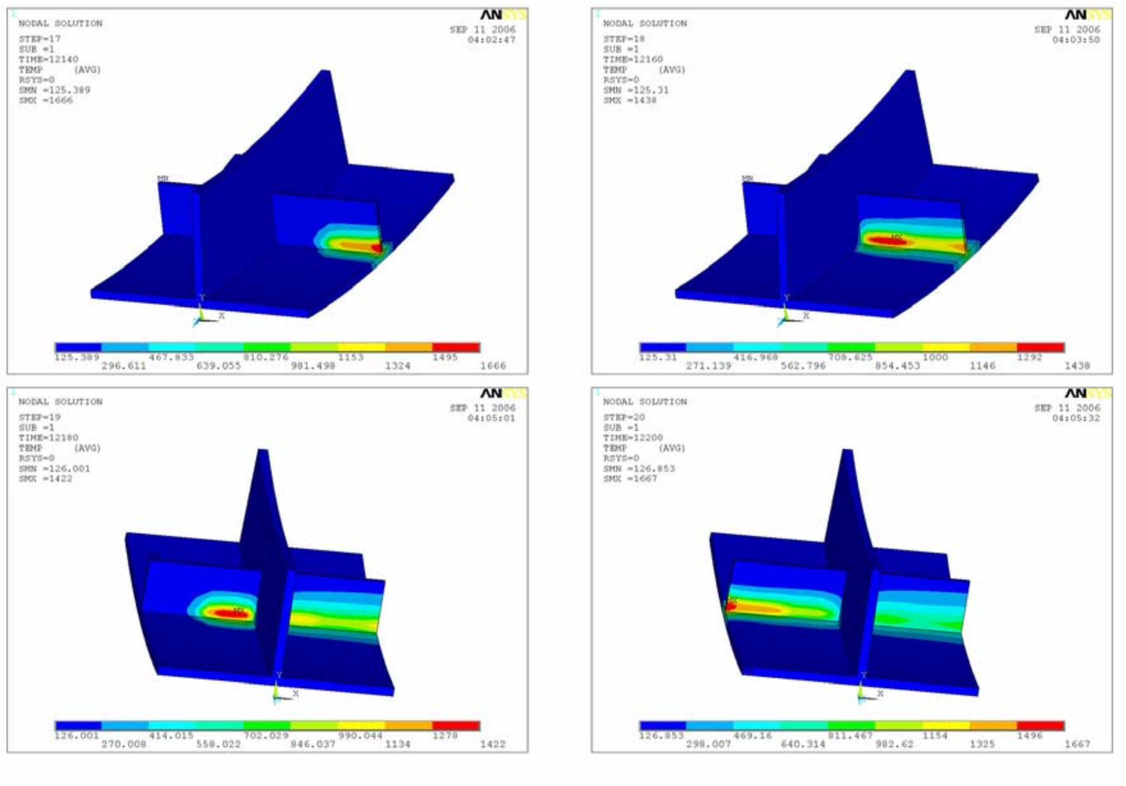

Fig. 37 Heat input process of 2nd model of stiffened curved plate

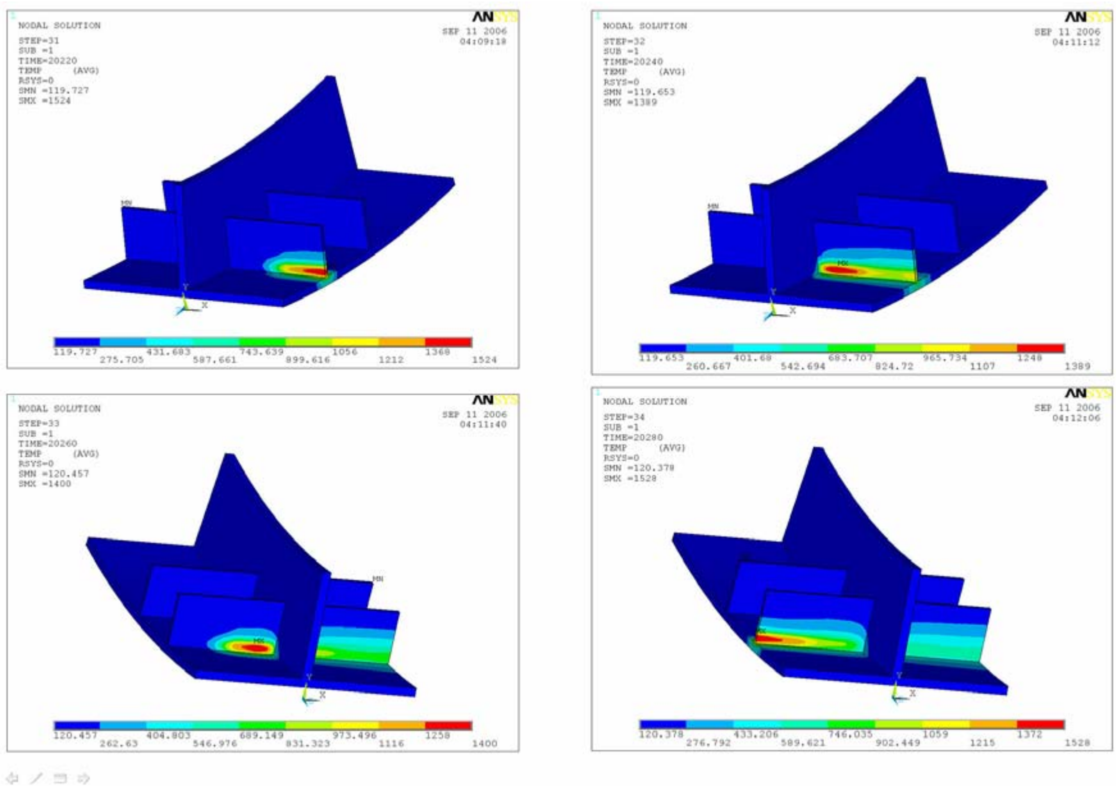

Fig. 38 Heat input process of 3rd model of stiffened curved plate

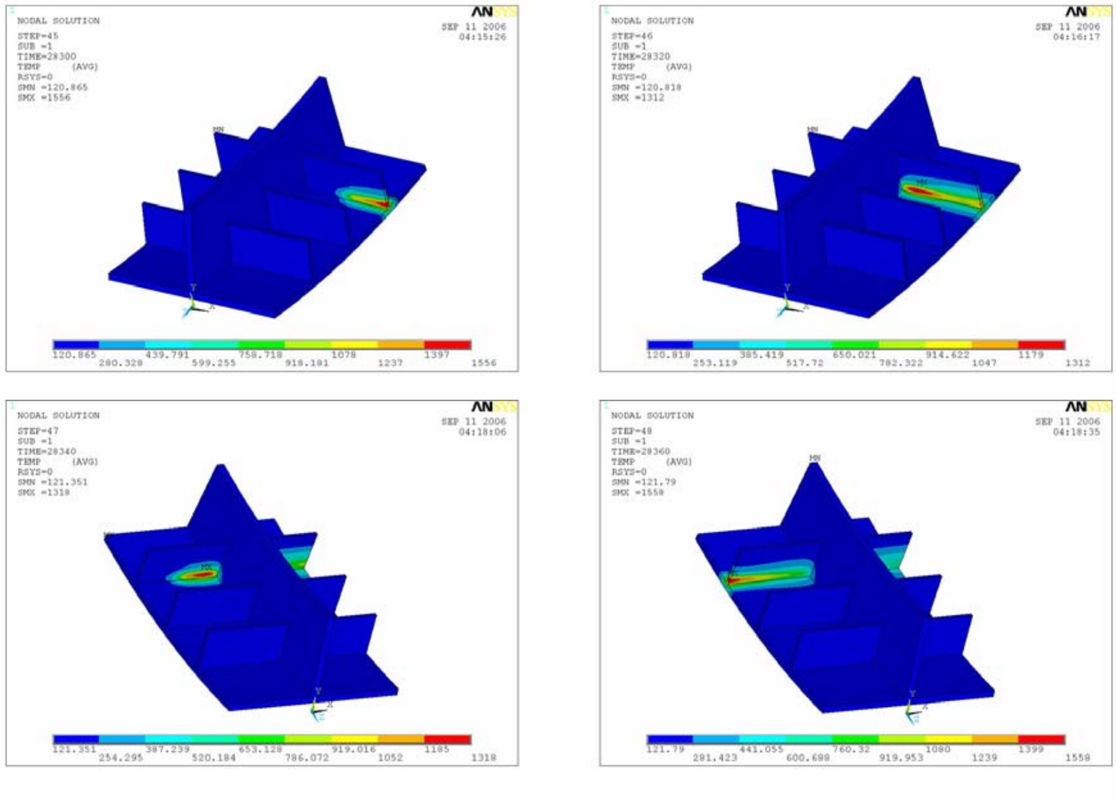

Fig. 39 Heat input process of 4th model of stiffened curved plate

3.2.5. Prediction of welding deformation of stiffened curved plates

(a) Boundary conditions

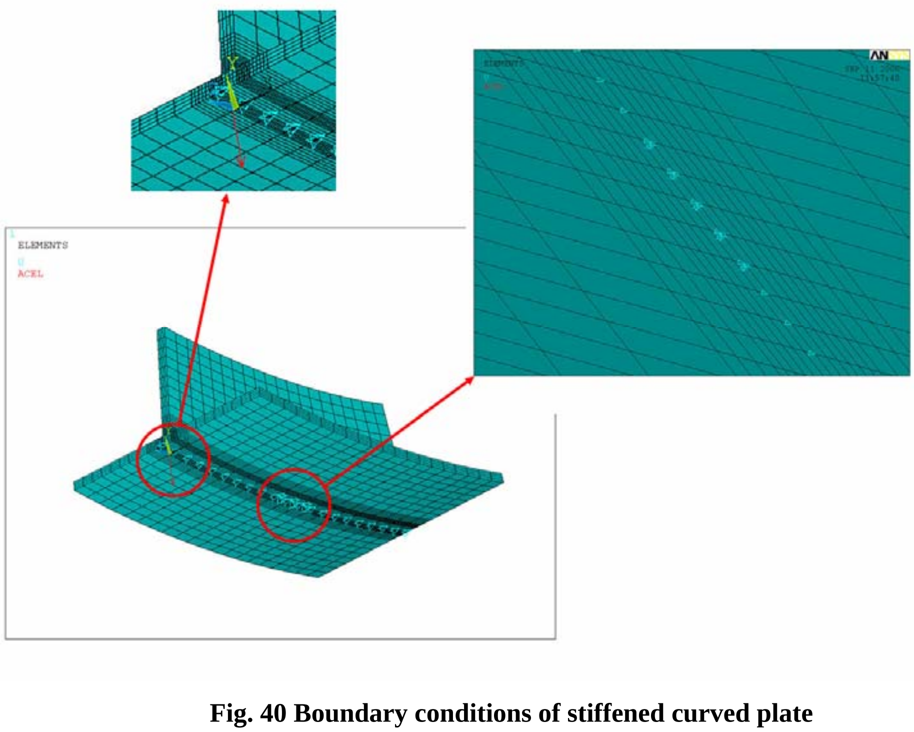

Fig. 40 Boundary conditions of stiffened curved plate

All of the boundary conditions of flat plate are applied at the bottom of main plate. As shown in Fig. 40 along the middle of the breadth direction (x=0), all of nodes are fixed to x direction. And in the middle of the length, some nodes are fixed all direction of x, y, and z. All applied boundary conditions of curved plate are same as the stiffened flat plate.

(b) Analysis results

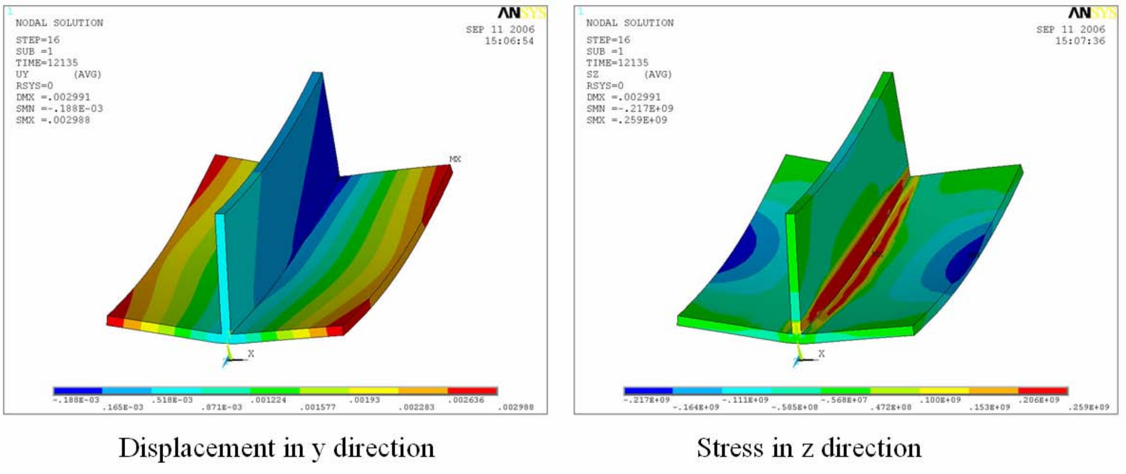

Fig. 41 Analysis result of 1st case of stiffened curved plate

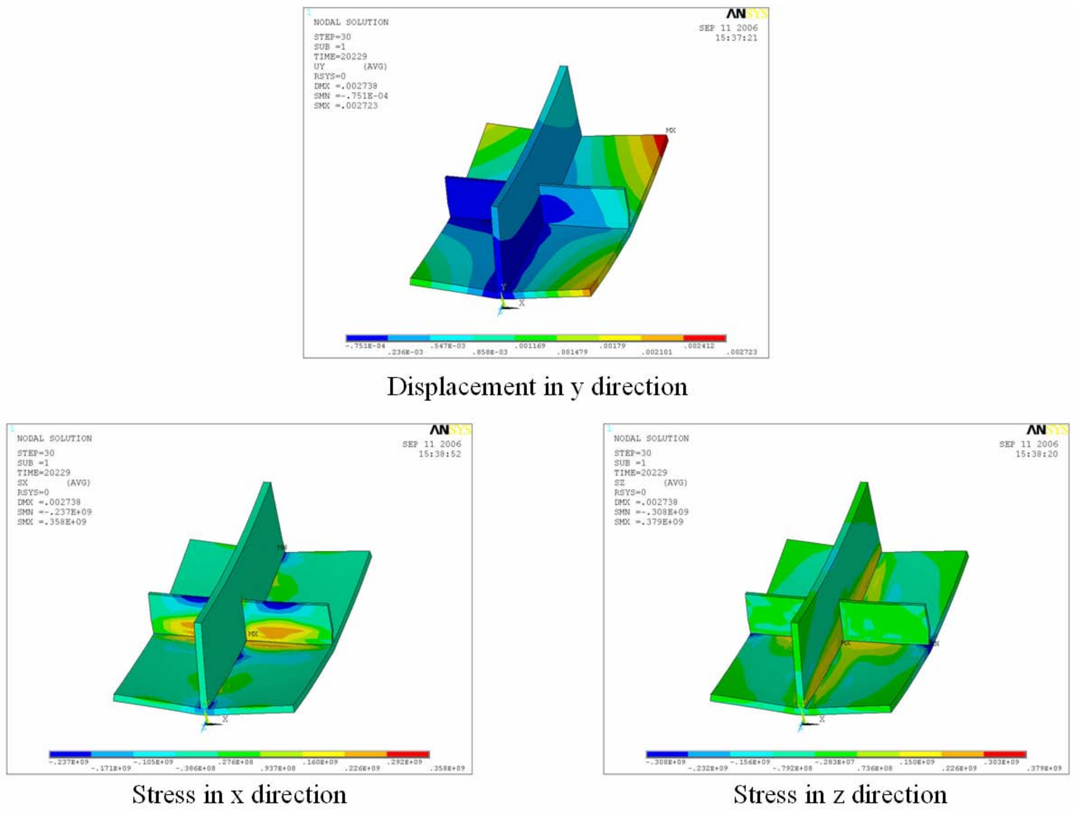

Fig. 42 Analysis result of 2nd case of stiffened curved plate

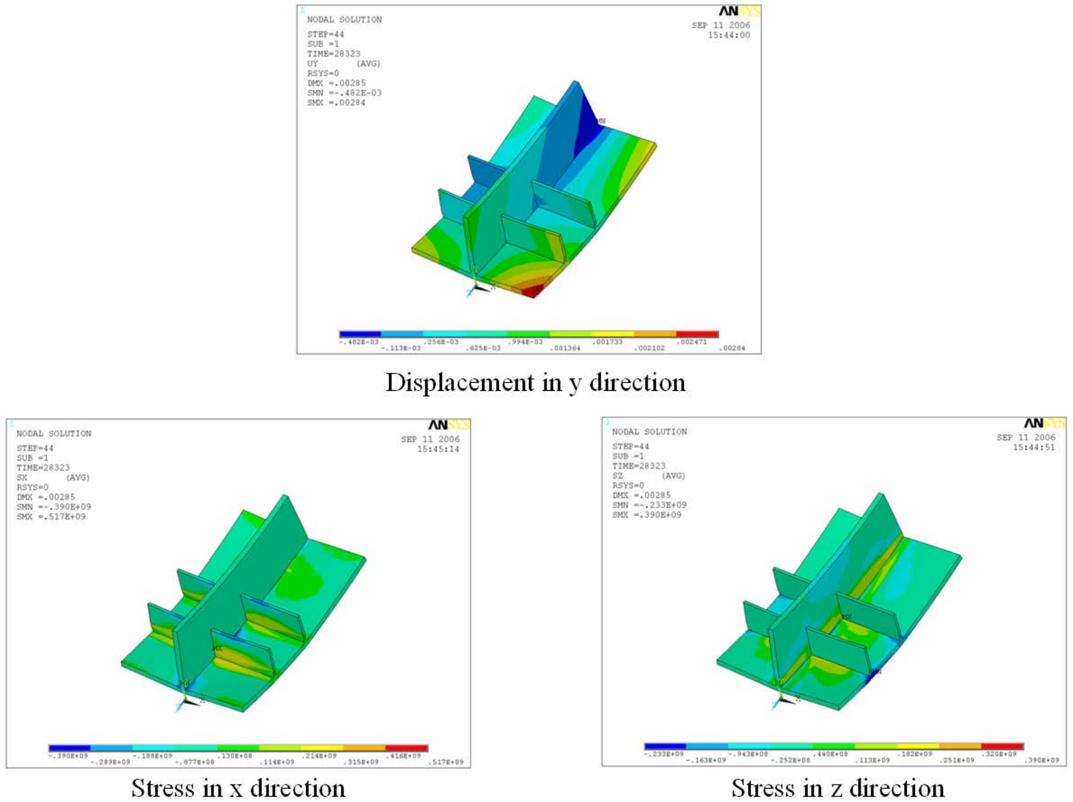

Displacement in y direction

Stress in x direction

Stress in z direction

Fig. 43 Analysis result of 3rd case of stiffened curved plate

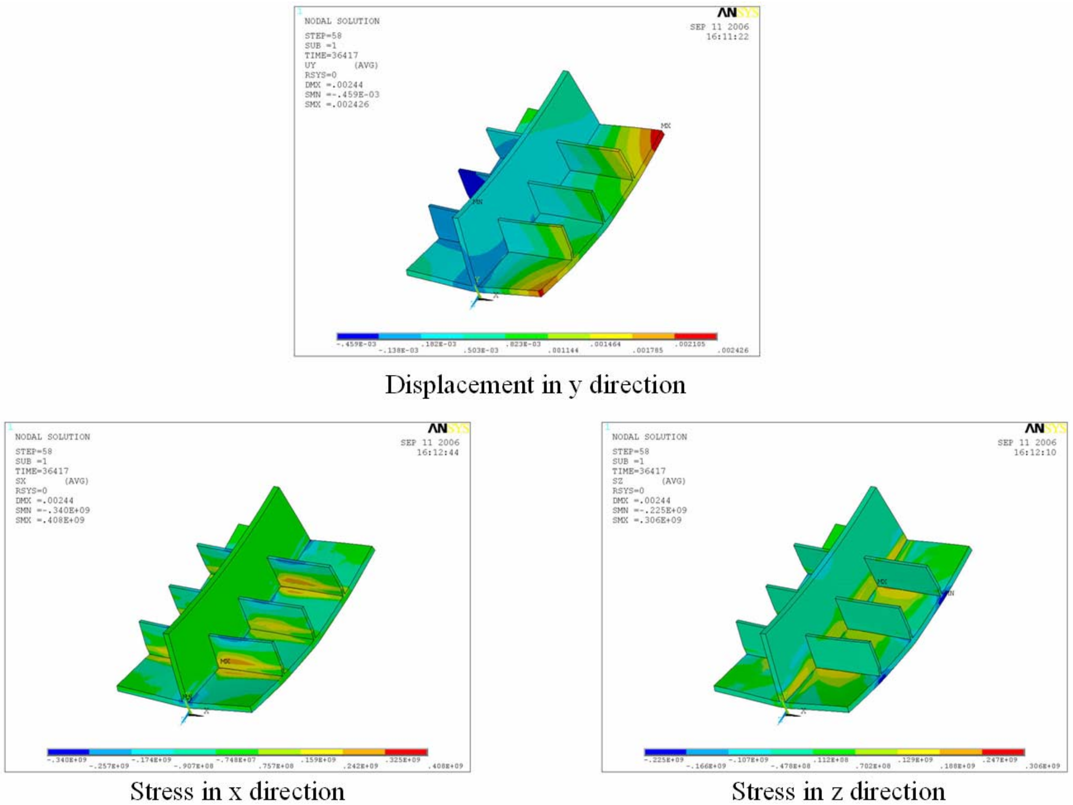

Displacement in y direction

Stress in x direction

Stress in z direction

Fig. 44 Analysis result of 4th case of stiffened curved plate

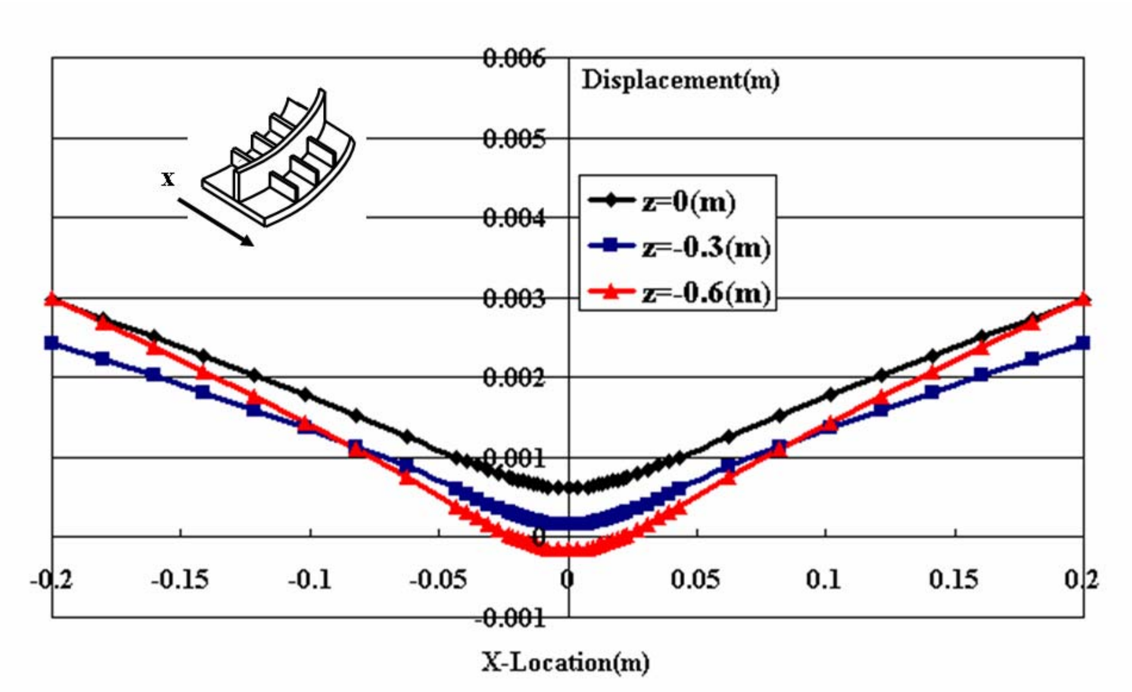

Fig. 45 Welding deformation of stiffened curved plates (Model 1)

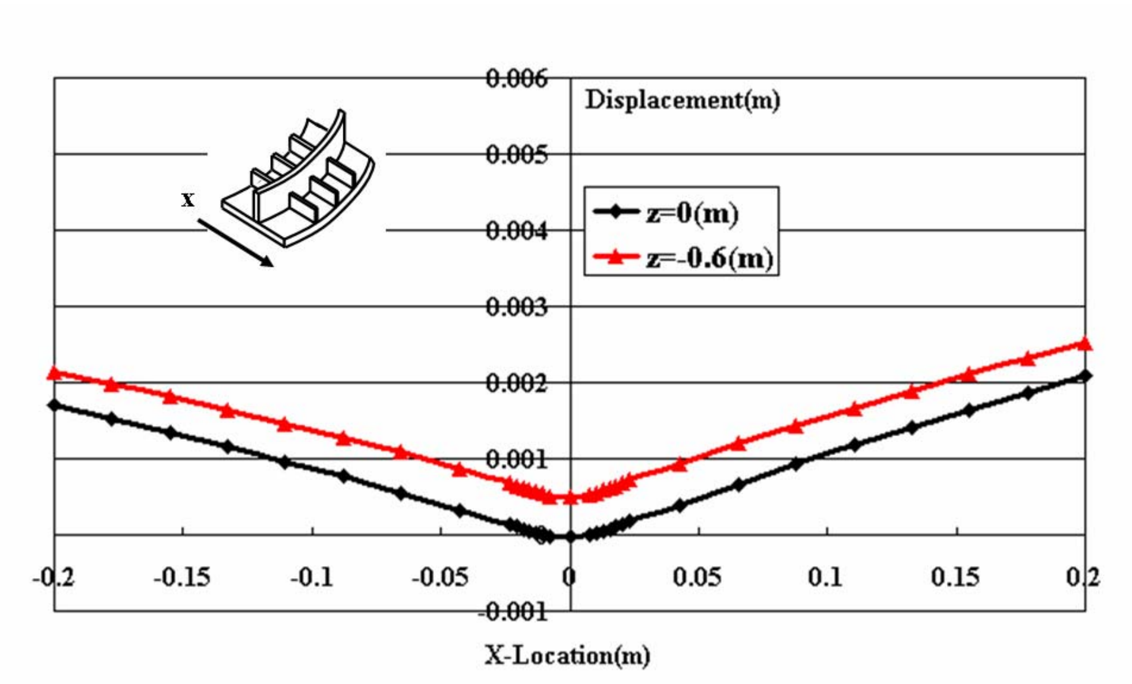

Fig. 46 Welding deformation of stiffened curved plates (Model 2)

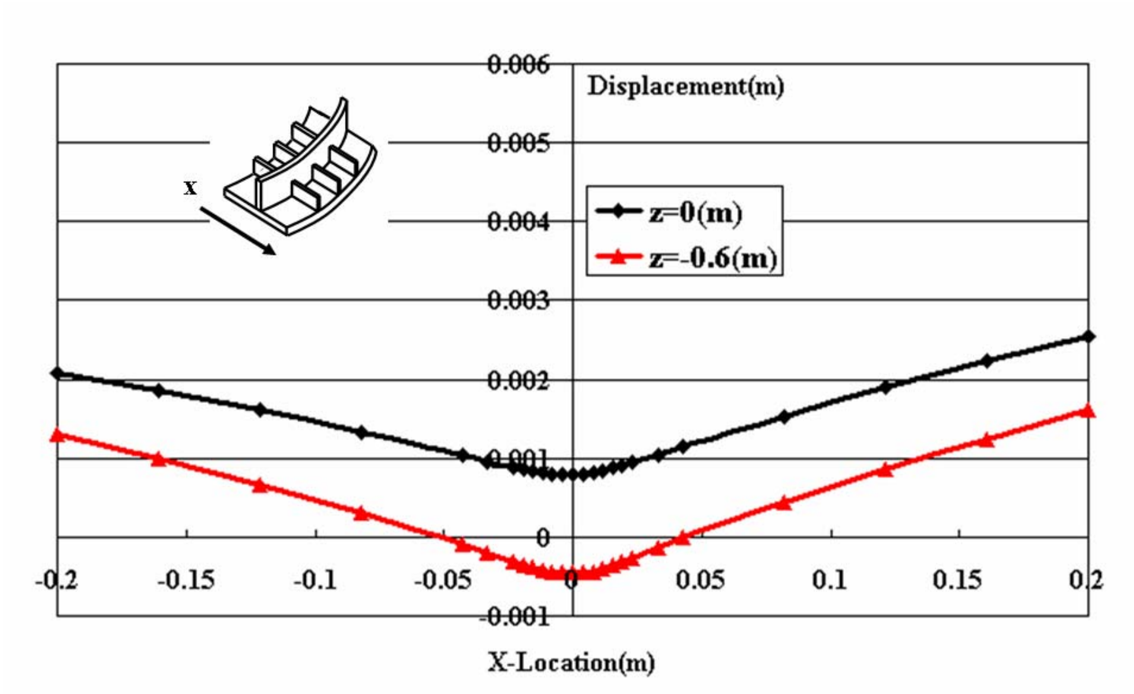

Fig. 47 Welding deformation of stiffened curved plates (Model 3)

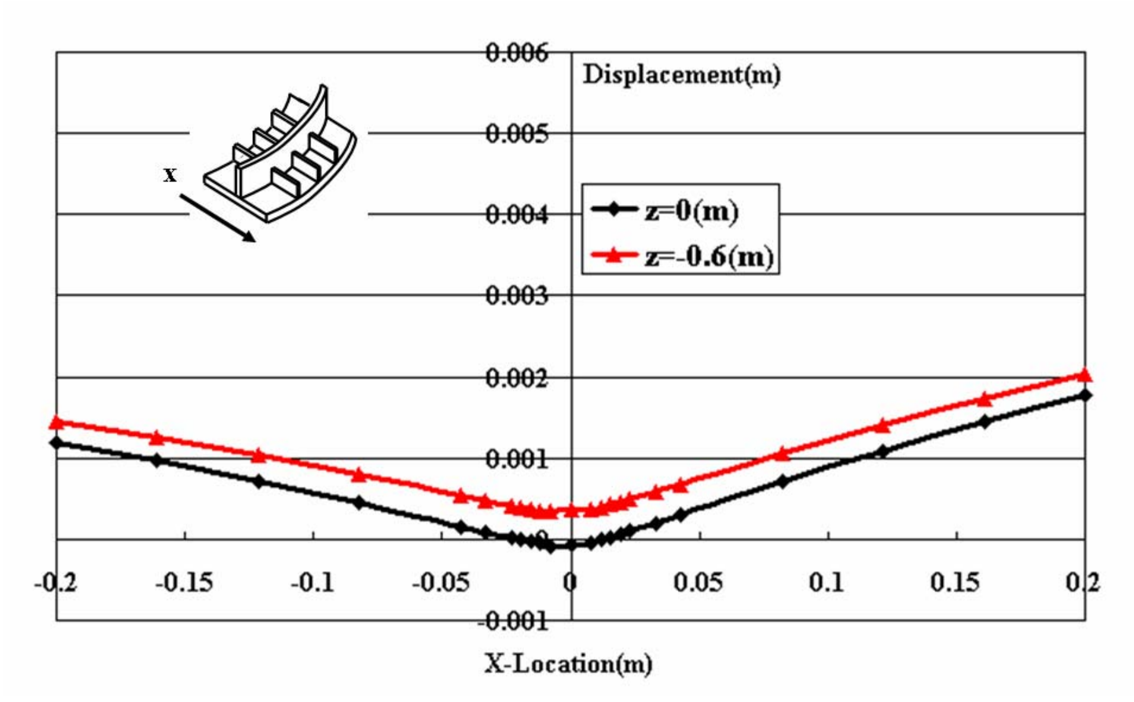

Fig. 48 Welding deformation of stiffened curved plates (Model 4)

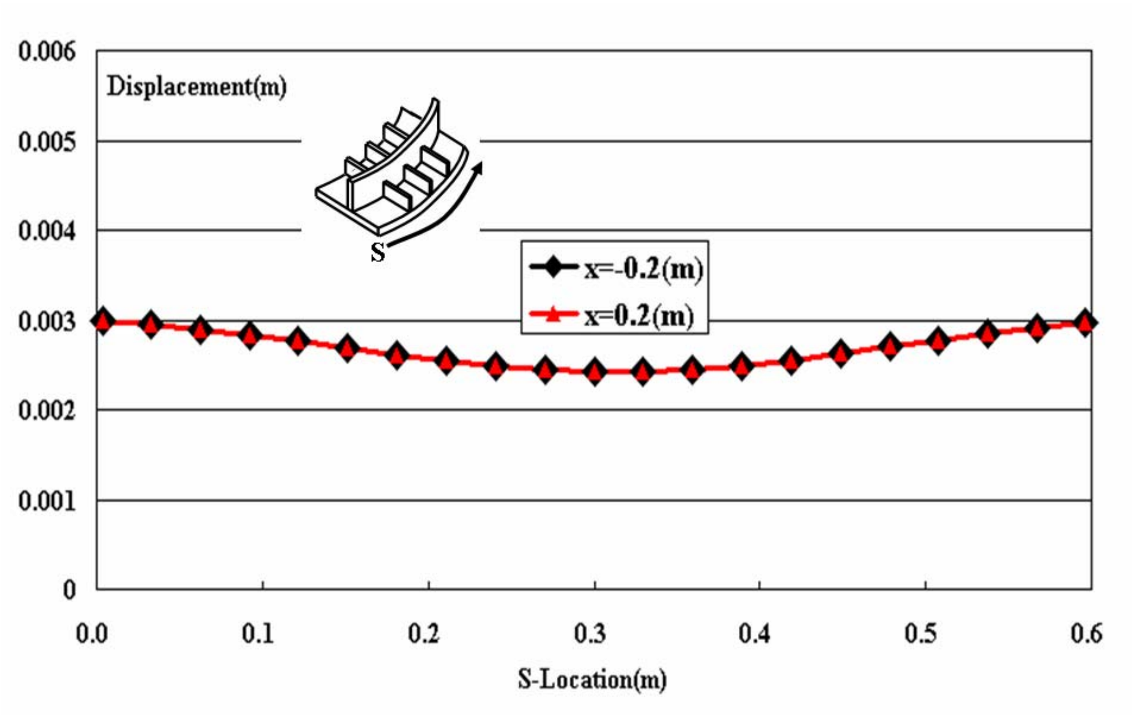

Fig. 49 Welding deformation of stiffened curved plates (Model 1)

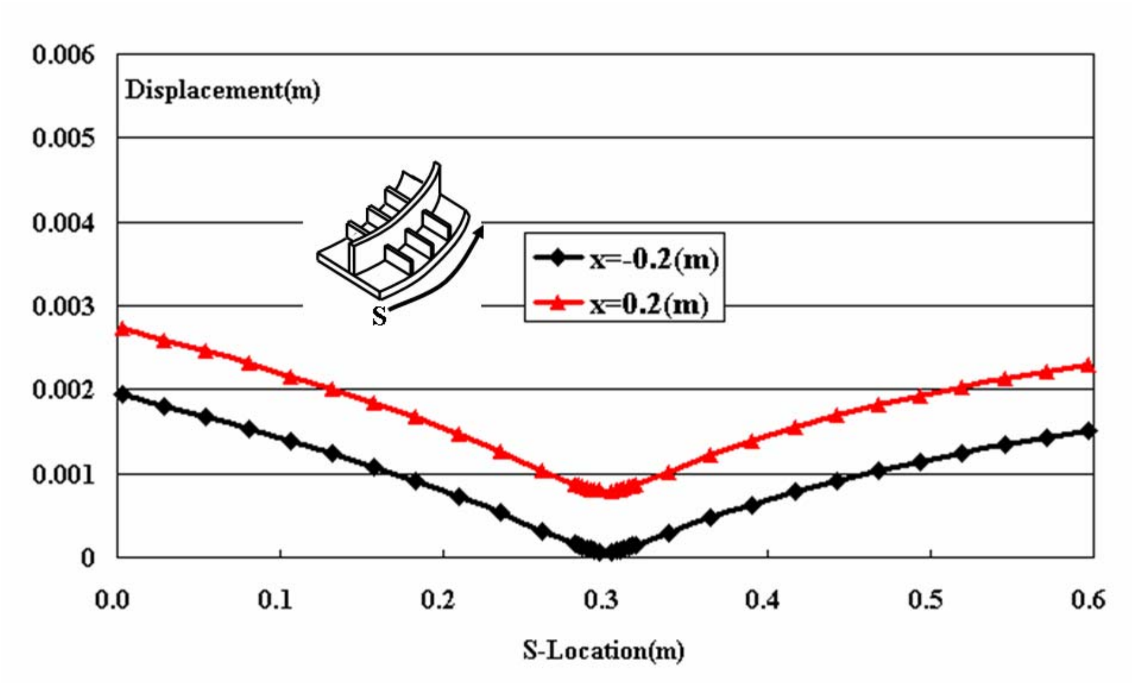

Fig. 50 Welding deformation of stiffened curved plates (Model 2)

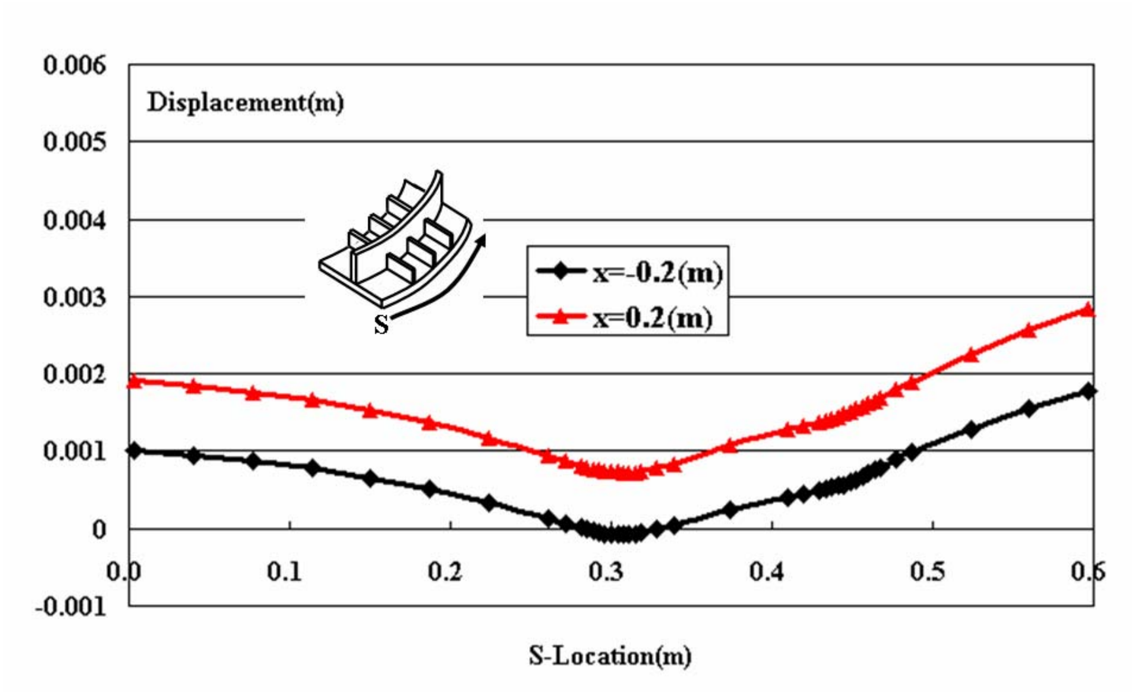

Fig. 51 Welding deformation of stiffened curved plates (Model 3)

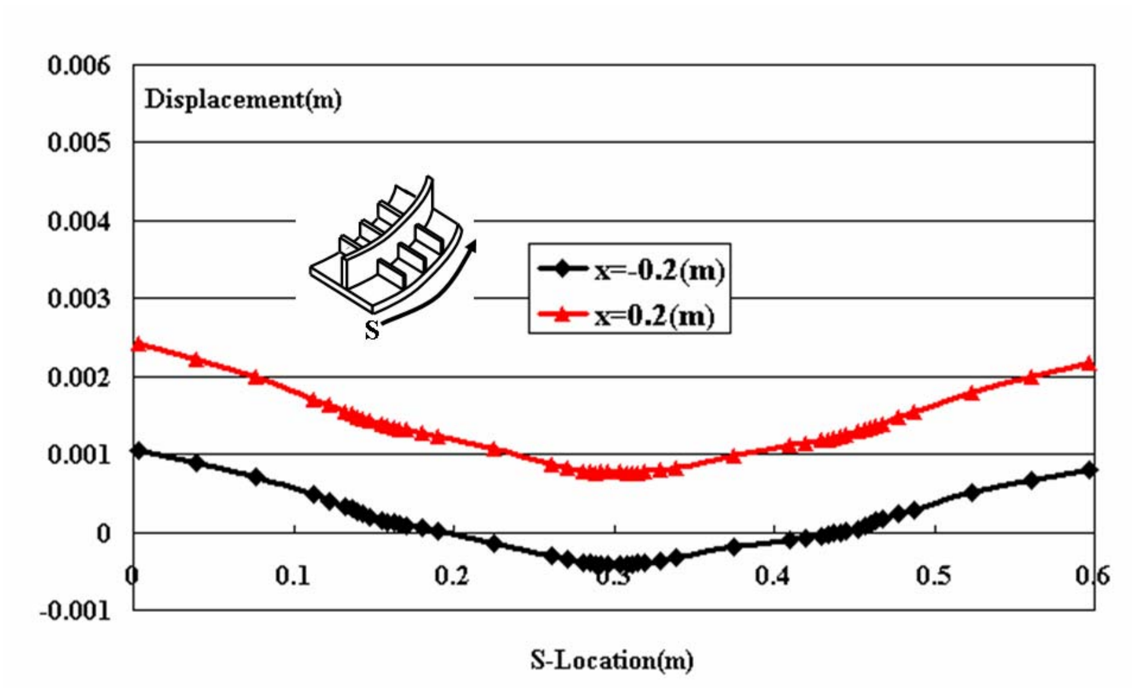

Fig. 52 Welding deformation of stiffened curved plates (Model 4)

4. Welding distortion analysis of stiffened flat plate by equivalent load method

By the equivalent load method, welding deformation analysis is performed for each case of the flat plate. Analysis results are shown in Fig. 53 - 60.

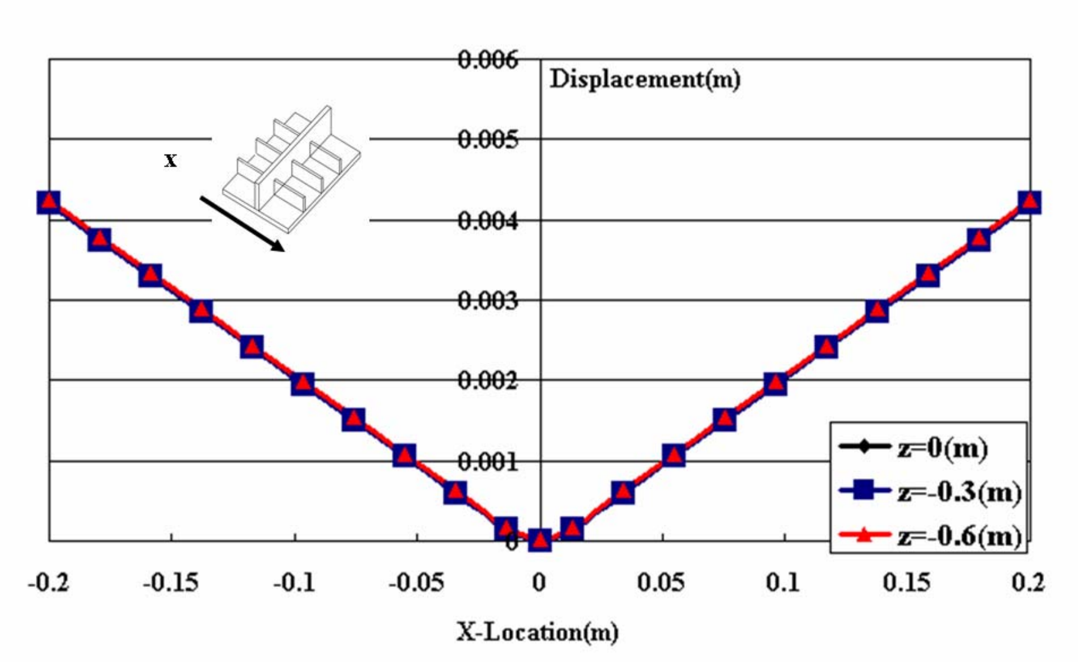

Fig. 53 Welding deformation of stiffened flat plates by equivalent load method (Model 1)

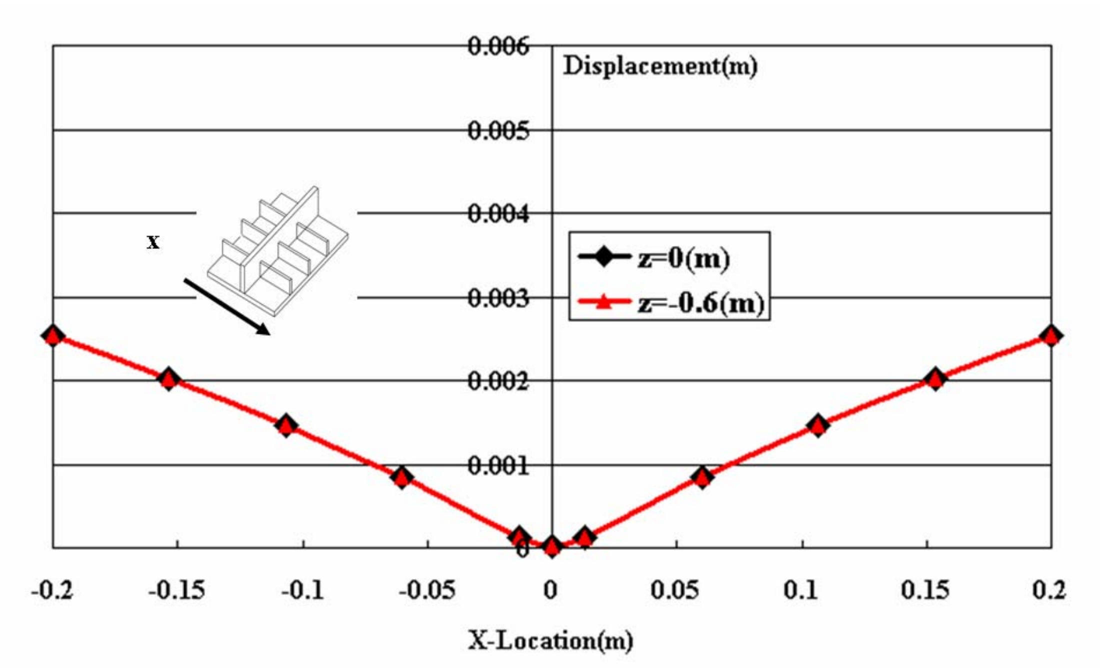

Fig. 54 Welding deformation of stiffened flat plates by equivalent load method (Model 2)

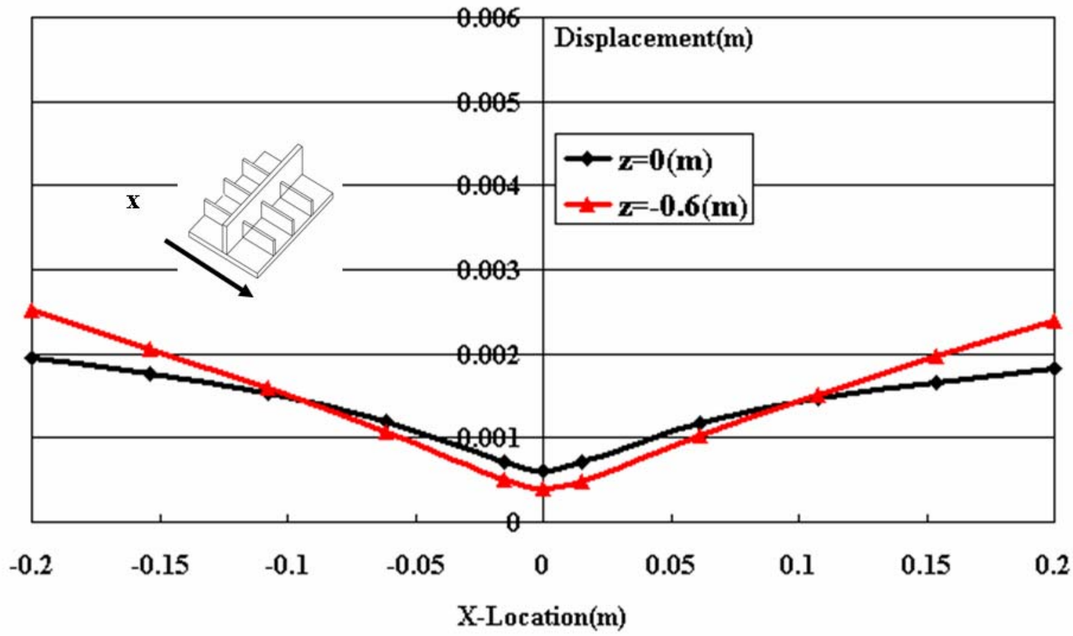

Fig. 55 Welding deformation of stiffened flat plates by equivalent load method (Model 3)

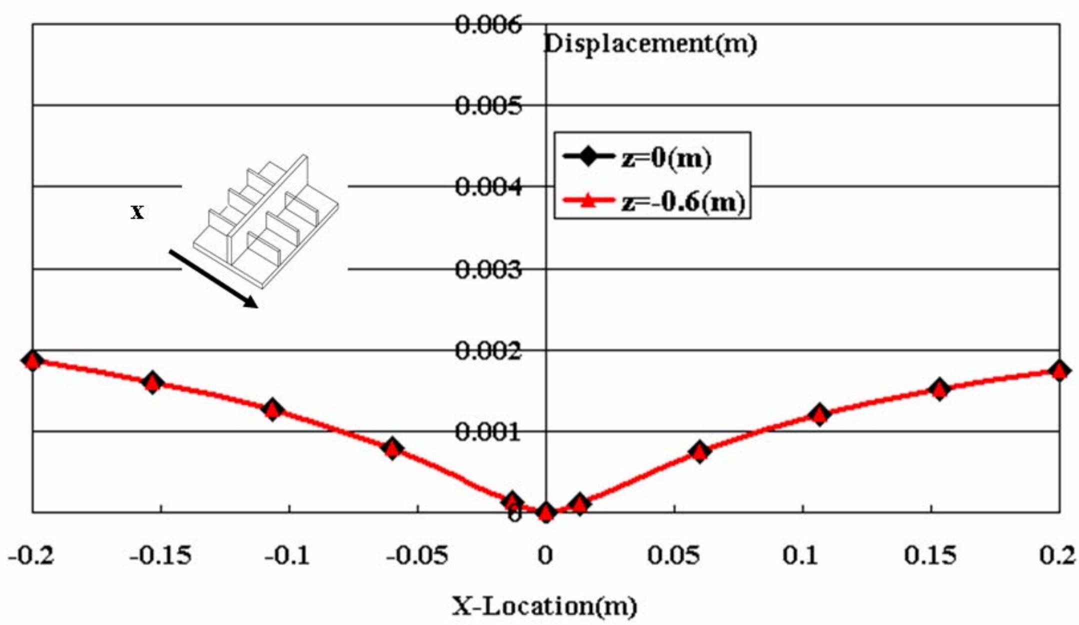

Fig. 56 Welding deformation of stiffened flat plates by equivalent load method (Model 4)

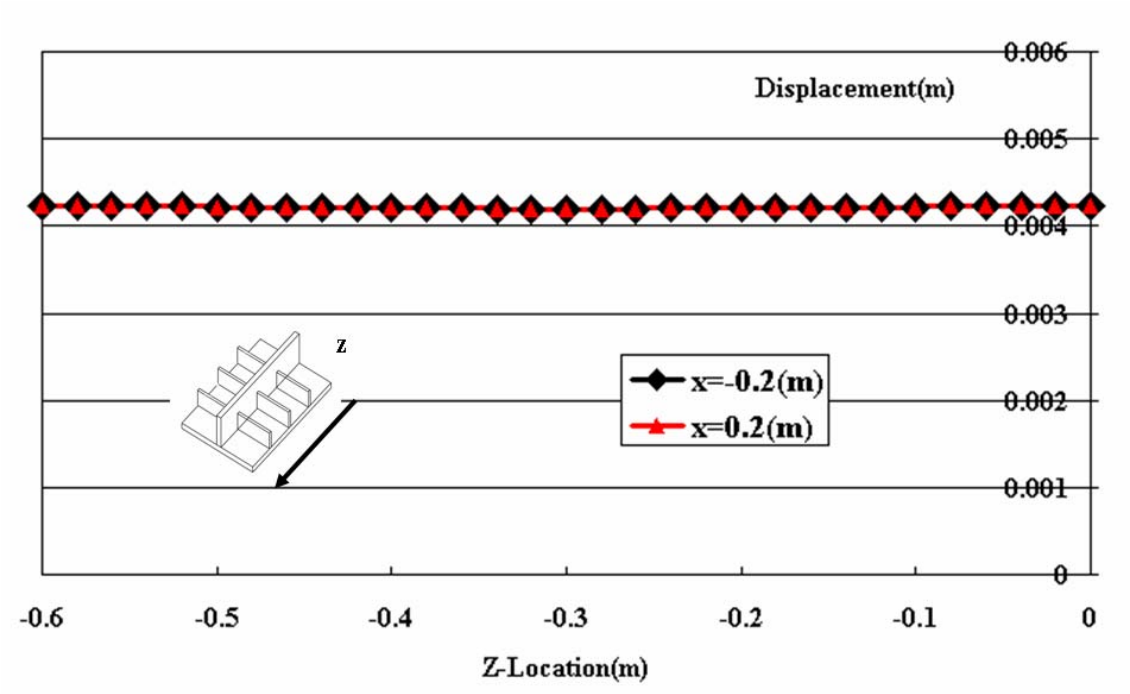

Fig. 57 Welding deformation of stiffened flat plates by equivalent load method (Model 1)

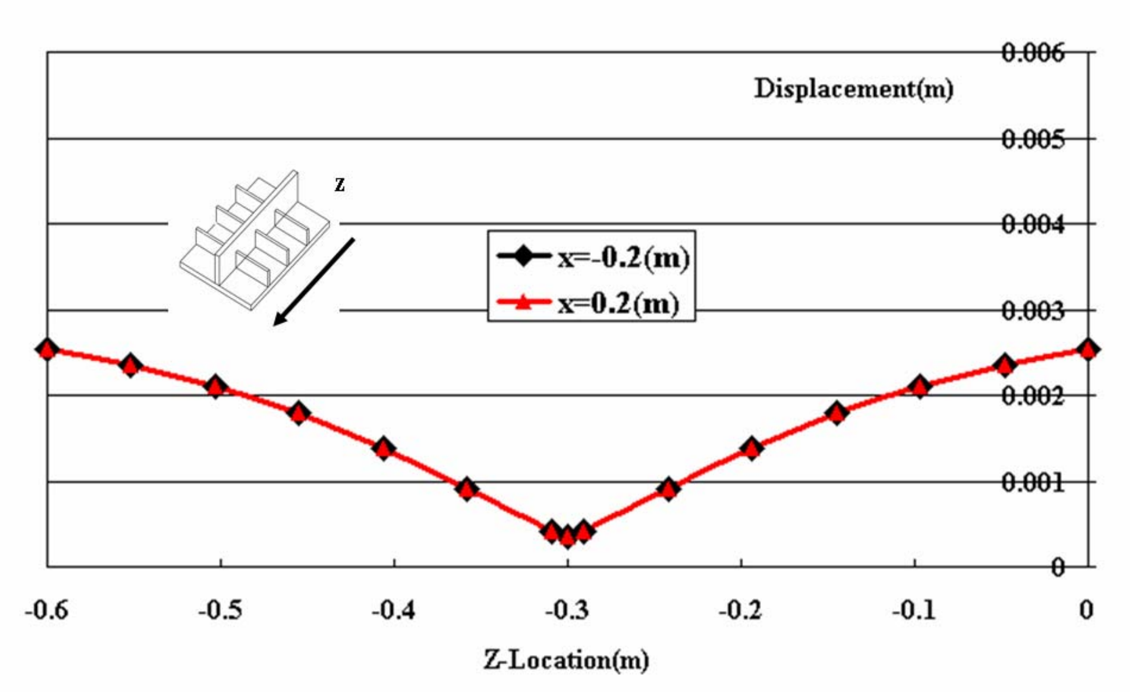

Fig. 58 Welding deformation of stiffened flat plates by equivalent load method (Model 2)

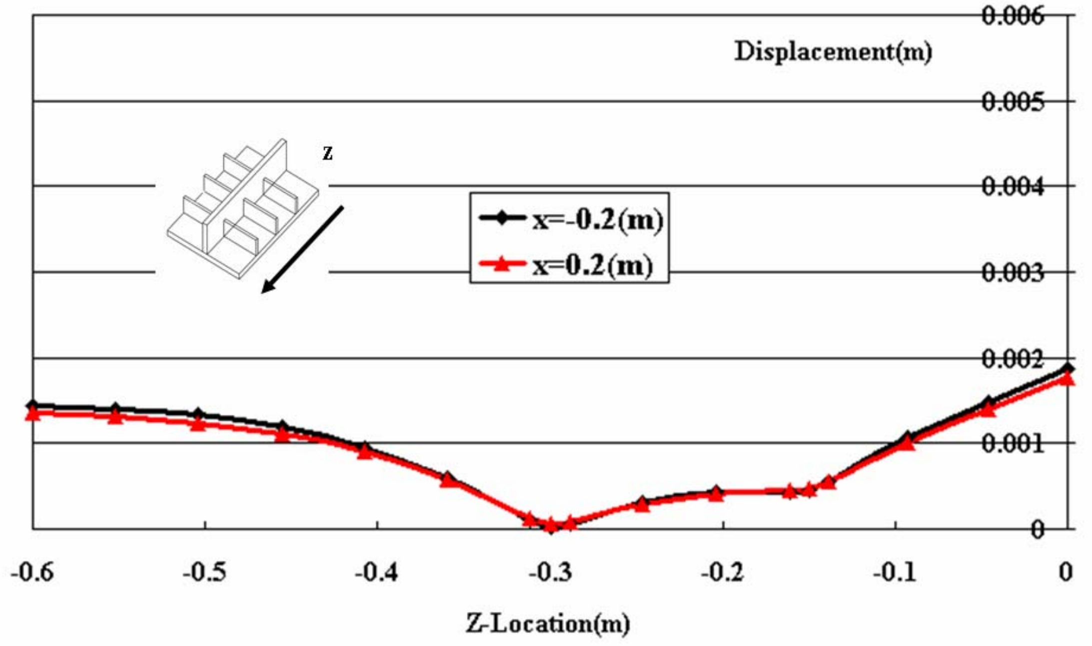

Fig. 59 Welding deformation of stiffened flat plates by equivalent load method (Model 3)

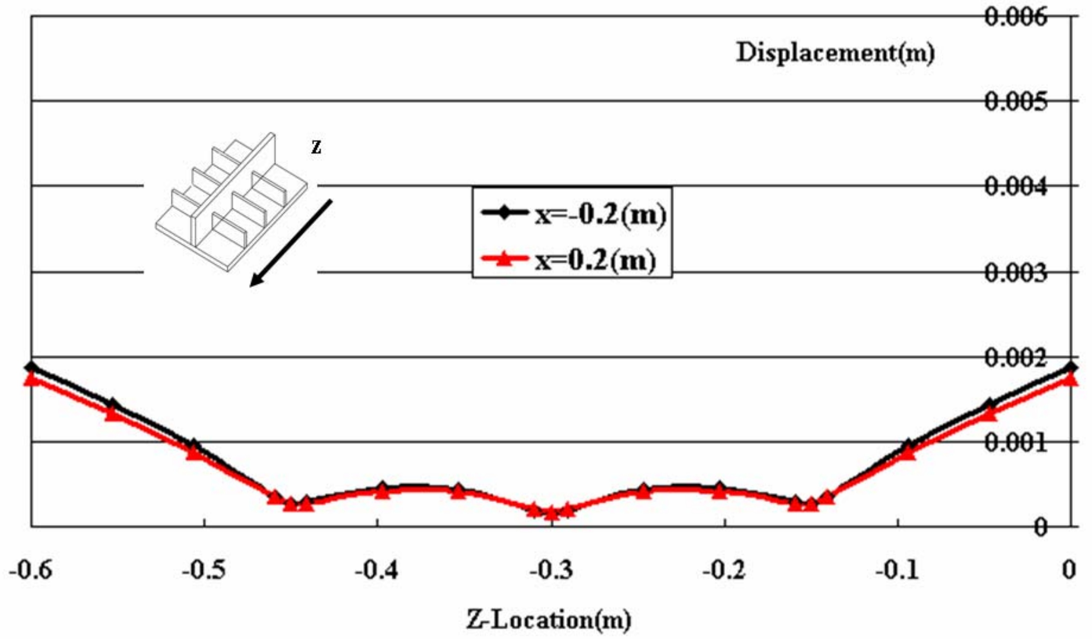

Fig. 60 Welding deformation of stiffened flat plates by equivalent load method (Model 4)

5. Comparison of thermal elasto-plastic analysis and equivalent load method of stiffened flat plates

The coordinates used in this report is shown in Fig. 60

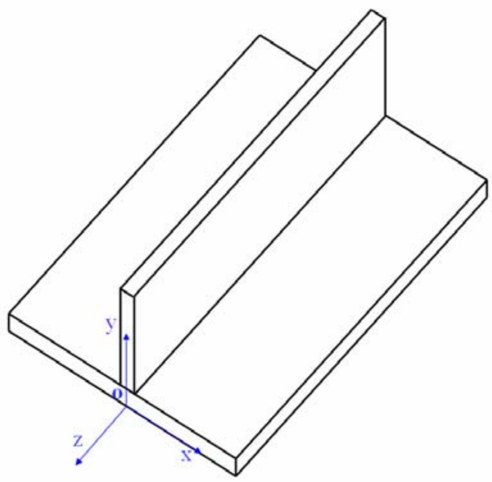

Fig. 61 Coordinates of stiffened flat plate

The welding distortions (at x=0.2m) calculated by two different methods (EPA: Elasto-Plastic Analysis, ELM : Equivalent Load Method) are compared in Table 1.

Both results show fairly good agreements with each other within 12% of average difference.

Table. 1 Comparison of welding distortions of stiffened flat plates(at x=0.2m)

	Stiffened Flat Plate Case 1		Stiffened Flat Plate Case 2		Stiffened Flat Plate Case 3		Stiffened Flat Plate Case 4		
z-location(m)	z=0	z=-0.6	z=0	z=-0.6	z=0(m)	z=-0.6	z=0	z=-0.6	
Displacement(m) by EPA	0.004344	0.005444	0.00218	0.0022383	0.002062	0.0014908	0.0013609	0.0015404	
Displacement(m) by ELM	0.004239	0.004239	0.00254	0.00254	0.001815	0.00239	0.001745	0.001745	**Average Ratio**
Ratio	0.9757	0.7786	1.1652	1.1348	0.8802	1.6032	1.2822	1.1328	1.1191

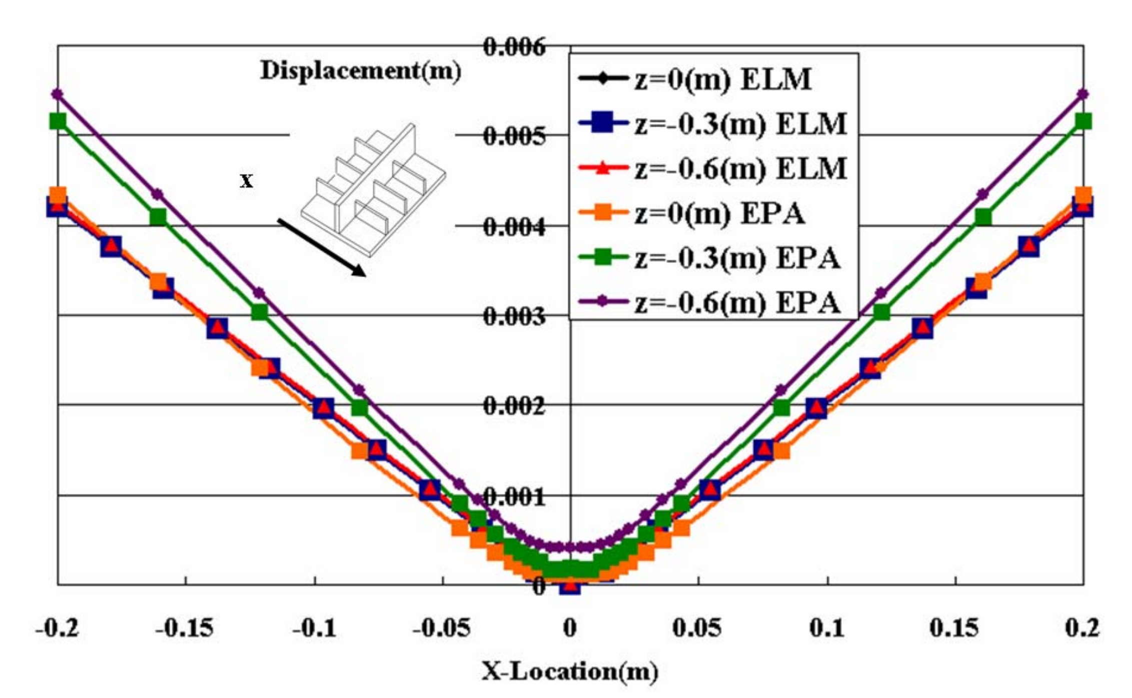

Fig. 62 Comparison of welding deformation of stiffened flat plates (Model 1)

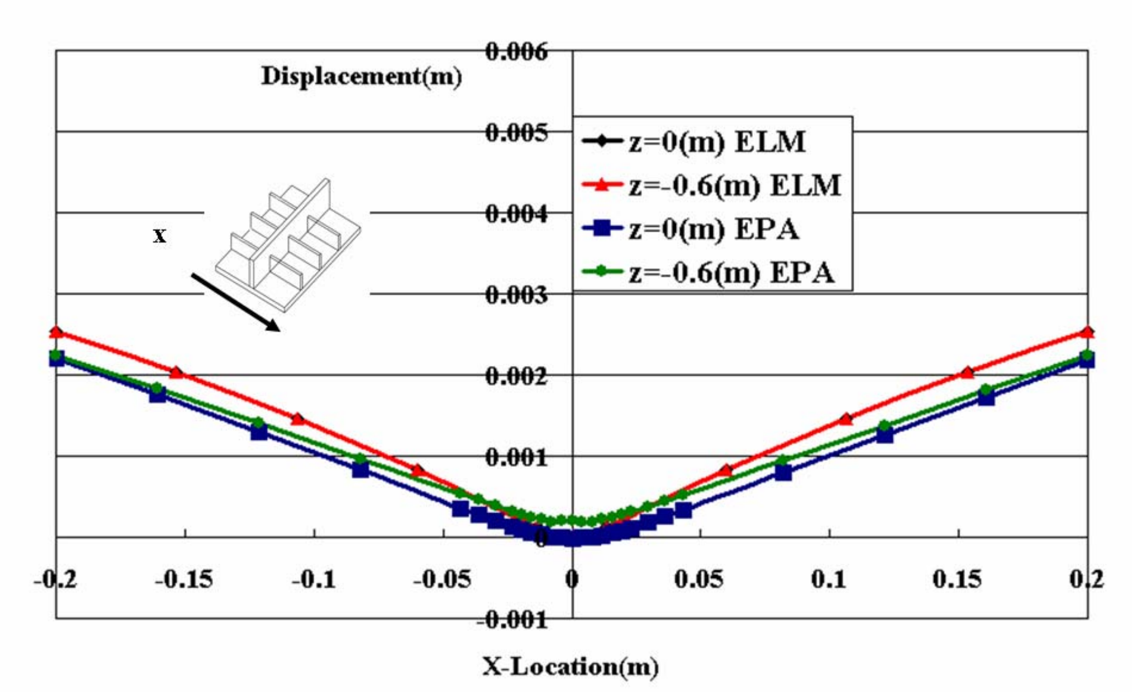

Fig. 63 Comparison of welding deformation of stiffened flat plates (Model 2)

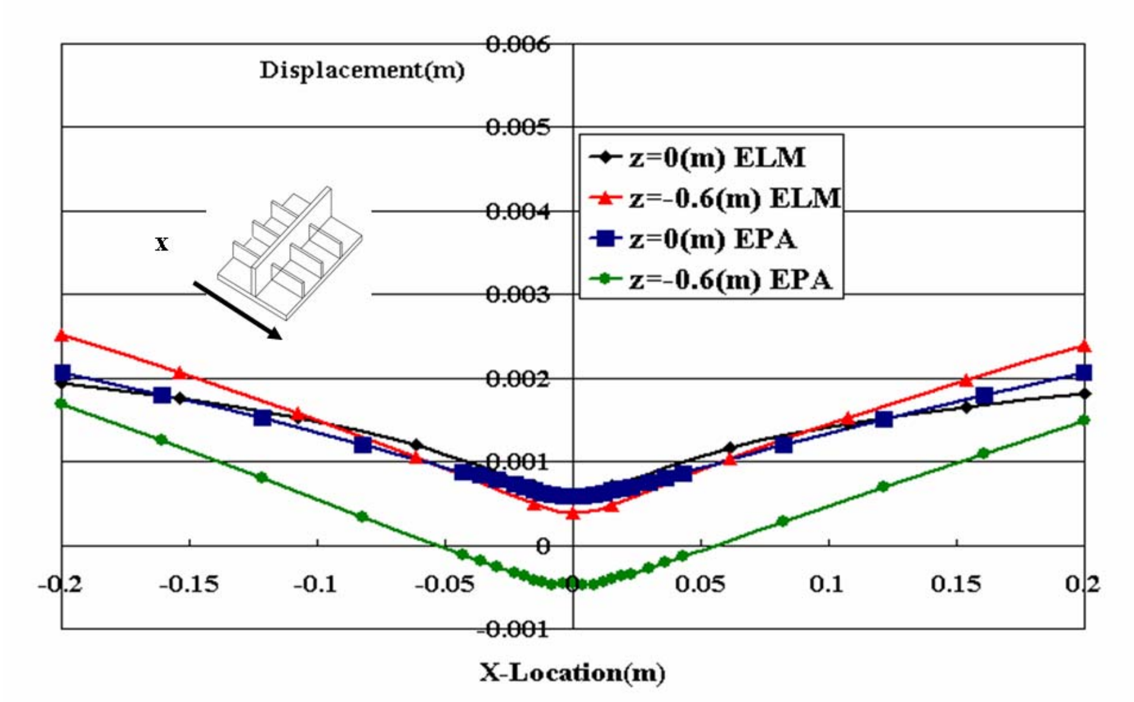

Fig. 64 Comparison of welding deformation of stiffened flat plates (Model 3)

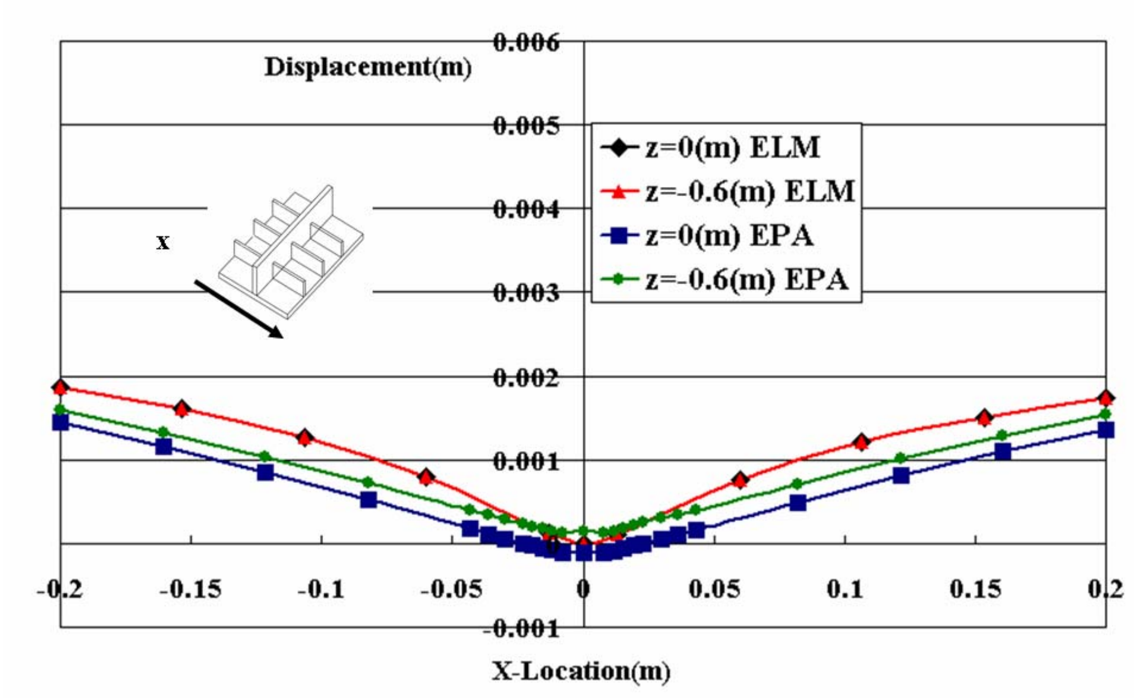

Fig. 65 Comparison of welding deformation of stiffened flat plates (Model 4)

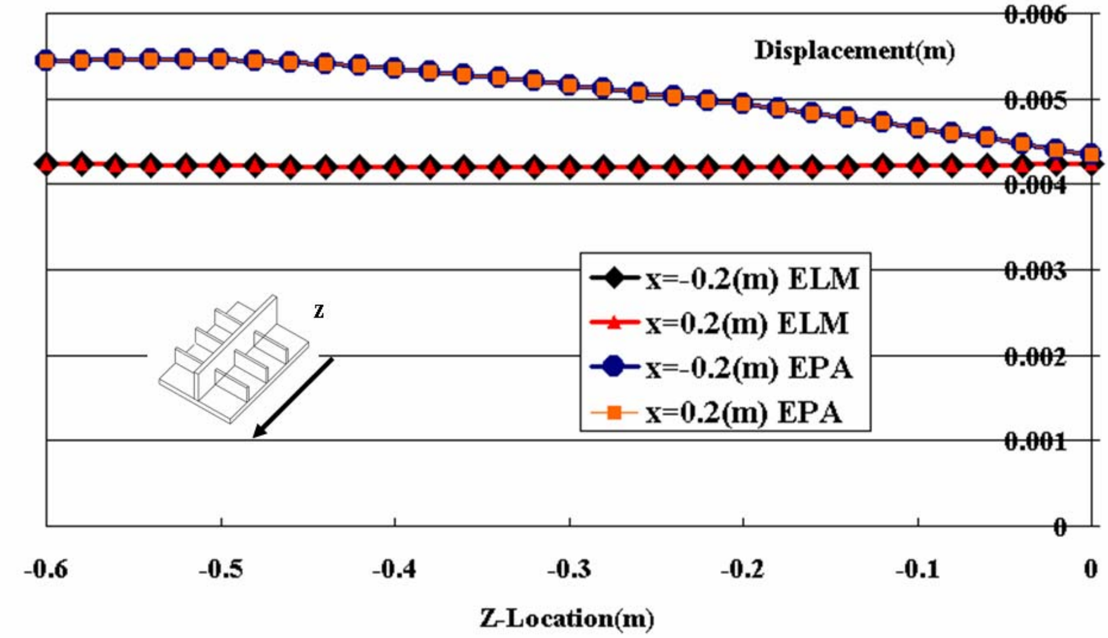

Fig. 66 Comparison of welding deformation of stiffened flat plates (Model 1)

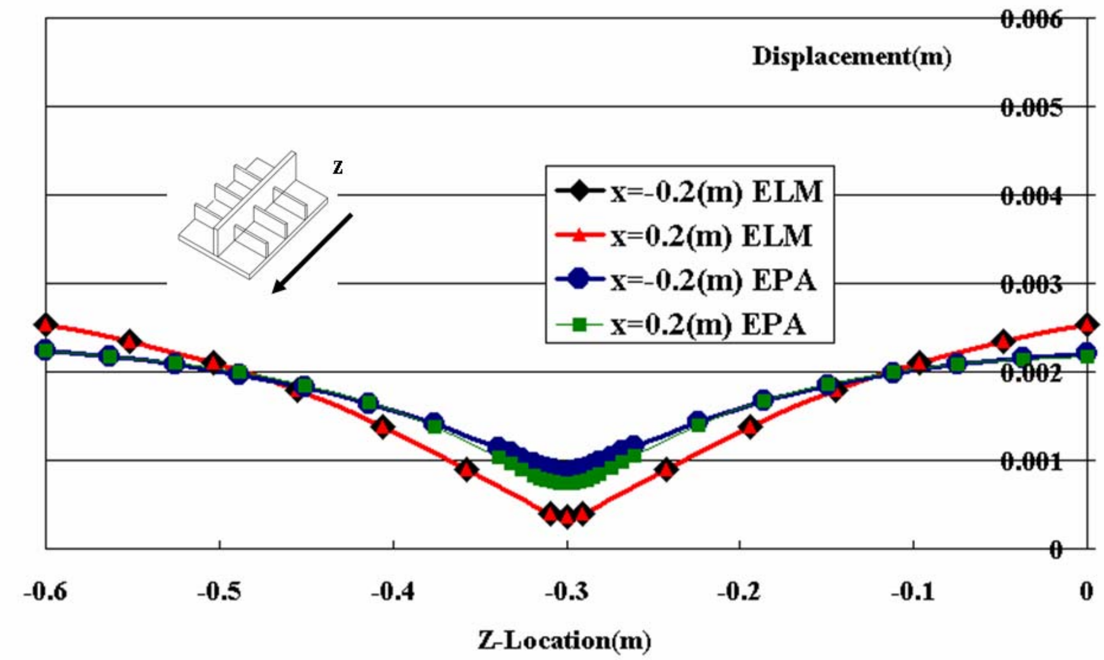

Fig. 67 Comparison of welding deformation of stiffened flat plates (Model 2)

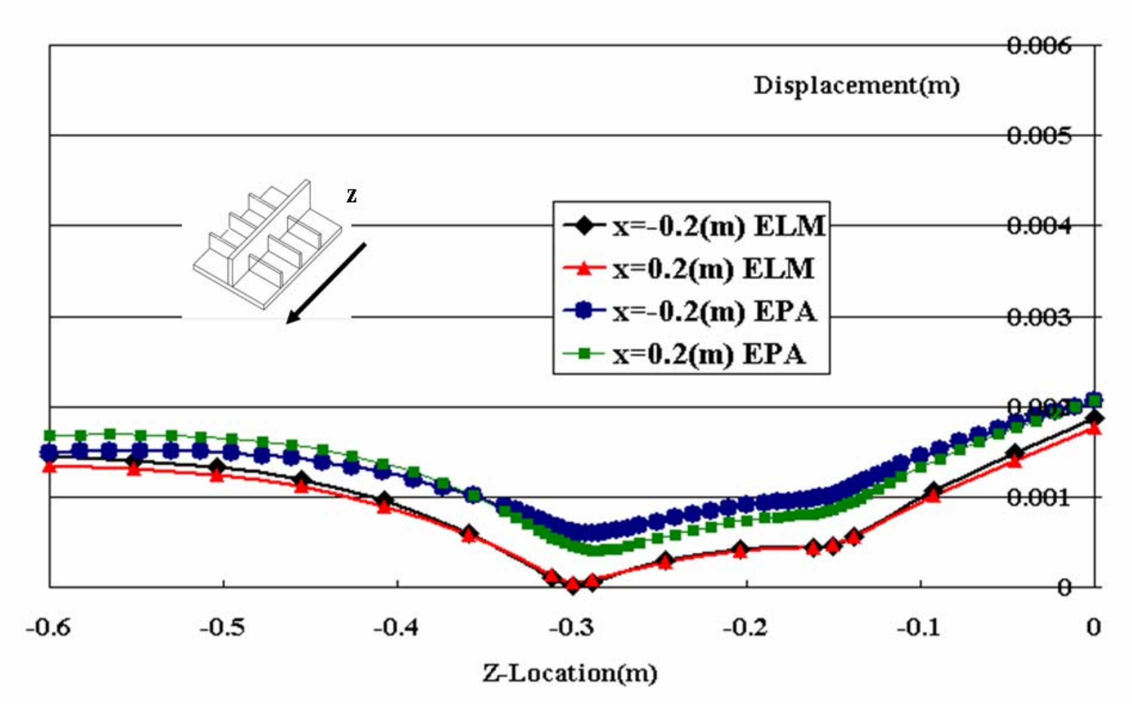

Fig. 68 Comparison of welding deformation of stiffened flat plates (Model 3)

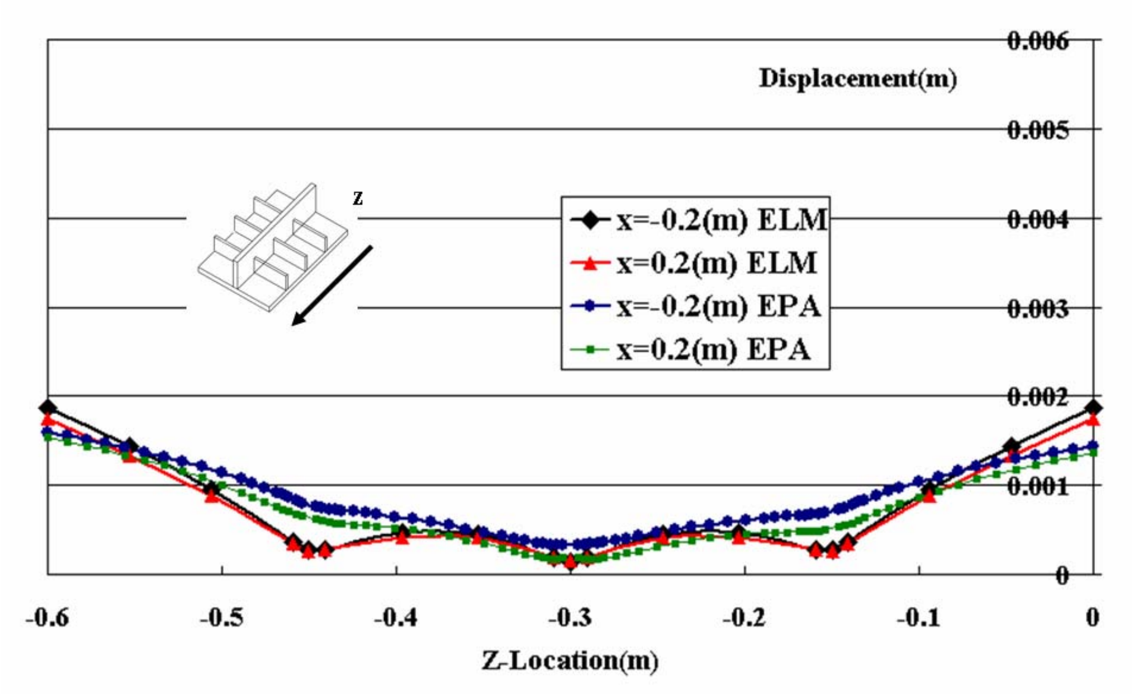

Fig. 69 Comparison of welding deformation of stiffened flat plates (Model 4)

As shown in Fig. 62 - 69, Y-direction displacements of stiffened flat plates by elasto-plastic analysis and equivalent load method are similar.

6. Welding distortion analysis of stiffened curved plates by equivalent load method

6.1. Analysis methods of stiffened curved plates by equivalent load method

6.1.1. Heat transfer analysis

The heat transfer analysis is performed to find the maximum temperature of each node. As explained in § 1, the highest temperature is an important factor with the degree of restraint for calculating the equivalent loads.

(a) Element type

2-D thermal solid element and 2-D thermal surface element are used for heat transfer analysis.

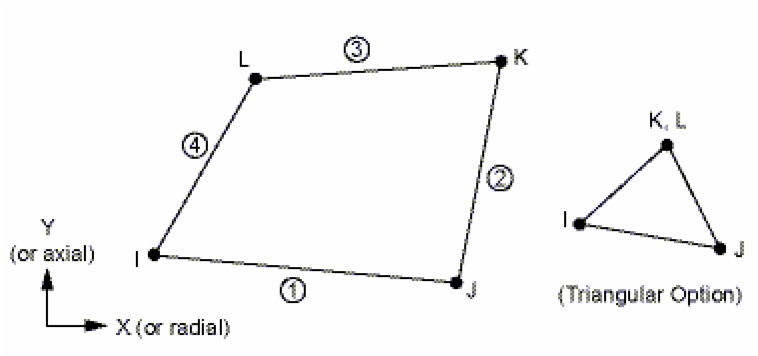

Fig. 70 2-D thermal solid element

The element has four nodes with a single degree of freedom, temperature, at each node. The element is applicable to a 2-D, steady-state or transient thermal analysis. The element can also compensate for mass transport heat flow from a constant velocity field. The geometry, node locations and the coordinate system for this element are shown in Fig. 70.

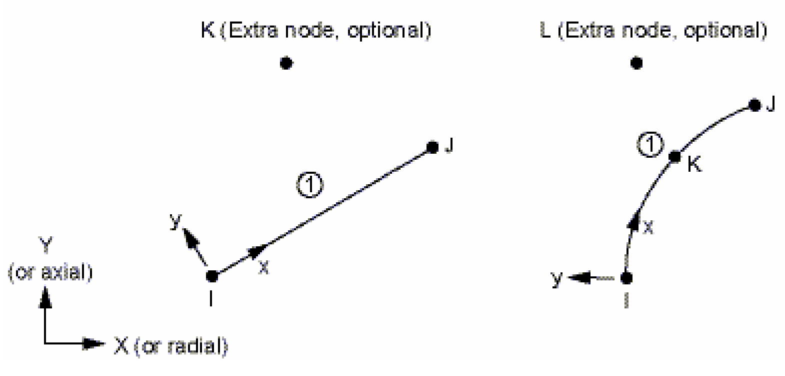

Fig. 71 2-D thermal surface element

The 2-D thermal surface element overlaid onto a face of any 2-D thermal solid element. The element is applicable to 2-D thermal analyses. The geometry, node location and the coordinate system for this element are shown in Fig. 71. The element is defined by two to four node points and the material properties. An extra node may be used for convection or radiation effects.

(b) 2-D heat transfer analysis

The heat transfer analysis is assumed that the temperature history of all section is same. So as shown in Fig. 72, the heat transfer analysis is performed by 2-D thermal analysis.

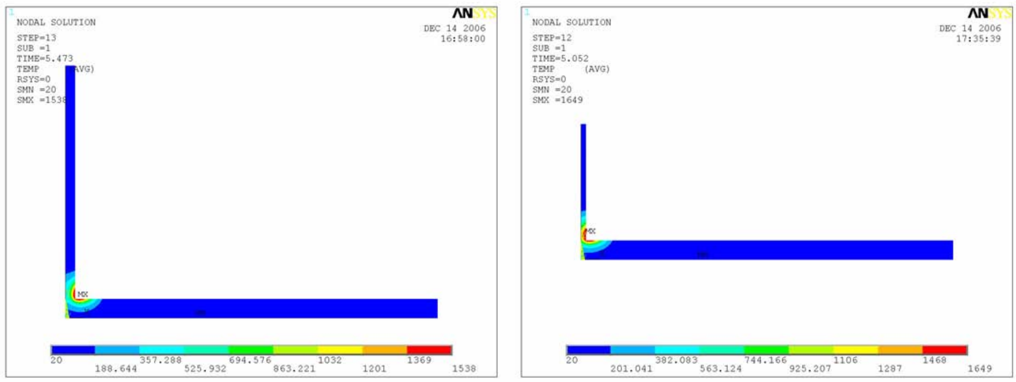

Longitudinal direction welding　　Transversal direction welding

Fig. 72 2-D thermal analysis

All of the welding process is analyzed through 20 steps and the cooling process is analyzed during 4 steps. Because the object of the heat transfer analysis is to find the highest temperature of each node, the cooling process has a few steps unlike the thermal elasto-plastic analysis. After the thermal analysis, all of the highest temperature at each node is saved to calculate the nodal loads.

6.1.2. Calculation of degree of restraint

In order to calculate the degree of restraint, it is necessary to know the rigidity of welding area and surround area. The unit load method is used to calculate the rigidity. The deformation from the elastic analysis of stiffened plate under the unit load along weld line is used to calculate the rigidity.

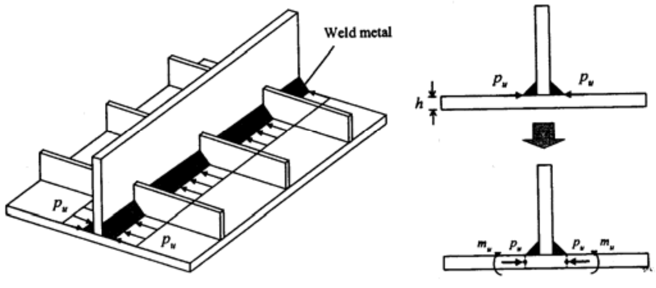

Fig. 73 Application of unit load along weld line

The distributed load p_u shown in Fig. 49 is applied at the end of leg length of the weld on the plate surface. So the distributed load p_u and bending moment m_u is applied in the middle plane of the plate.

$$m_u = \frac{h}{2} \times p_u$$

$$\delta_S = \delta + \frac{h}{2} \cdot \theta$$

$$R_S = \frac{p_u}{\delta_s} = \frac{p_u}{\delta + \frac{h}{2} \cdot \theta} = k_S + K_B$$

where m_u : *moment distributed along weld line*

p_u : *force distributed along weld line*

δ_S : *surface shrinkage*

θ : *rotation angle*

R_S : *stiffness of structure*

k_S : *stiffness of spring*

K_B : *stiffness of bar*

The elastic analysis of stiffened curved plate under unit load is as follow:

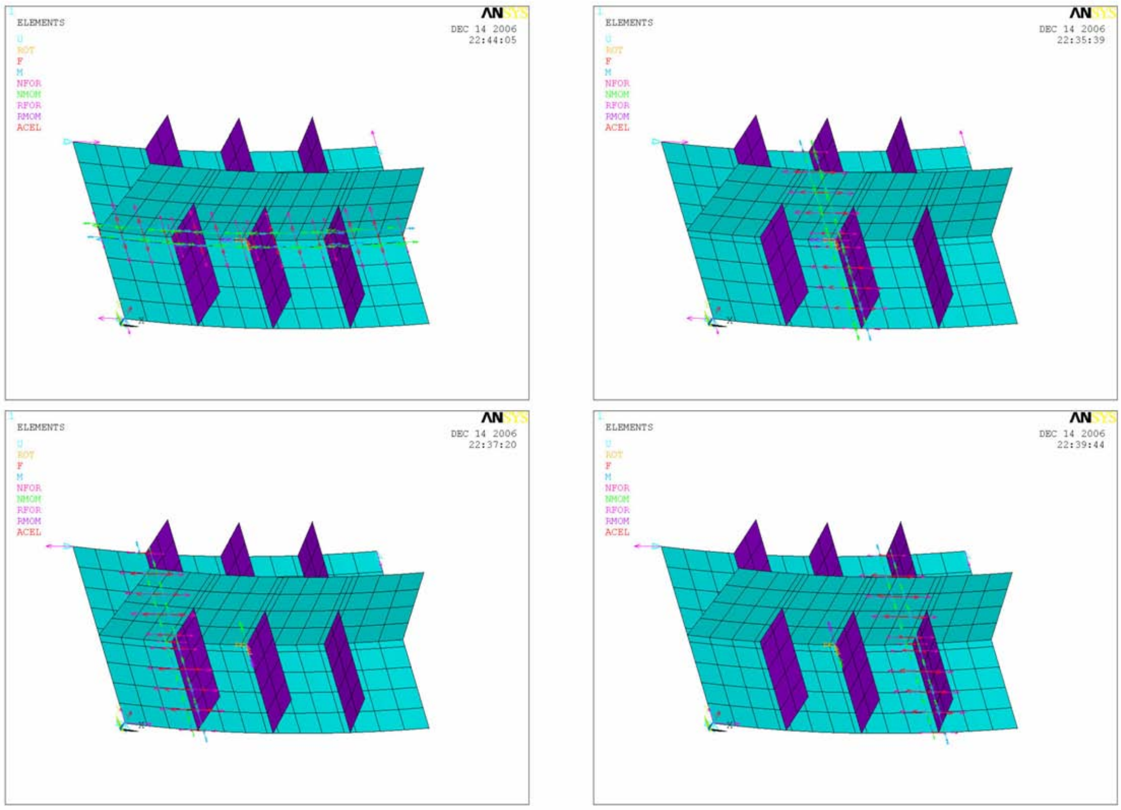

Fig. 74 Elastic analysis of stiffened curved plate under unit load

6.1.3. Calculation of equivalent loads

(a) Element type

Elastic shell element is used for equivalent load analysis.

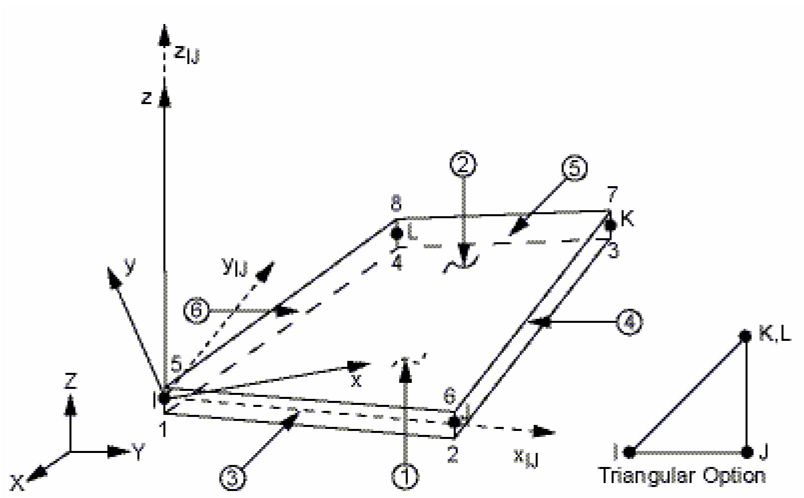

Fig. 75 Elastic shell element

The adopted elastic shell element has both bending and membrane capabilities. Both in-plane and normal loads are permitted. The element has six degrees of freedom at each node. Stress stiffening and large deflection capabilities are included. The geometry, node location, and the coordinate system for this element are shown in Fig. 75. The element is defined by four nodes, four thicknesses, elastic foundation stiffness, and the orthotropic material properties. Orthotropic material directions correspond to the element coordinate directions.

(b) Elastic analysis by equivalent load method

By the highest temperature and degree of restraint, the inherent strain can be obtained from the inherent strain chart. The shrinkage forces and moments can be calculated as explained in §1.2(Calculation of equivalent loads).

The shrinkage forces of stiffened flat plate and of stiffened curved plate should be applied in different way. As shown in Fig. 76, the shrinkage force of the flat plate is applied at the both ends of the plate. But in the curved plate case, the shrinkage force should be applied to each node along the weld line in the tangential direction.

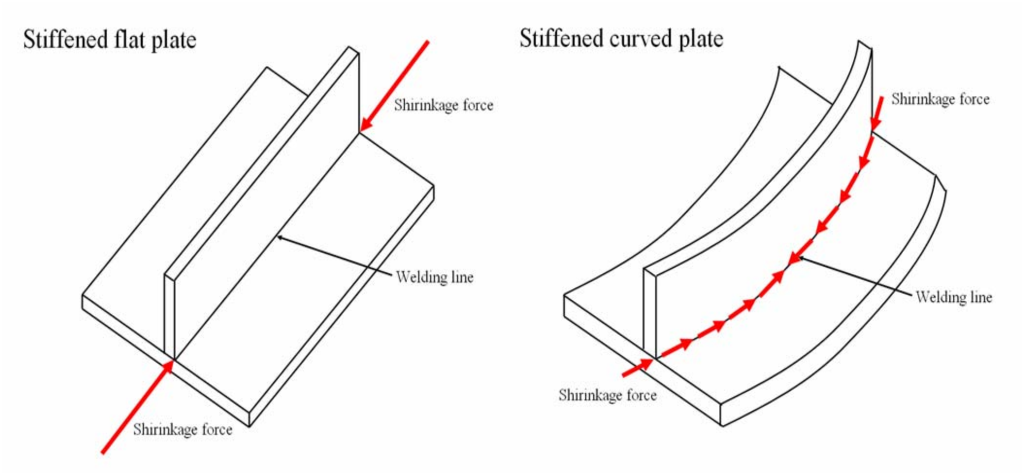

Fig. 76 Application of shrinkage forces

The applications of equivalent load to four cases of stiffened curved plate model are shown in Fig. 77.

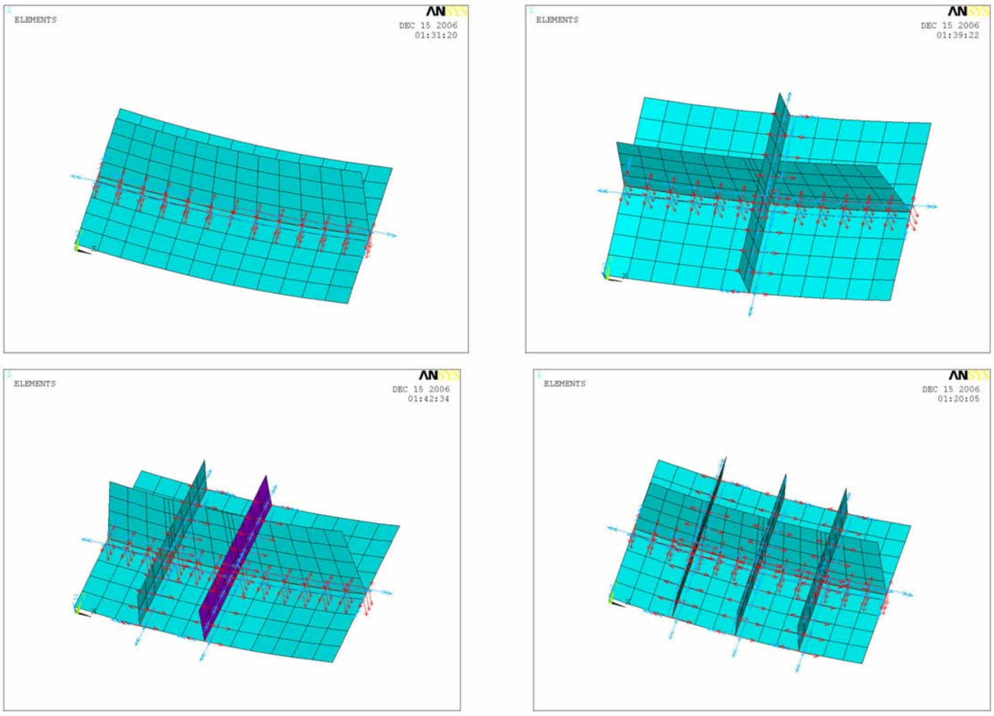

Fig. 77 Application of equivalent loads

6.2. Prediction of welding distortion of stiffened curved plates by equivalent load method

Fig.78 shows the adopted coordinates system for the stiffend curved plate.

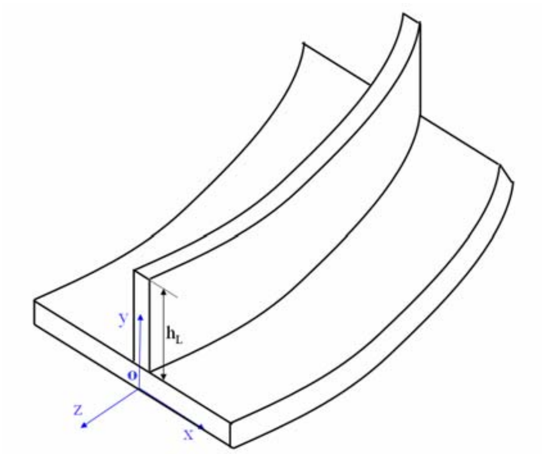

Fig. 78 Coordinate of stiffened curved plate

By the equivalent loads method, welding deformation analysis is performed for 4 cases of the stiffened curved plate. Analysis results are shown in Fig. 79 - 87.

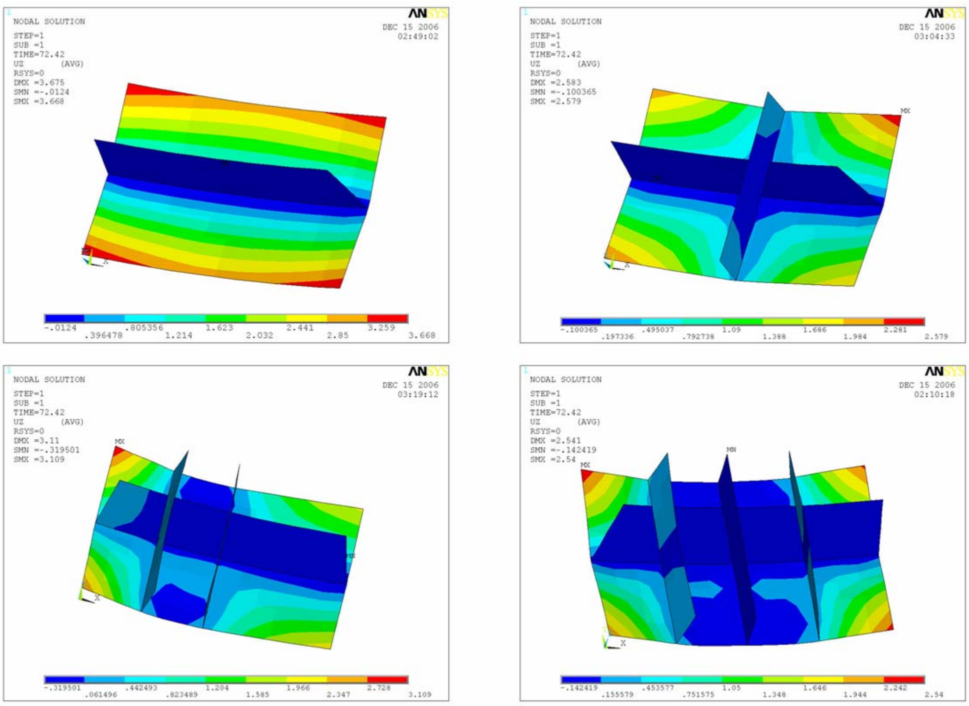

Fig. 79 Welding deformation of stiffened curved plates by equivalent load method

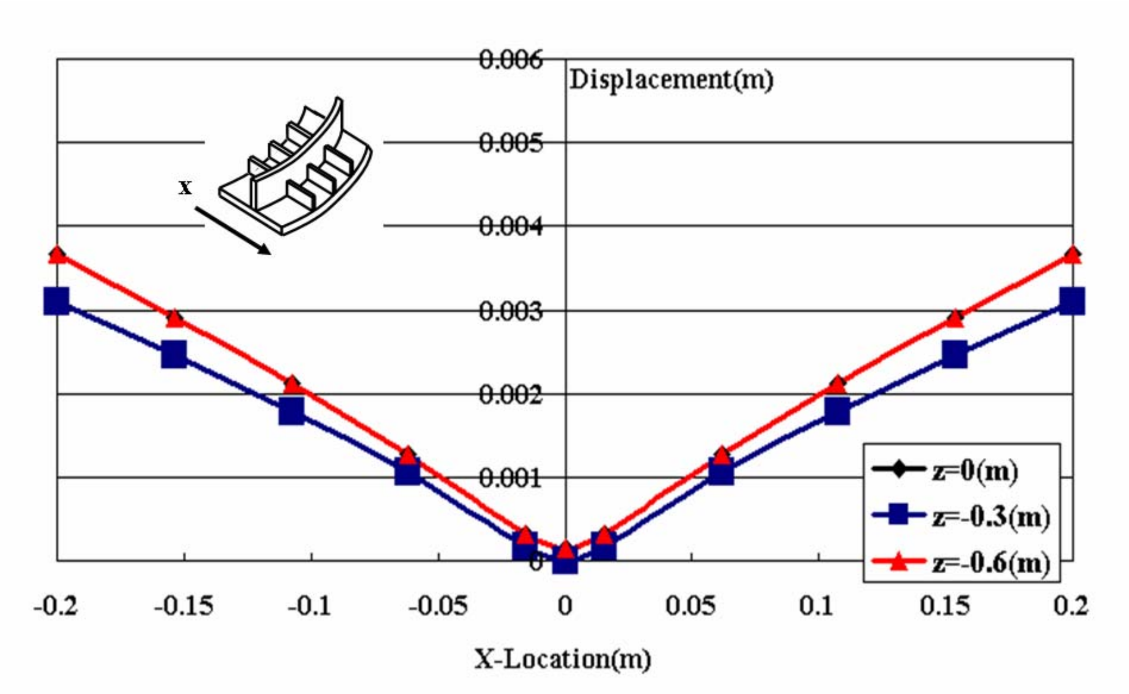

Fig. 80 Welding deformation of stiffened curved plates by equivalent load method (Model 1)

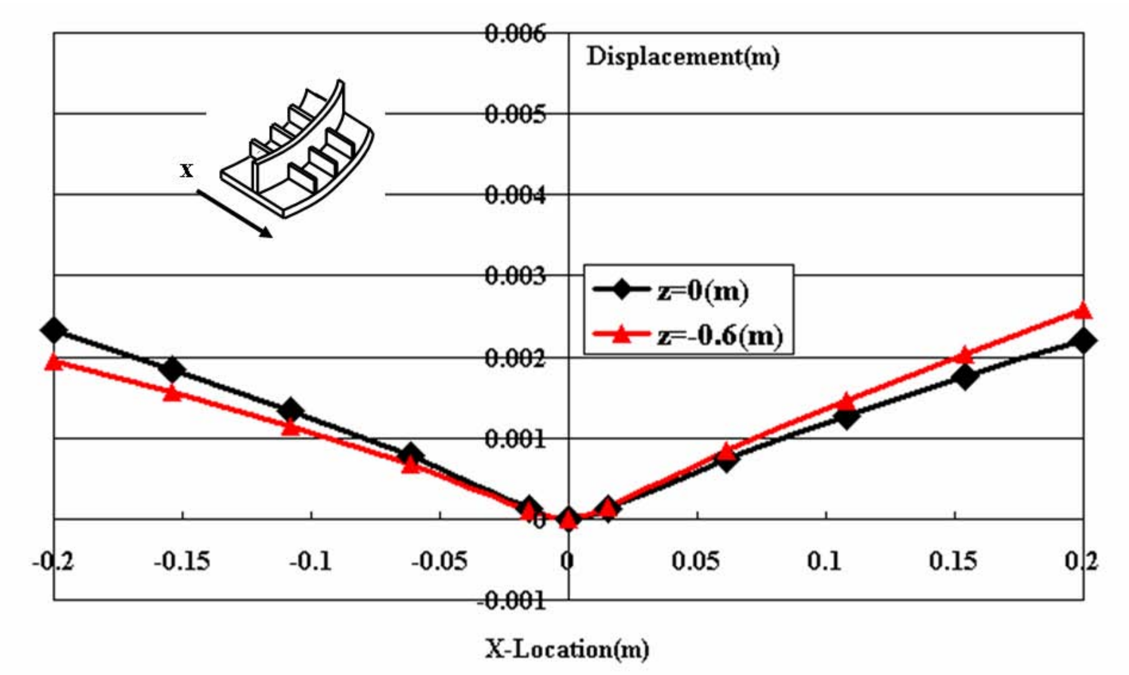

Fig. 81 Welding deformation of stiffened curved plates by equivalent load method (Model 2)

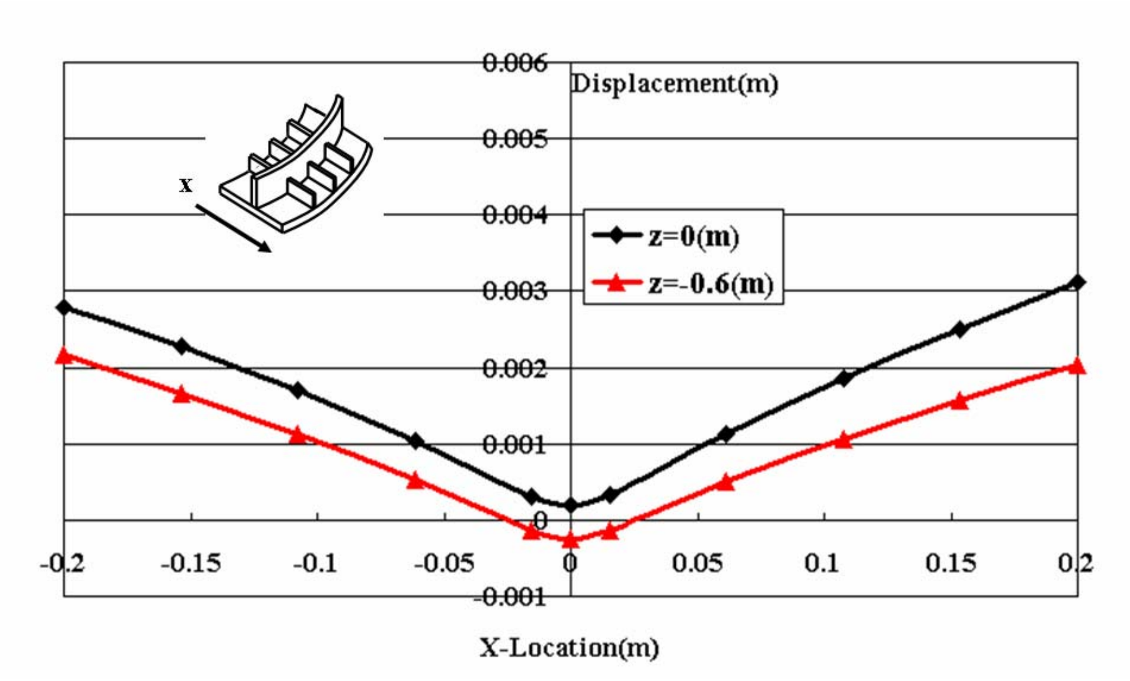

Fig. 82 Welding deformation of stiffened curved plates by equivalent load method (Model 3)

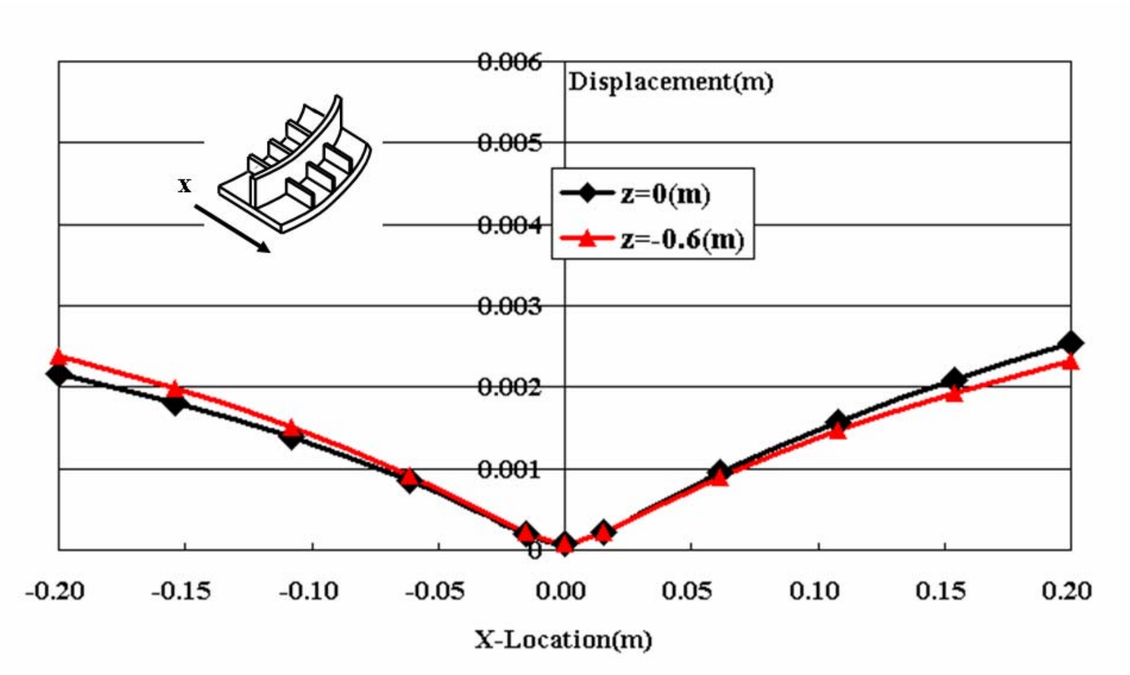

Fig. 83 Welding deformation of stiffened curved plates by equivalent load method (Model 4)

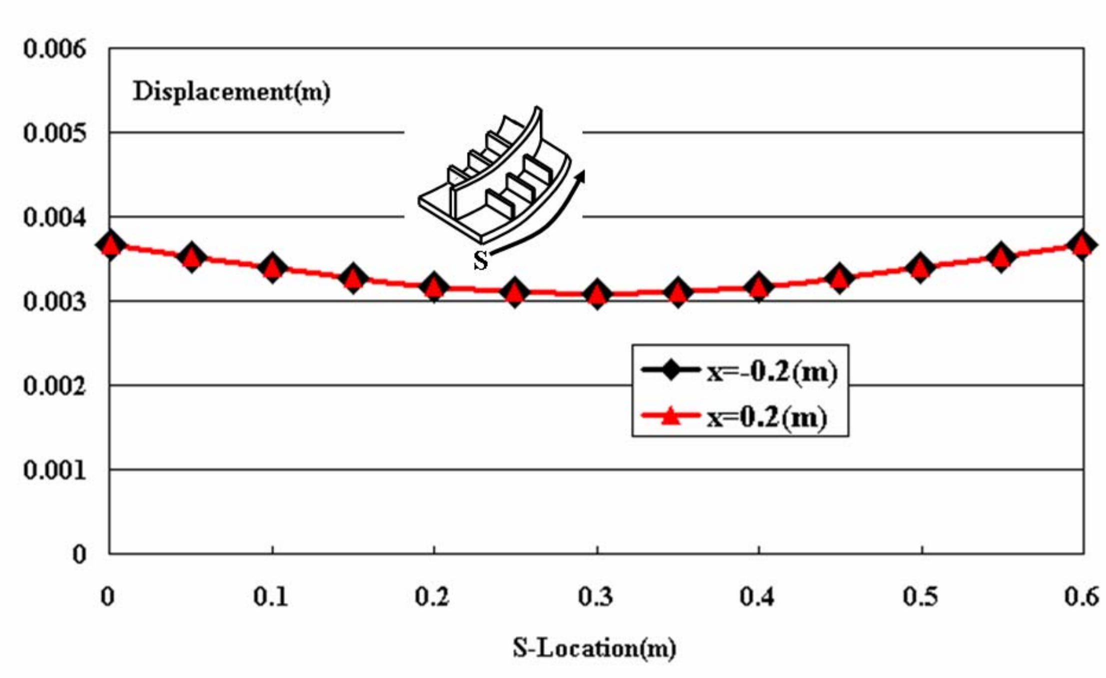

Fig. 84 Welding deformation of stiffened curved plates by equivalent load method (Model 1)

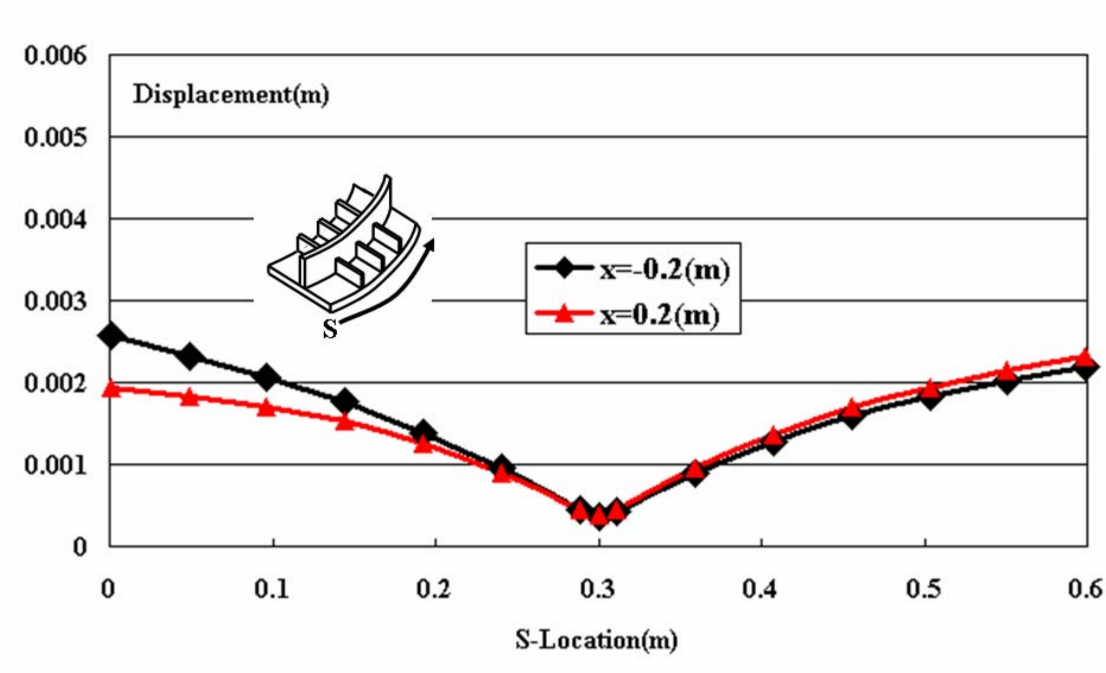

Fig. 85 Welding deformation of stiffened curved plates by equivalent load method (Model 2)

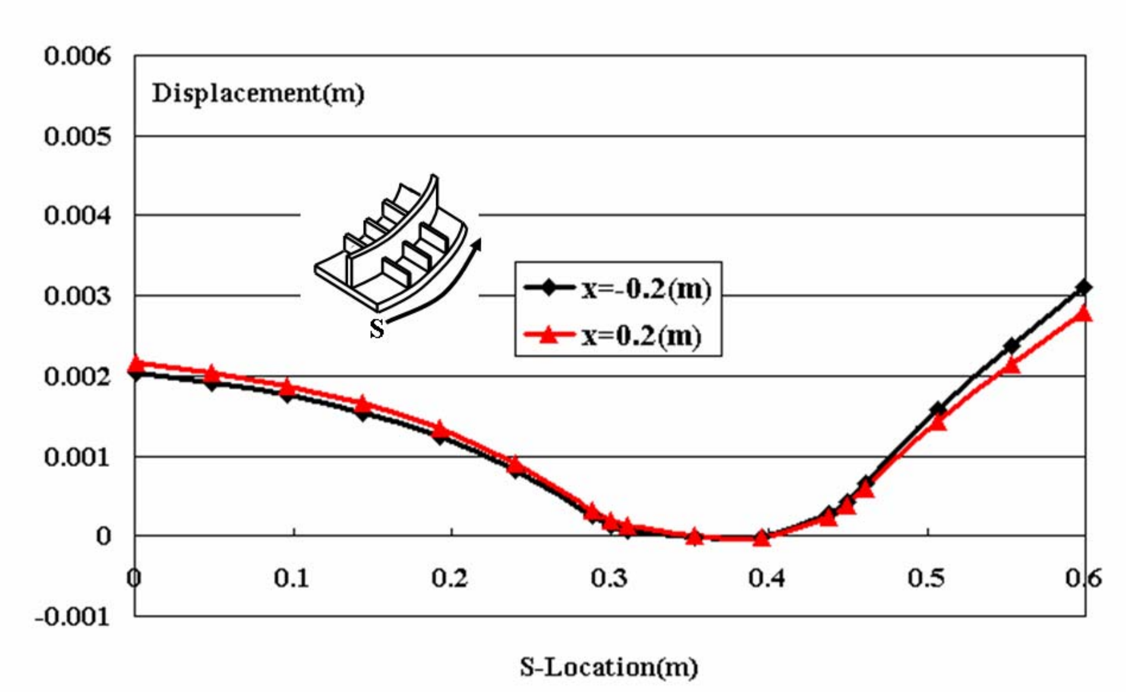

Fig. 86 Welding deformation of stiffened curved plates by equivalent load method (Model 3)

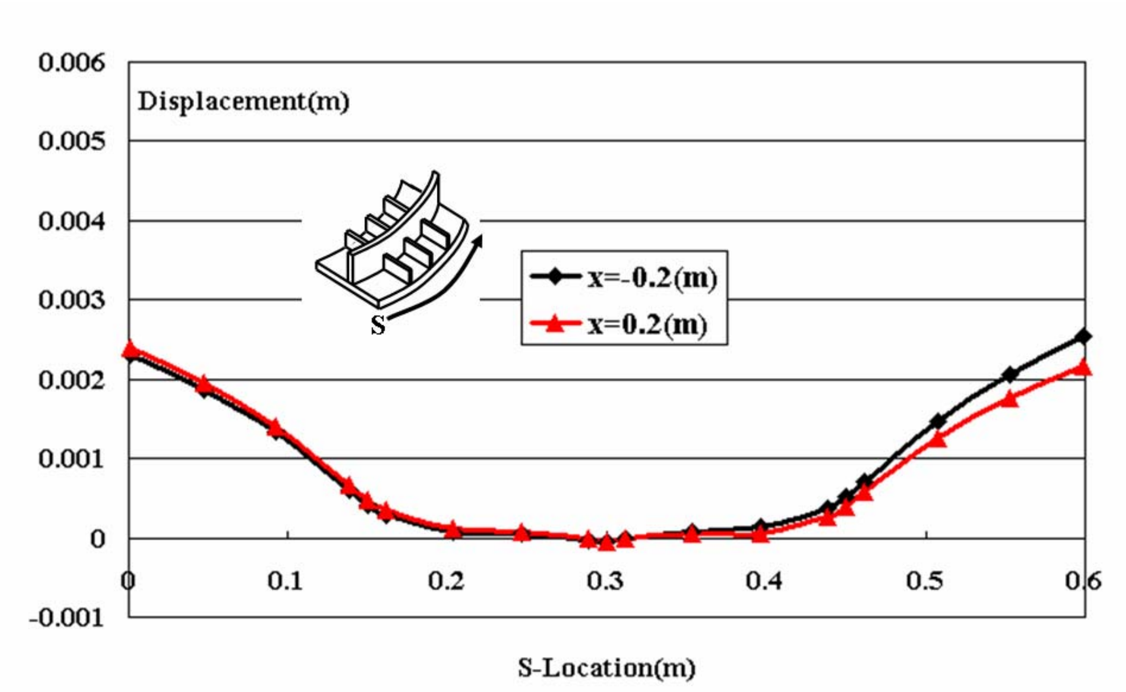

Fig. 87 Welding deformation of stiffened curved plates by equivalent load method (Model 4)

7. Comparison of thermal elasto-plastic analysis and equivalent load method of stiffened curved plates

The welding deformation (at x=0.2m) calculated by two different methods (EPA: thermal Ealsto-Plastic Analysis, ELM: Equivalent Load Method) are compared in Table2.

Both results show fairly good agreements with each other within 20% of average difference.

Table. 2 Welding distortion of stiffened curved plate(at x=0.2m)

	Stiffened Curved Plate Case 1		Stiffened Curved Plate Case 2		Stiffened Curved Plate Case 3		Stiffened Curved Plate Case 4		
z-location(m)	z=0	z=-0.6	z=0	z=-0.6	z=0	z=-0.6	z=0	z=-0.6	
Displacement(m) by EPA	0.0030	0.0030	0.0021	0.0025	0.0025	0.0016	0.0018	0.0020	
Displacement(m) by ELM	0.0037	0.0037	0.0022	0.0026	0.0031	0.0020	0.0025	0.0023	**Average Ratio**
Ratio	1.2329	1.2272	1.0465	1.0221	1.2244	1.2661	1.4338	1.1445	1.2080

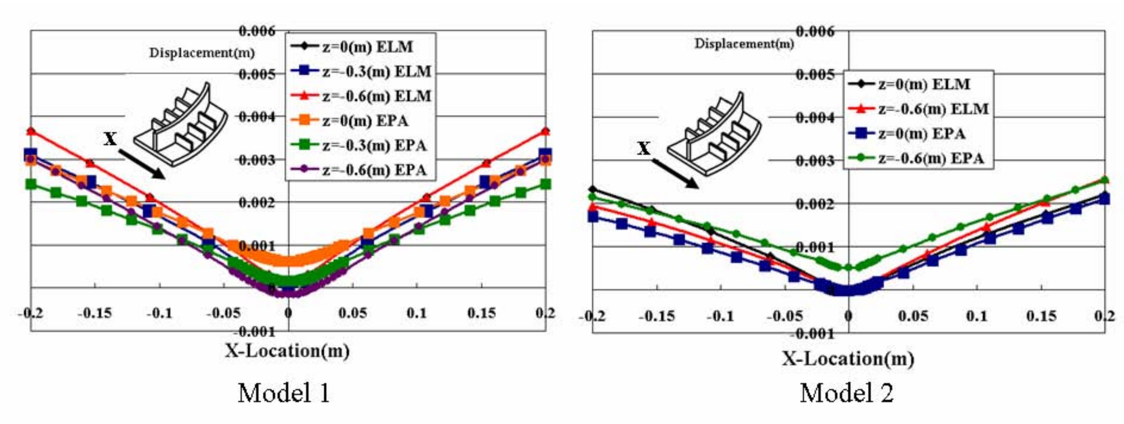

Fig. 88 Comparison of welding deformation of stiffened curved plates (model 1 & 2)

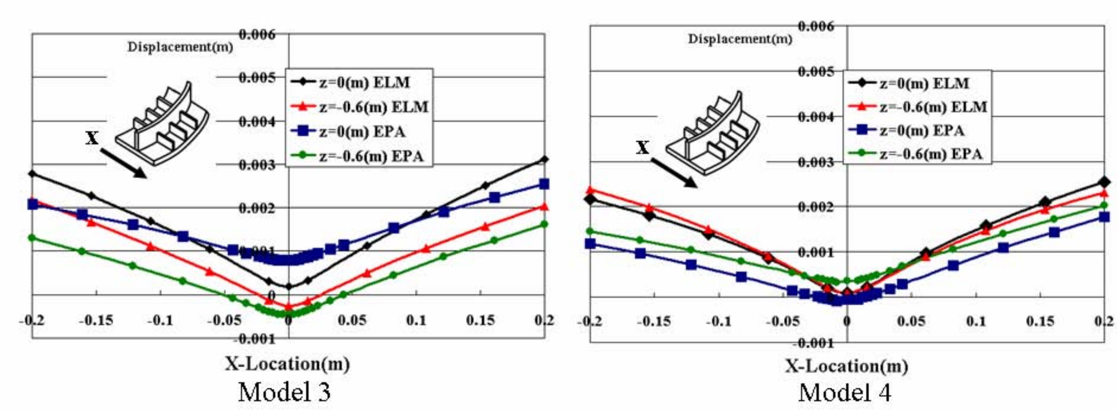

Fig. 89 Comparison of welding deformation of stiffened curved plates (Model 3 & 4)

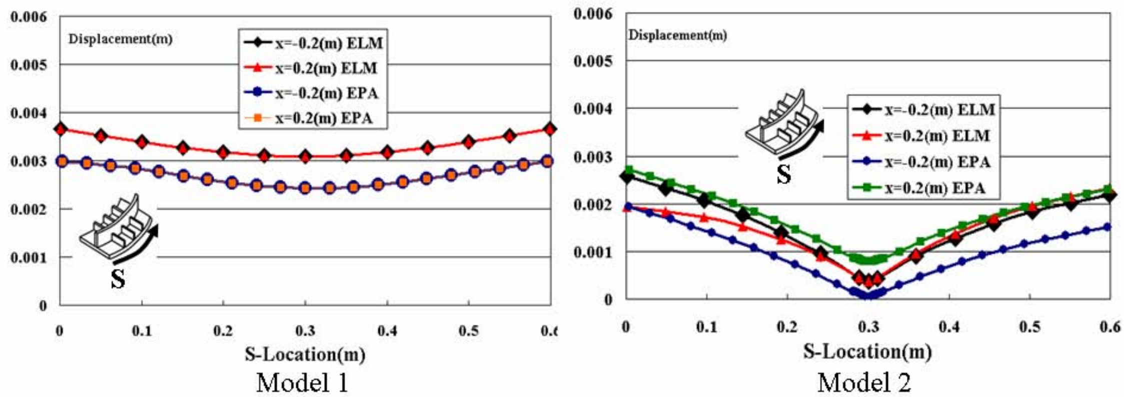

Fig. 90 Comparison of welding deformation of stiffened curved plates (Model 1 & 2)

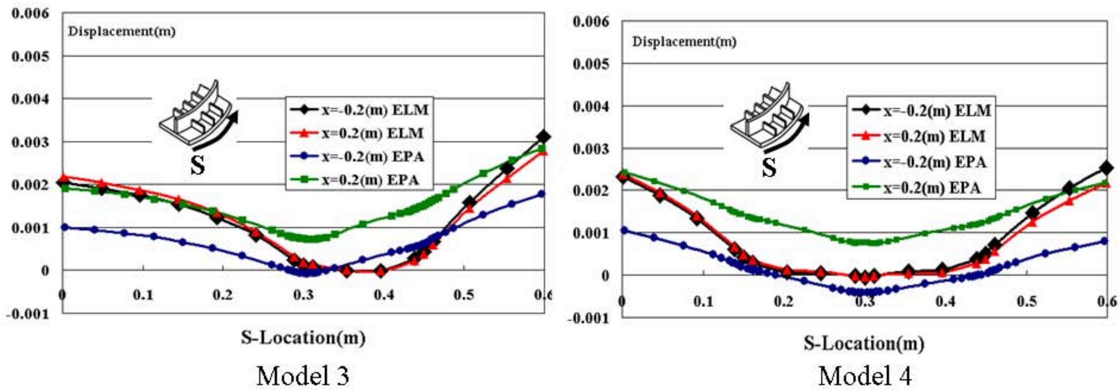

Fig. 91 Comparison of welding deformation of stiffened curved plates (Model 3 &4)

As shown in Fig. 88-91, Y-direction displacements of stiffened curved plates by thermal elasto-plastic analysis and equivalent load method are similar. The welding deformation by the equivalent load method is generally bigger than the welding deformation by the thermal elasto-plastic analysis. The reason of this tendency is due to the precision to evaluate the degree of restraint of base welding structure. Based on the welding experiment of stiffened curved plates, more precise degree of restraint of base welding structure can be evaluated. So, the welding deformation of stiffened curved plate by the equivalent loads method could give better agreement with the numerical and experimental results of welding deformation.

8. Plan of experiments

8.1. Welding deformation experiment

The welding deformation experiment was performed for four kinds of stiffened curved plates. As shown in Fig. 92, the experimental models have three kinds of curvatures ($\rho = 1000$mm, 2000mm, and 5000mm). The curvatures were selected by investigating actual fabrication data in the shipyards.

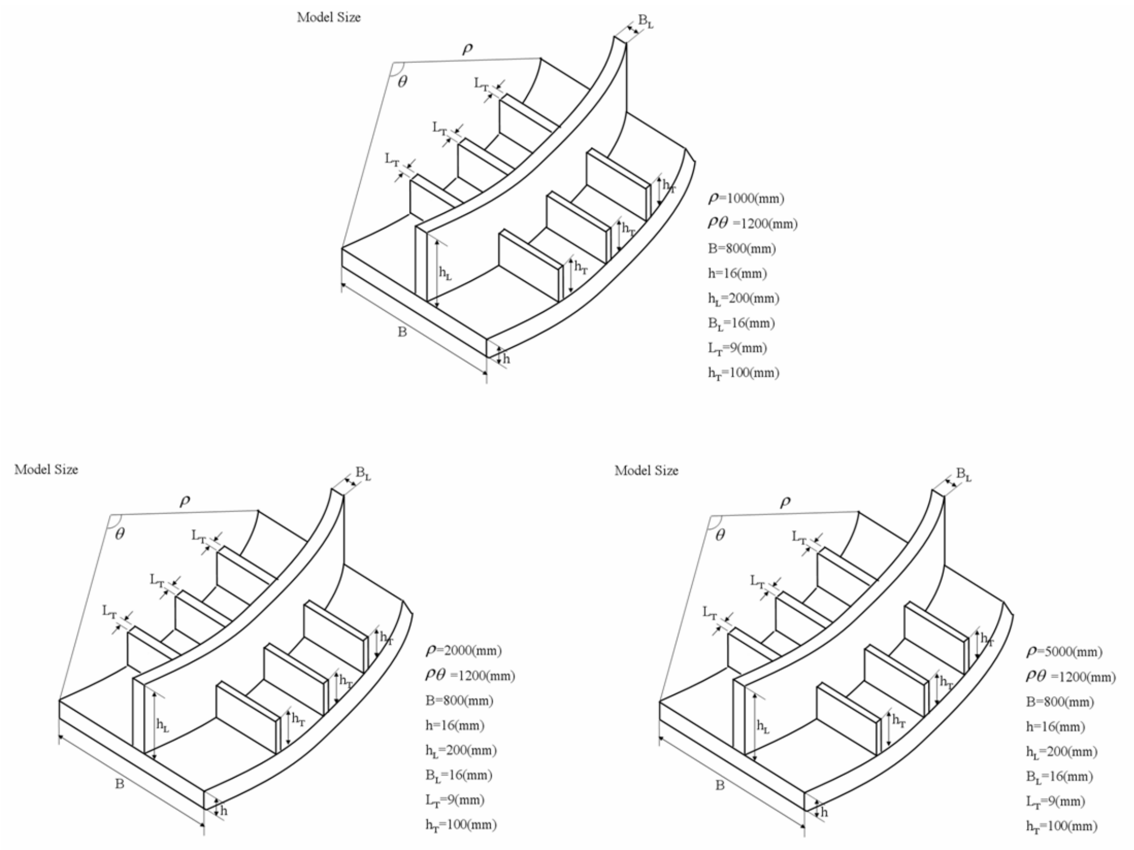

Fig. 92 Size of the experimental models for welding distortion

In order to study the effect of welding sequence on the welding distortion, the experimental model has two kinds of welding sequences shown in Fig. 93. Case 1 is that the longitudinal stiffener is welded after all the transverse stiffeners are welded in order. Case 2 is that the longitudinal stiffener is welded at first and then the transverse stiffeners are welded in order. It is generally known by the welding experts that the welding deformation of case 2 is smaller than that of case 1.

This fact will be examined and verified by numerical calculation and experiment later in Fig.100 - 107. In many shipyards, however, welding sequence of case 1 has been generally used because of the productivity. But, in case of some particular ships, if the welding deformation is more critical than the productivity, the case 2 will be more recommendable.

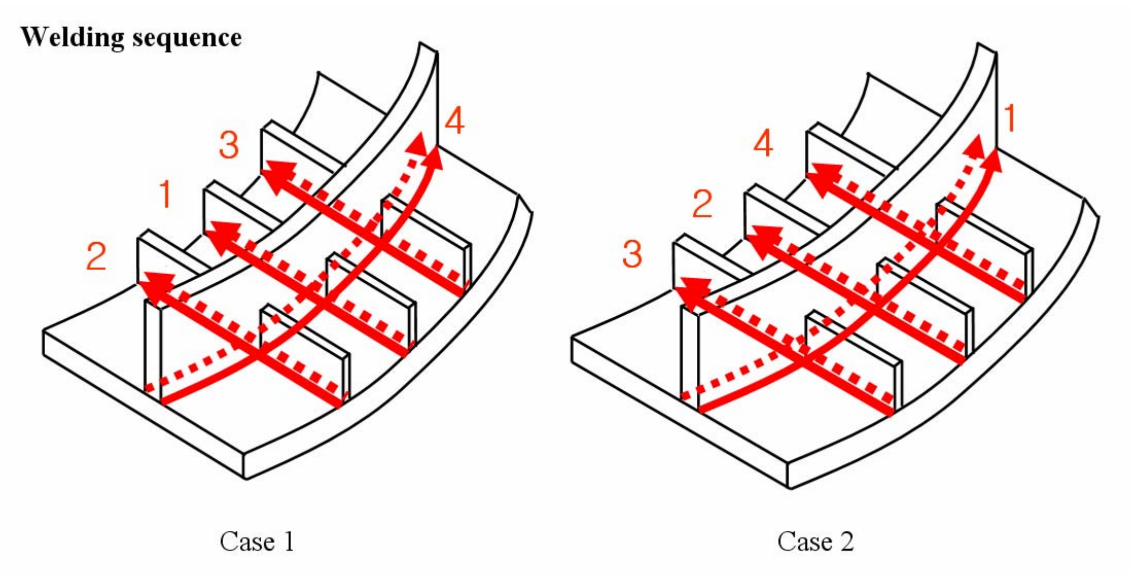

Fig. 93 Two different welding sequences of experimental model

The experimental models were selected by investigating the actual fabrication data in the shipyard. The 1st and 4th experimental model with $\rho = 1000$(mm) and $\rho = 5000$(mm) adopted the welding sequence of case 1, and the 2nd and 3rd experimental model with $\rho = 2000$(mm) adopted each welding sequence of case 1 and 2.

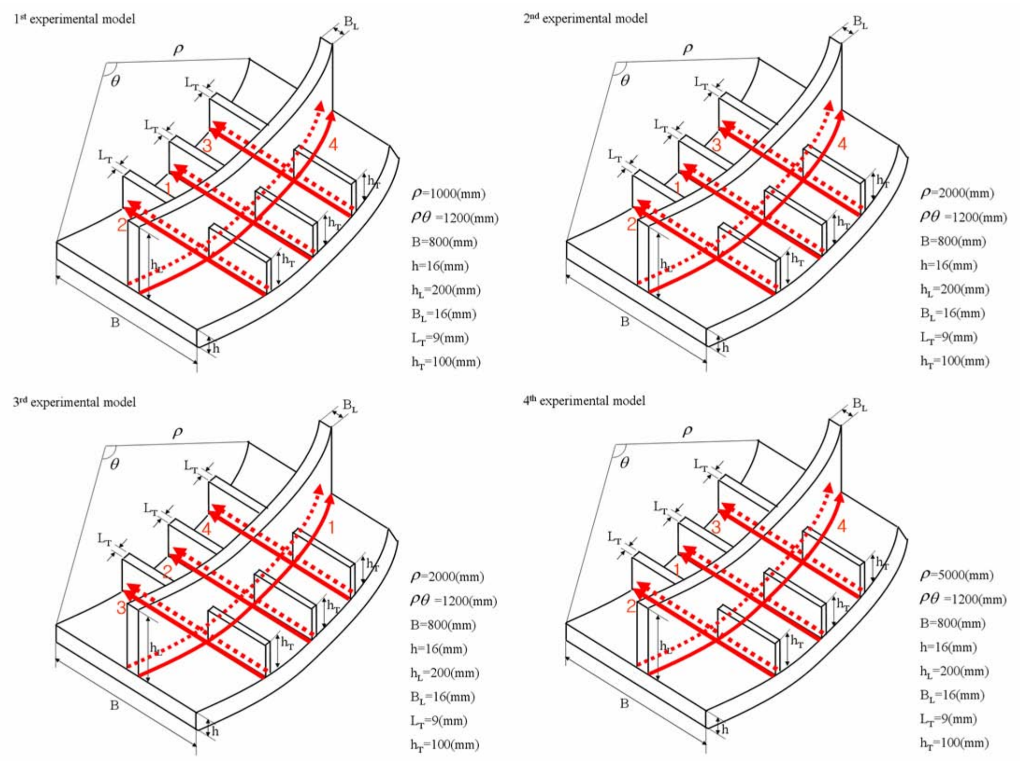

Fig. 94 Four experimental models with welding sequence

Fig. 95 Photographs of experimental steels

8.2. Tensile test

The experimental model has been constructed using two kinds of steel plates. The one has a thickness of 16(mm), while the other has a thickness of 9 (mm). The tensile tests for two kinds of steel plates were performed. Each steel plate is tested three times and the average yield strength and ultimate strength is used for the numerical calculation.

9. Results of experiments

9.1. Tensile test

Fig. 96 Specimens of tensile test

As shown in Fig. 96, two kinds of specimen (thickness=16mm, 9mm) was used for tensile test. In case of thickness=16(mm), the specimen was fabricated in round bar shape. In case of thickness=9(mm), the specimen was fabricated in plate shape because of the thin thickness.

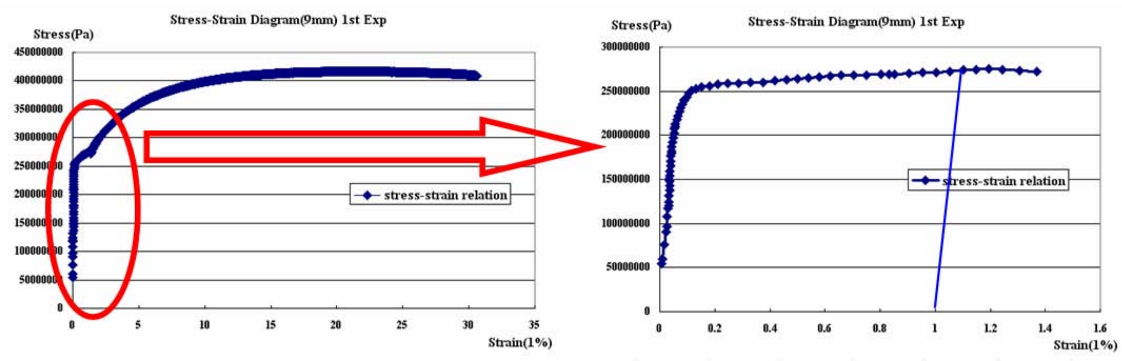

Fig. 97 Tensile test of 9(mm) plate

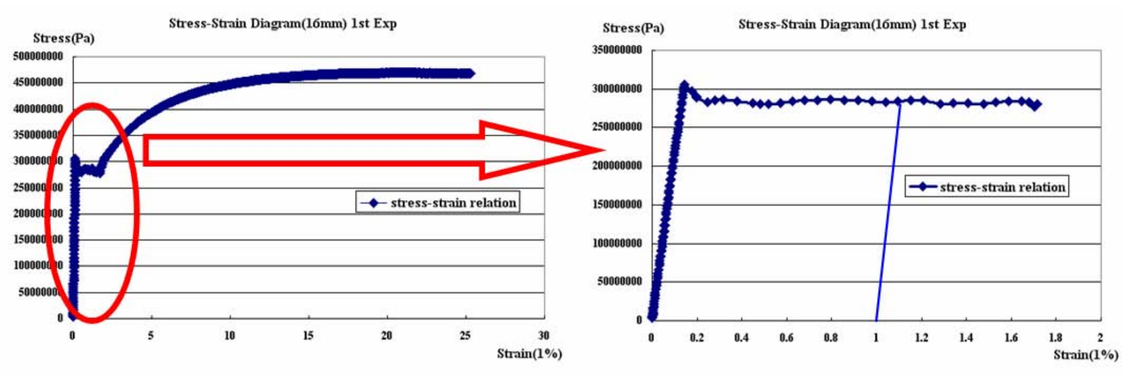

Fig. 98 Tensile test of 16(mm) plate

Table. 3 Tensile test result (yield stress)

	1st (MPa)	2nd (MPa)	3rd (MPa)	Average (MPa)
Thickness 16(mm)	283.6	288.4	289.4	287.1
Thickness 9(mm)	275.4	275.8	279.3	276.8

Fig.97 - 98 show the stress-strain curves of tensile tests of the specimen. In general, 0.2% offset yield stress has been customary used to determine the yield stress for some other material except mild steel which has no definite yield stress. However, 1% offset yield stress is adopted here since sufficient plastic flow at 0.2% offset could not be expected for 9mm specimen shown in Fig.101. But the difference is very small.

Table 3 shows the yield stresses of two kinds of specimen. The average yield stress is used for analysis to estimate the welding deformation.

9.2. Welding deformation experiment

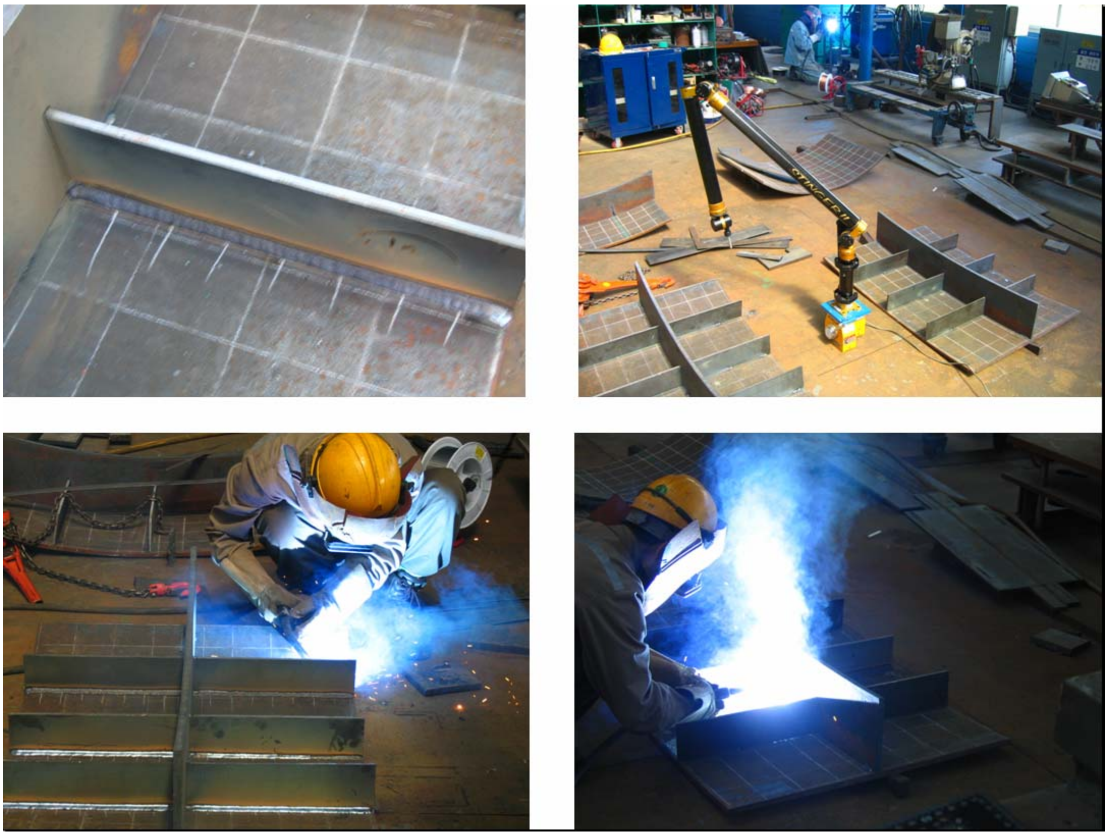

Fig. 99 Pictures of welding experiment

Welding expert with more than 20 year's experience performed the experiment. The welding speed was checked every 5 seconds that the welding velocity could be kept nearly constant with

5(mm/sec). The welding deformation is measured by 3-D digitizer which can measure 3-D position shown in Fig. 99.

9.3. Comparison of welding deformation between experiment and analysis

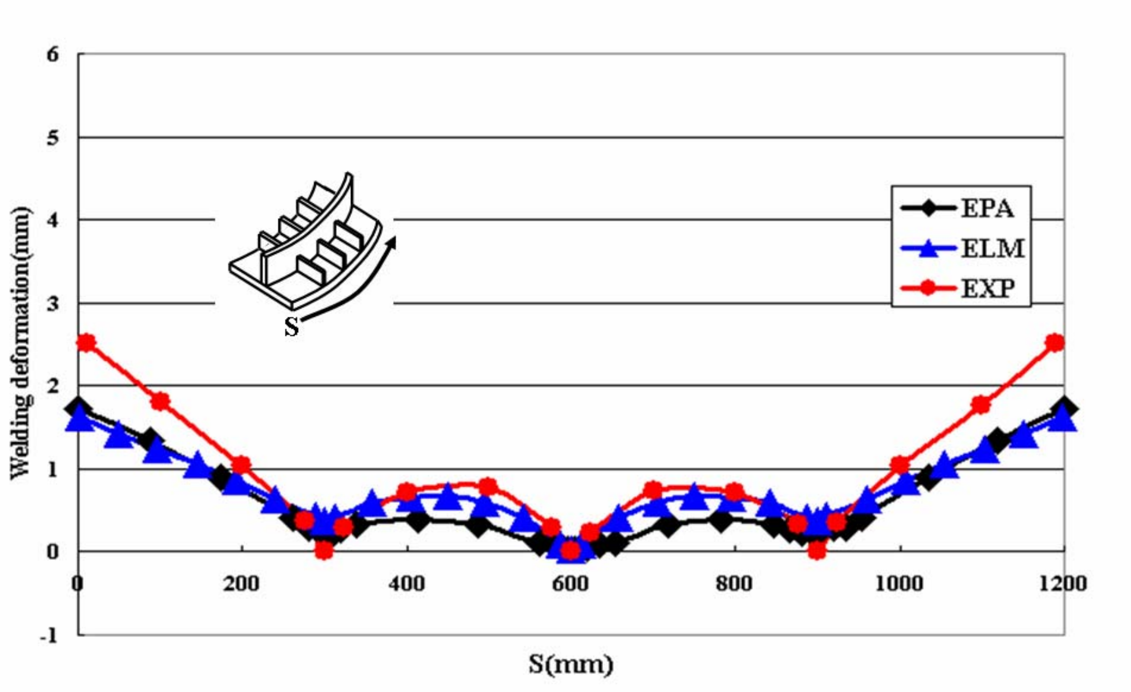

Fig. 100 Comparison of welding deformation with R=1000(mm)

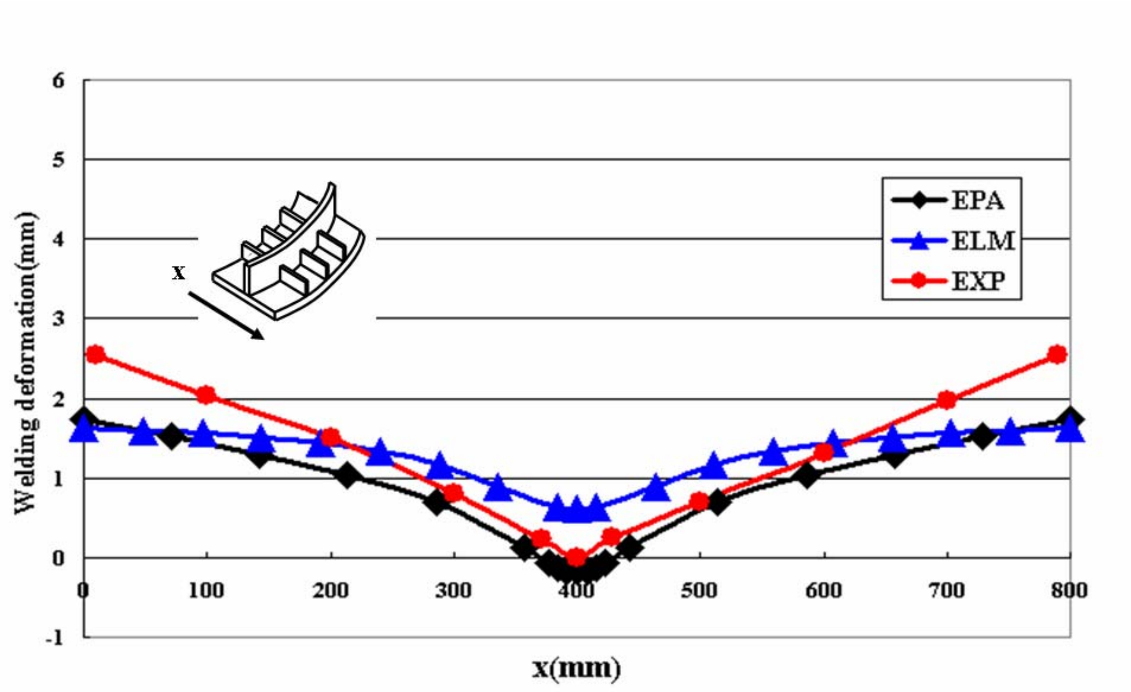

Fig. 101 Comparison of welding deformation with R=1000(mm)

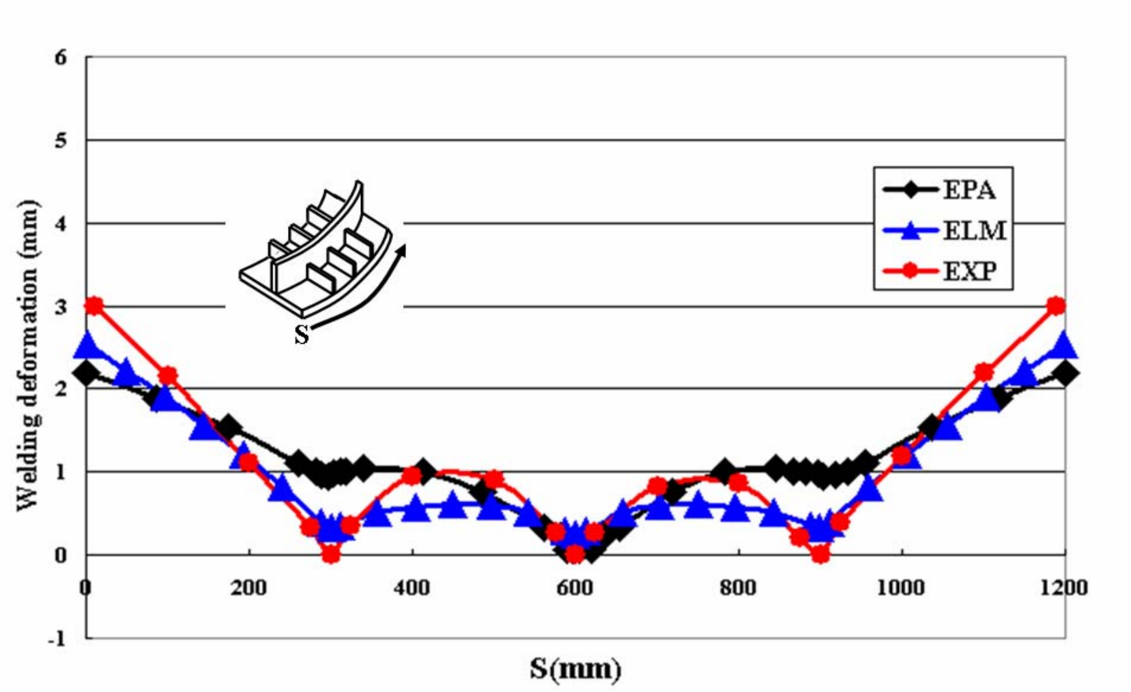

Fig. 102 Comparison of welding deformation with R=2000(mm), case 1

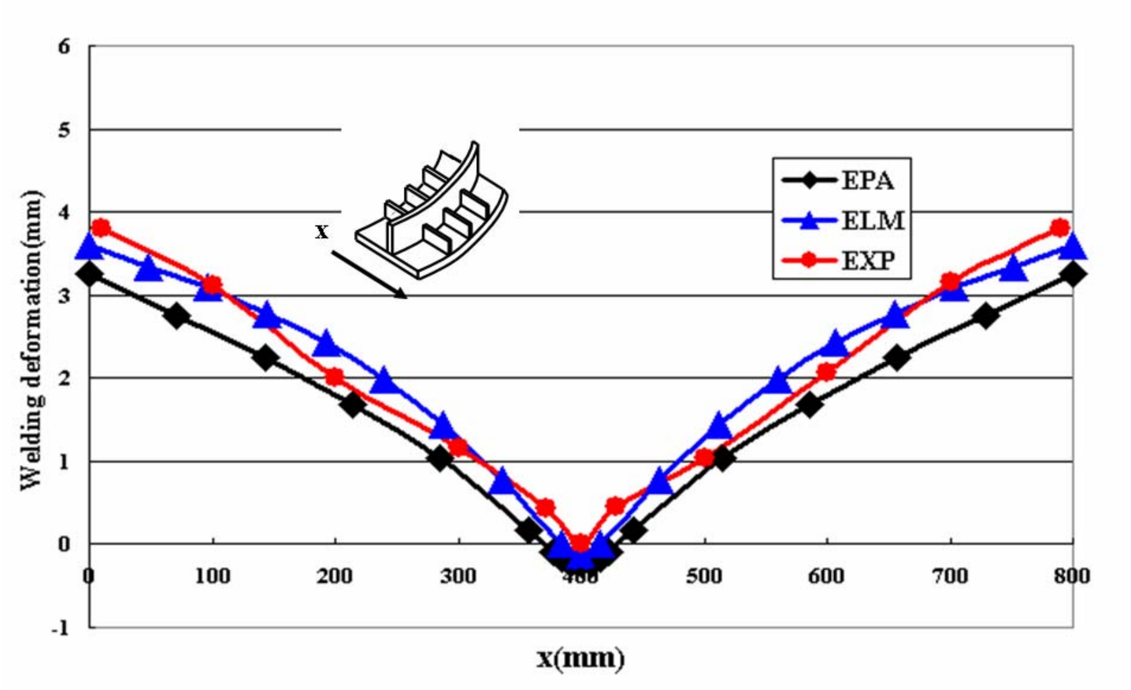

Fig. 103 Comparison of welding deformation with R=2000(mm), case 1

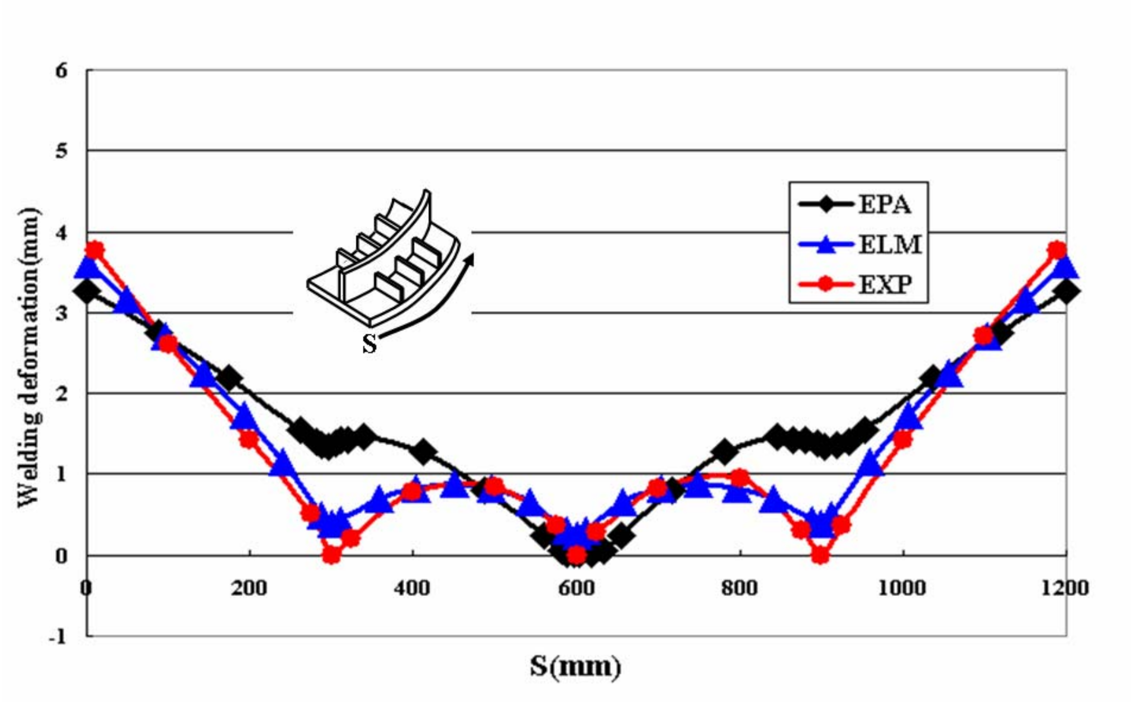

Fig. 104 Comparison of welding deformation with R=2000(mm), case 2

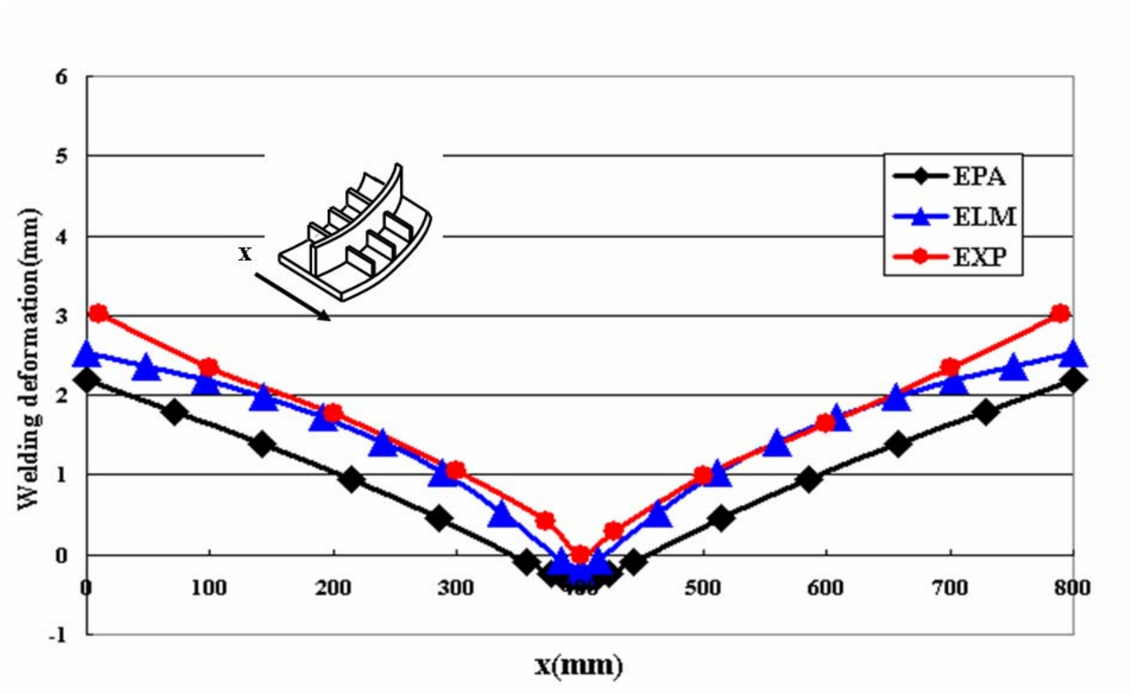

Fig. 105 Comparison of welding deformation with R=2000(mm), case 2

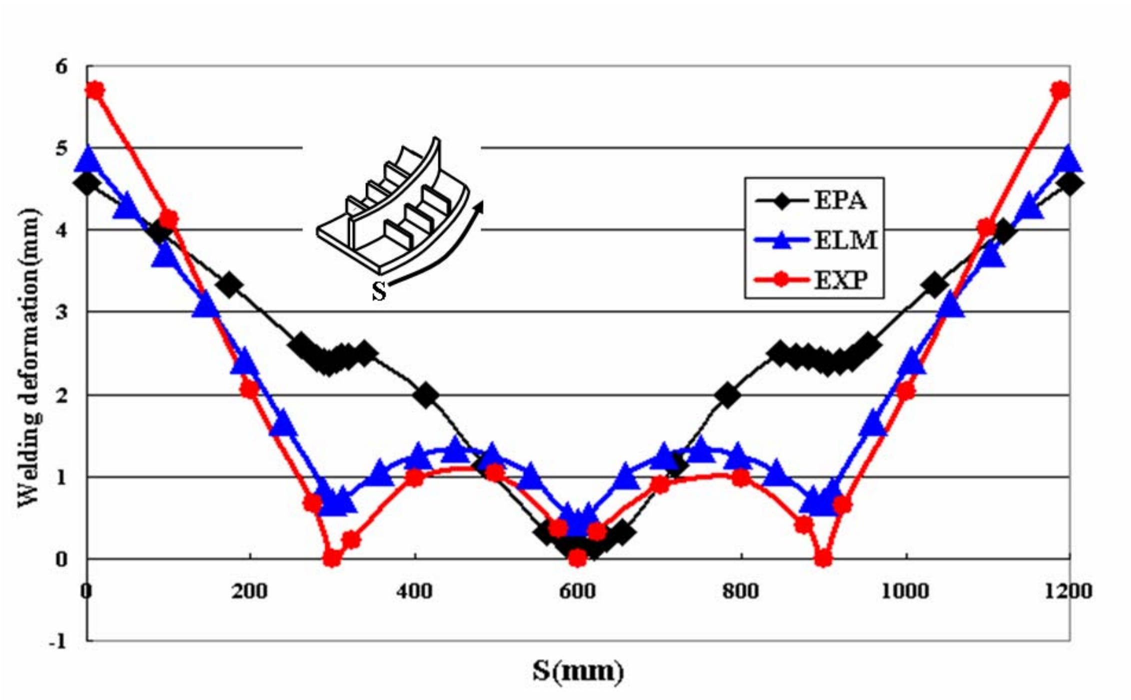

Fig. 106 Comparison of welding deformation with R=5000(mm)

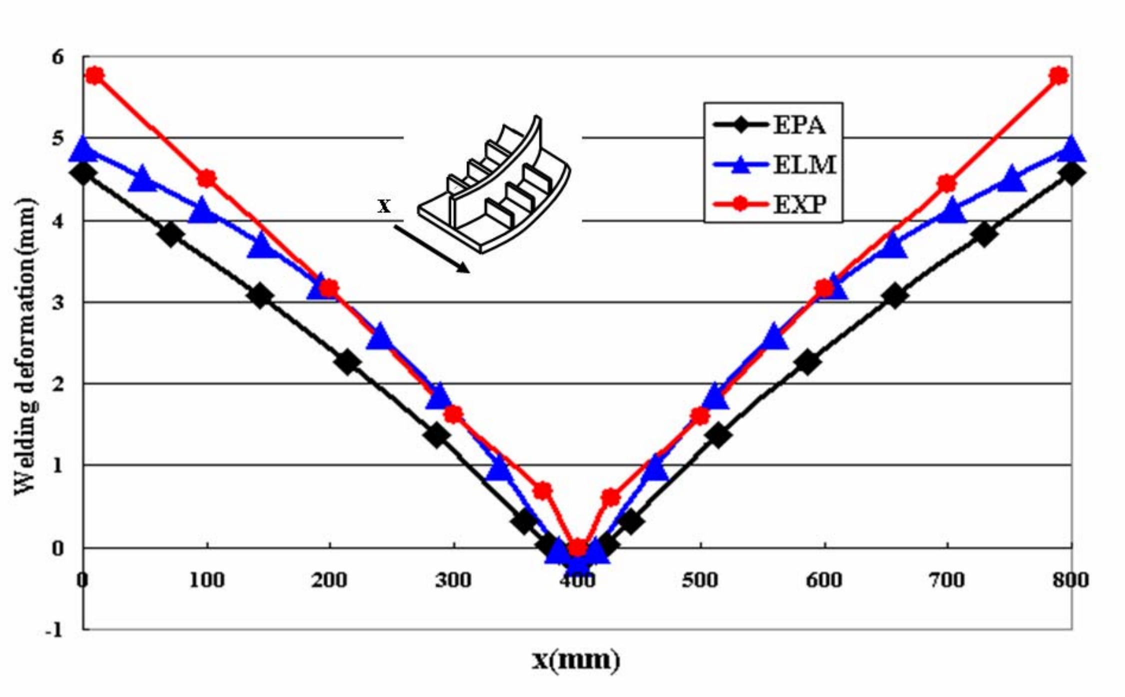

Fig. 107 Comparison of welding deformation with R=5000(mm)

By the analysis results, the welding deformation is getting larger as the radius of curvature becomes large value, and the welding deformation of case 1 is larger than that of case 2. From this result, it is recommended that the curved longitudinal stiffener should be welded first before the smaller transverse stiffeners are welded from the view point of welding distortion control.

The welding deformations by the experiment show fairly good agreements with those by the ELM(Equivalent Load Mehod) suggested in this paper, but the welding deformation by the EPA(Thermal Elasto-Plastic Analysis) has a different tendency compared with the cases of ELM and EXP(Experiment).

In case of ELM and EXP, the deformation at the transverse stiffener has a small value, but in case of EPA, the deformation at the transverse stiffener has a large value.

10. Welding distortion analysis of a stiffened curved panel block by equivalent load method

10.1. Dimension and welding heat input of a curved double bottom block

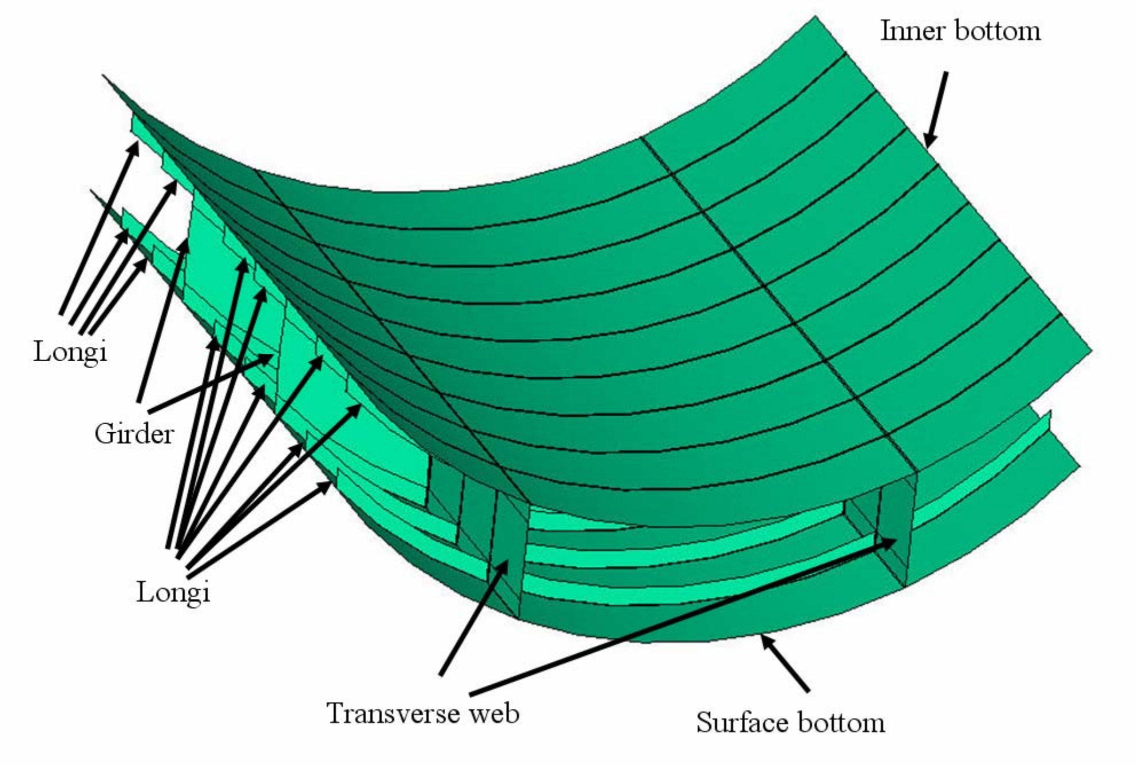

Fig. 108 Curved double bottom block for analysis

The analysis model has 6 longitudinal stiffeners (Longi) on the surface bottom plate and 6 longitudinal stiffeners on the inner bottom plate. 2 girders and 2 transverse webs between the surface and inner bottom plate shown in Fig. 108. A curvature of the plate (ρ) is 5000(mm) in the longitudinal direction.

Table. 4 Dimension and welding heat input

	Size(mm)	**Thickness(mm)**	**Heat input(cal/mm)**
Surface bottom	8000×7200, ρ=5000	12	-
Inner bottom	8000×7200, ρ=5000	12	-
Girder	8000×1200	12	252
Transverse Web	7200×1200	12	252
Longitudinal Stiff.	8000×200	10	218.4

The dimension of the curved double bottom block is shown in Table. 4. The value of the heat input is determined by considering the data in the shipyards. In this analysis, it is assumed that the voltage and welding velocity has a constant value with 30(V) and 5(mm/s). The current is controlled for exact heat input.

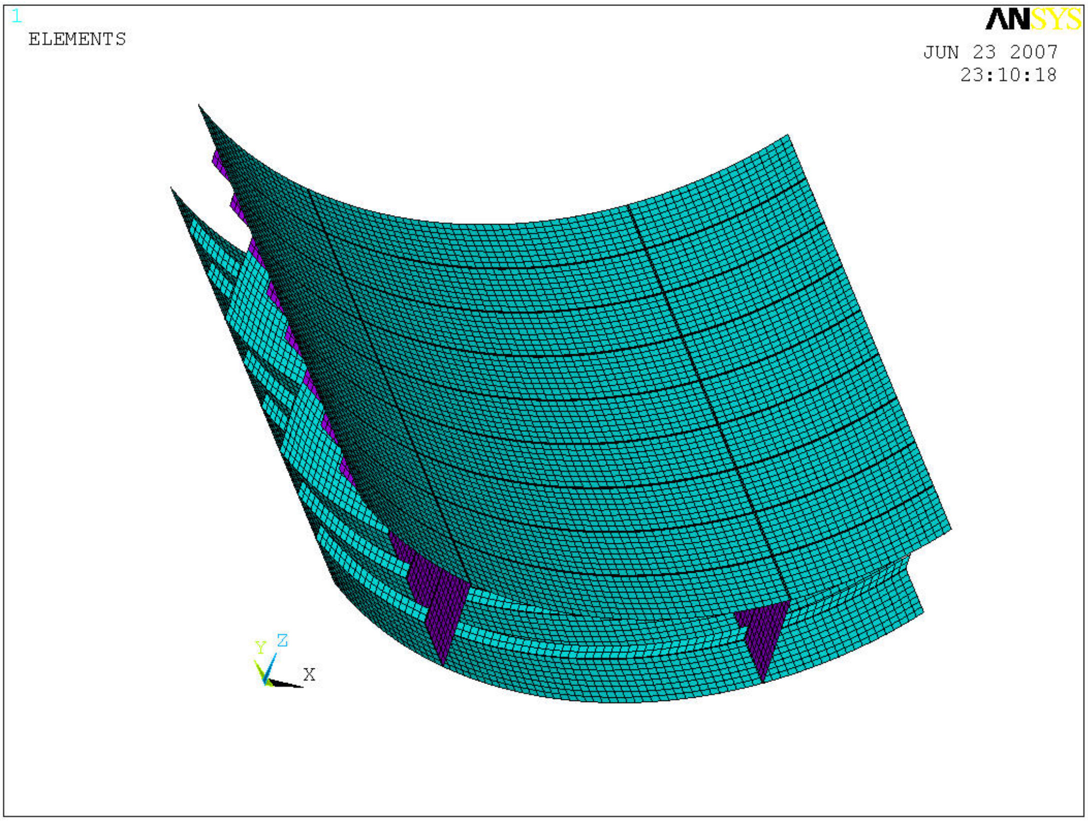

Fig. 109 Modeling for finite element analysis

The model of the curved double bottom block has 20864 elements and 20906 nodes. The number of elements has a large value for elasto-plastic analysis. Actually, the elasto-plastic analysis for this block is nearly impossible. The ELM, however, is adopting an elastic analysis, so the welding deformation can be predicted.

In this analysis, the longitudinal direction is x-direction, the transversal direction is y-direction and the height direction is z-direction as shown in Fig. 109.

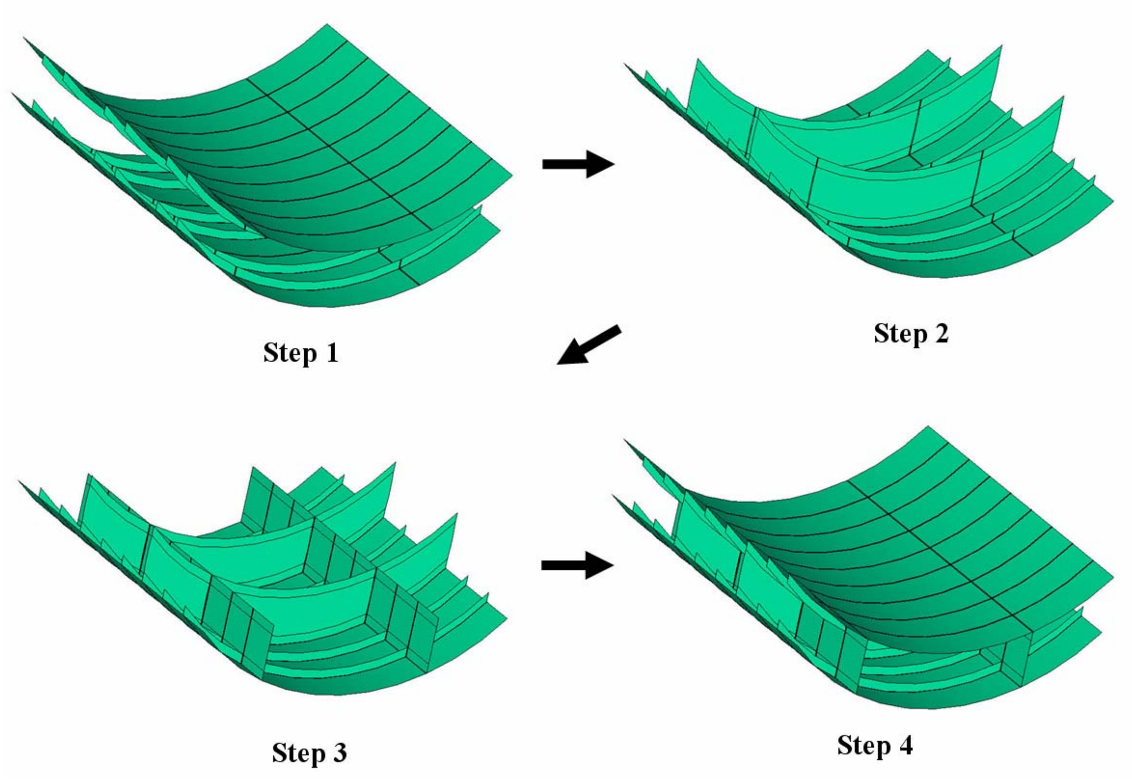

Fig. 110 Welding sequences

The welding sequence is determined by considering the welding sequence in ship yard. First, the longitudinal stiffener on the surface and inner bottom is welded as shown in step 1. Second, the Girder, and transverse web frame is welded in order as shown in step 2 and 3. The inner bottom with the longitudinals is welded lastly as shown in step 4.

10.2. Heat transfer analysis

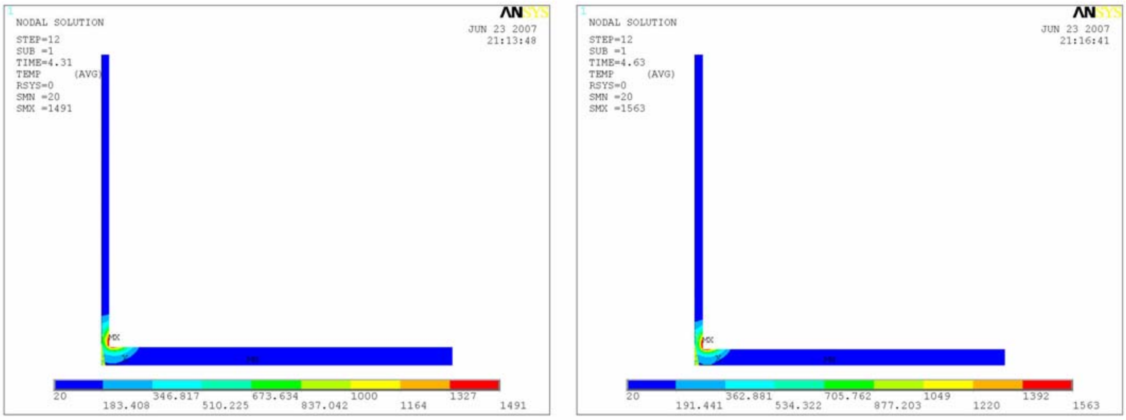

Fig. 111 Heat transfer analysis

All of the welding process is analyzed through 20 steps and the cooling process is analyzed during 4 steps. Because it is assumed in previous chapter that the temperature history of all section is same, as shown in Fig. 111, the heat transfer analysis is performed by 2-D thermal analysis. In this case, because the base plates (surface bottom, inner bottom) have same thickness, and the stiffeners have two kinds of thickness, the heat transfer analysis is performed twice.

10.3. Calculation of degree of restraint

The degree of restraint is calculated by the unit load method as introduced in previous chapter. For calculating the degree of restraint, it needs to perform two unit load elastic analysis, a free state and a restrained state.

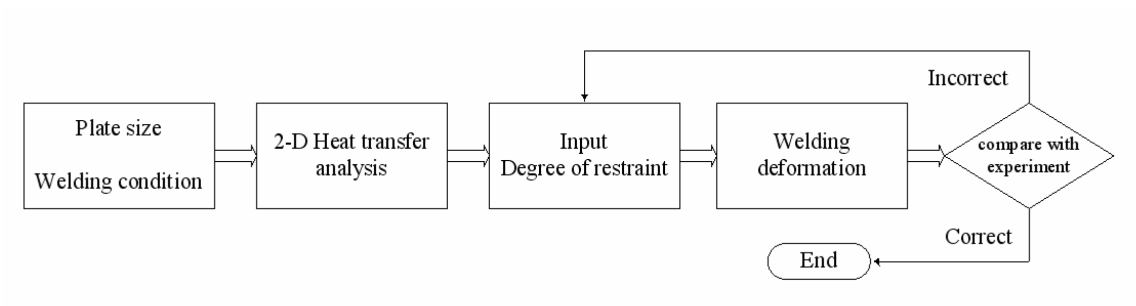

Fig. 112 Calculation of the restraint of Free State

The experimental result is necessary for calculating the degree of restraint of a free state. As shown in Fig. 112, by the 2-D heat transfer analysis, the highest temperature is calculated. Because the inherent strain is determined by the highest temperature and the degree of restraint, if the degree of restrain is assumed, the welding deformation can be calculated. If the calculated welding deformation is different with the experimental result, changed degree of restraint is used to calculate the welding deformation. By this loop, the exact degree of restraint of a free state is calculated.

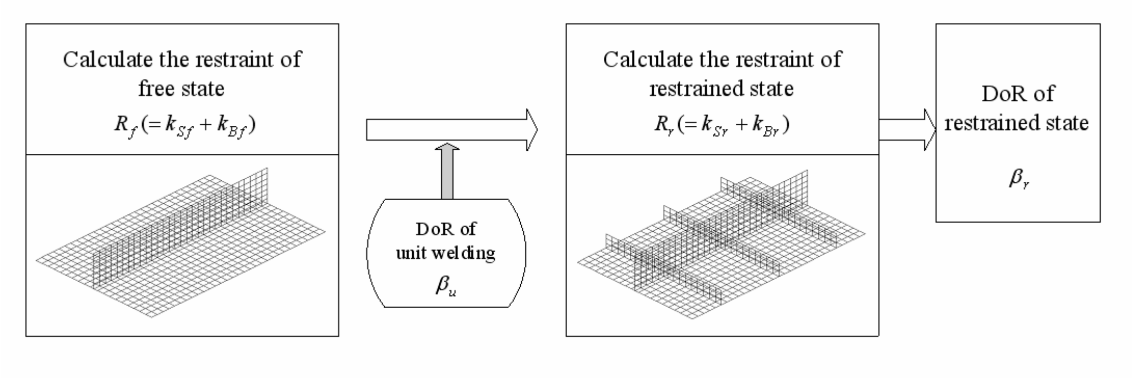

Fig. 113 Calculation of degree of restraint

The degree of restraint of a free state β_f is expressed by the stiffness of bar and plate in bar-spring model.

$$\beta_f = \frac{k_{Sf}}{k_{Sf}+k_{Bf}}$$
$$\textit{where} \quad k_{Sf} : \textit{stiffness of spring in free state}$$
$$k_{Bf} : \textit{stiffness of bar in free state}$$

Substituting the stiffness by the unit load method in a free state R_f, the k_{Sf} and k_{Bf} is calculated.

$$k_{Sf} = \beta_f \times (k_{Sf}+k_{Bf}) = \beta_f \times R_f$$
$$k_{Bf} = R_f - k_{Sf} = (1-\beta_f) \times R_f$$

Substituting the degree of restraint of restrained state β_r

$$\beta_r = \frac{k_{Sr}}{k_{Sr}+k_{Br}}$$
$$\textit{where} \quad k_{Sr} : \textit{stiffness of spring in restrained state}$$
$$k_{Br} : \textit{stiffness of bar in restrained state}$$

In this expression, because the k_{Br} is the stiffness of the heat input area (bar) in restrained state, the stiffness of spring in restrained state k_{Br} has a same value with the stiffness of spring in free state k_{Bf}. Therefore the stiffness of spring and the stiffness of bar in restrained state are calculated.

$$k_{Br} = k_{Bf}$$
$$k_{Sr} = R_r - k_{Br} = R_r - k_{Bf}$$

10.4. Prediction of welding deformation of a curved double bottom block by equivalent load method

The welding deformation by the equivalent load method is shown in Fig. 114 - 116. The analysis shows that the buckling phenomena (deformation) occurred in surface and inner bottom plate along the longitudinal direction.

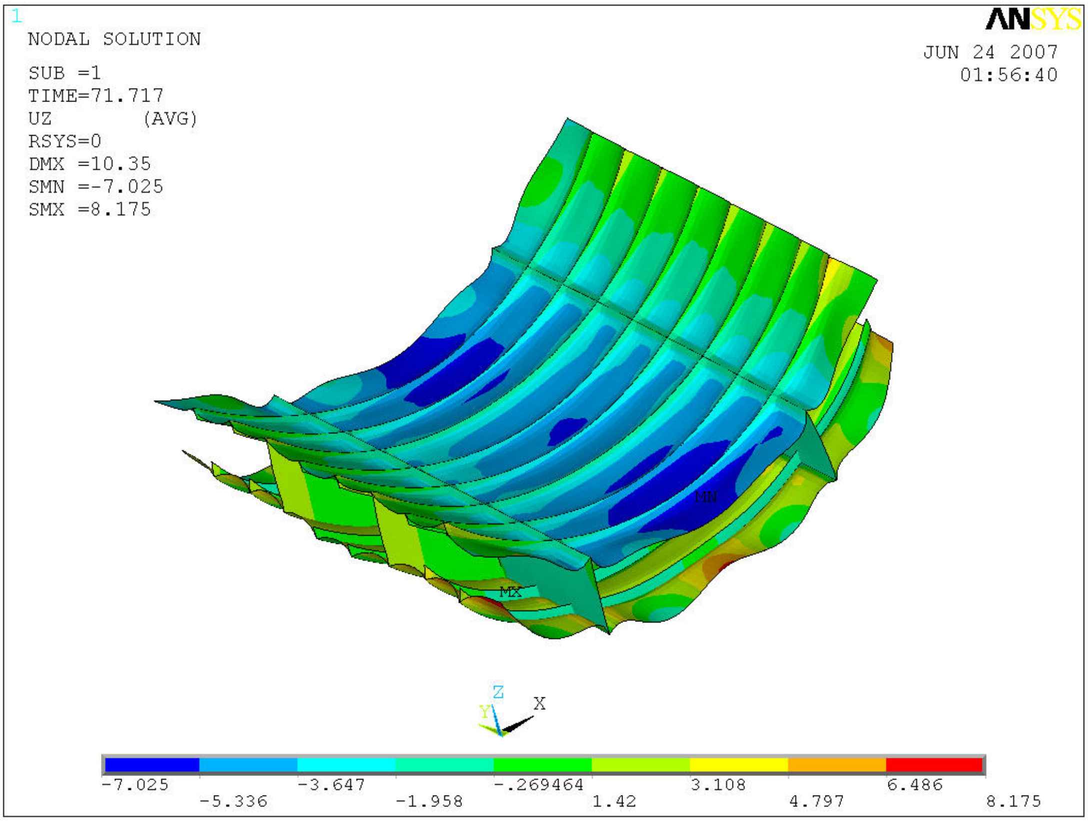

Fig. 114 Welding deformation of curved double bottom block

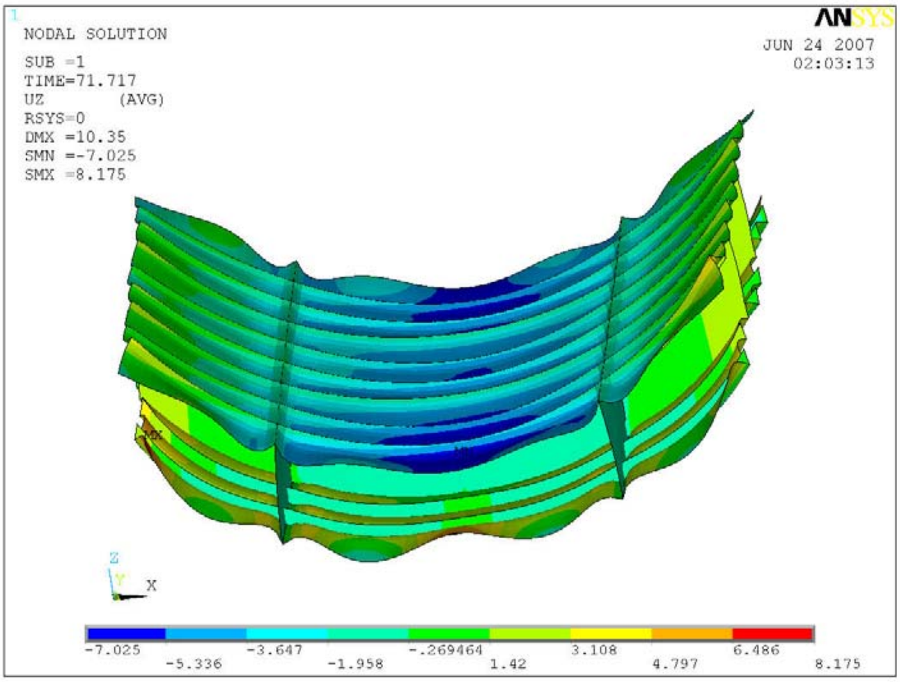

Fig. 115 Welding deformation of curved double bottom block

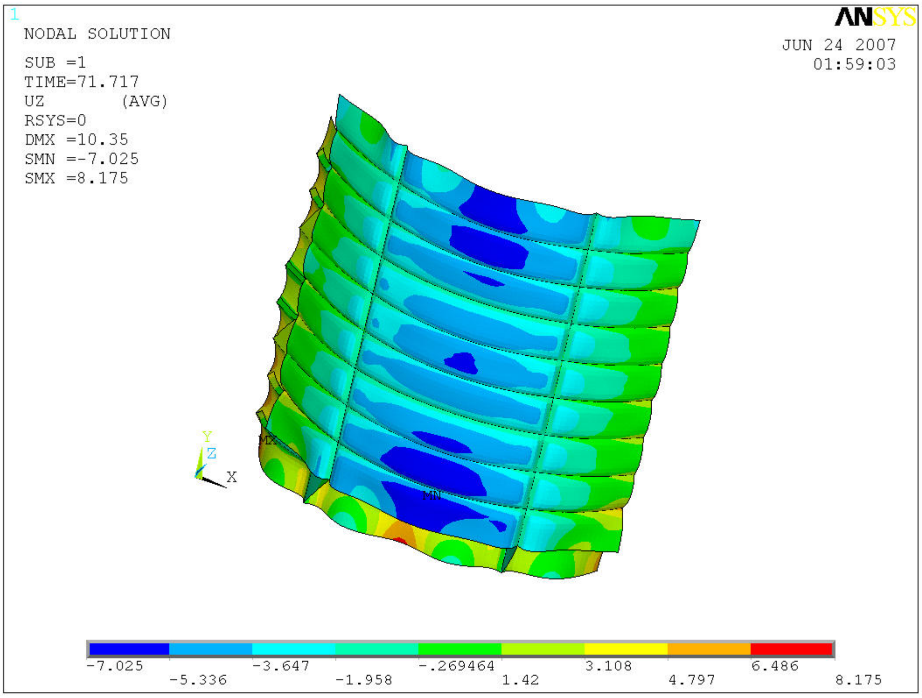

Fig. 116 Welding deformation of curved double bottom block

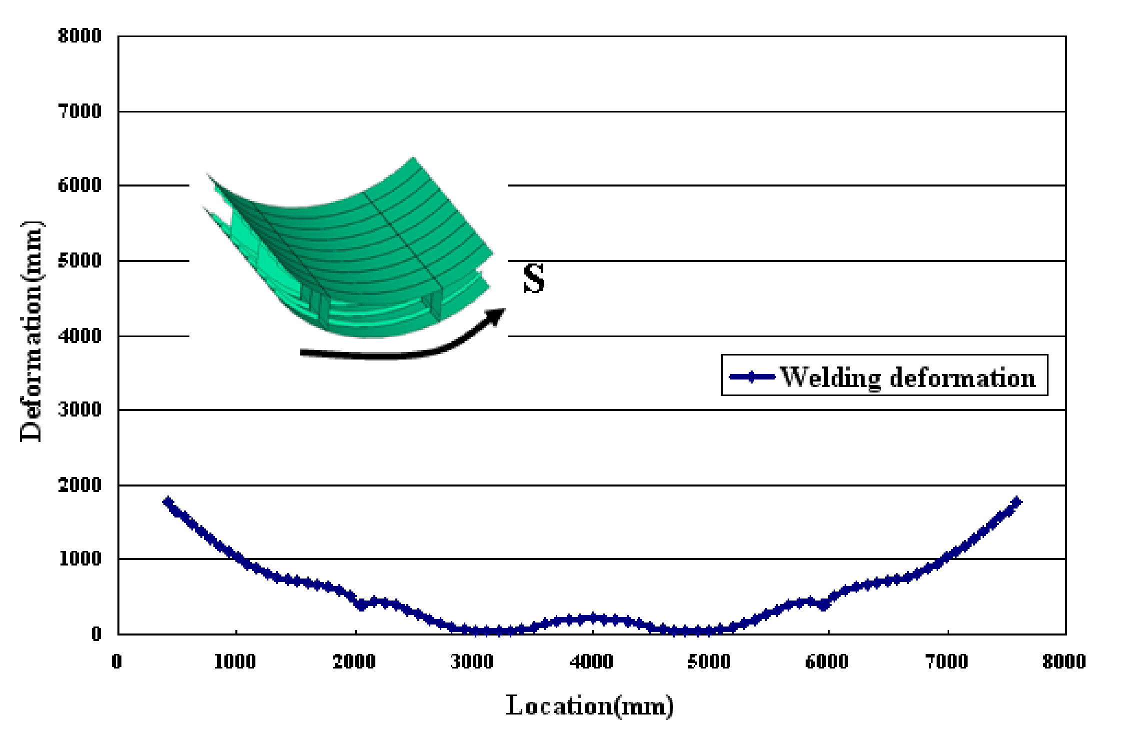

Fig. 117 Welding deformation in longitudinal direction of surface bottom

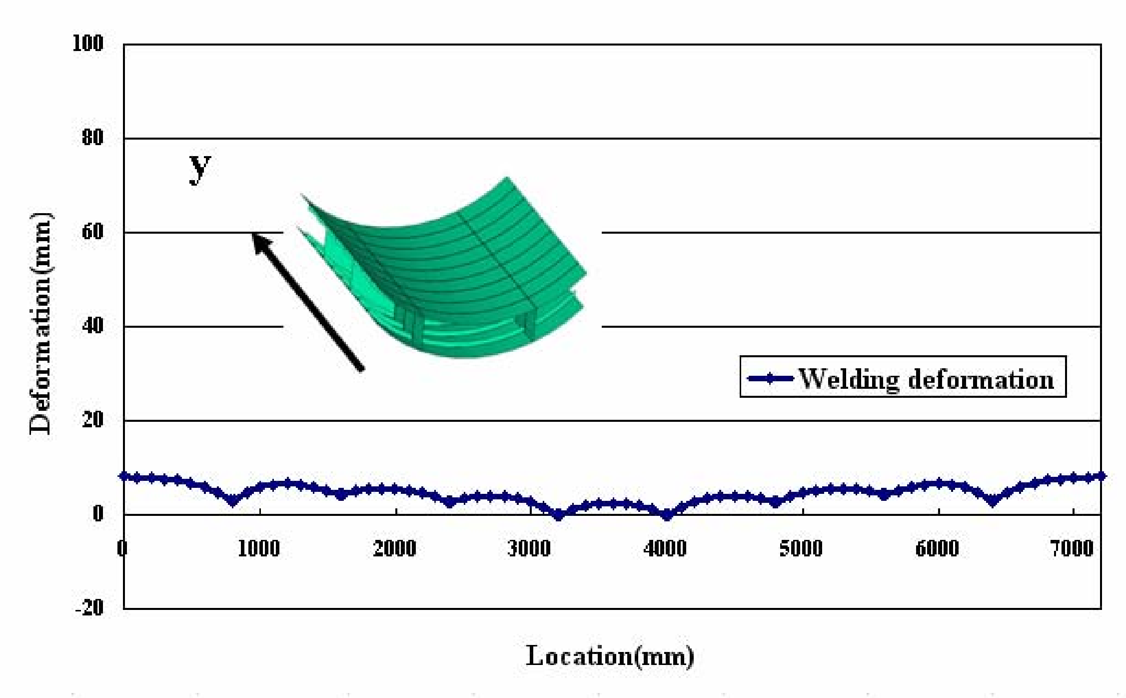

Fig. 118 Welding deformation in transversal direction of surface bottom

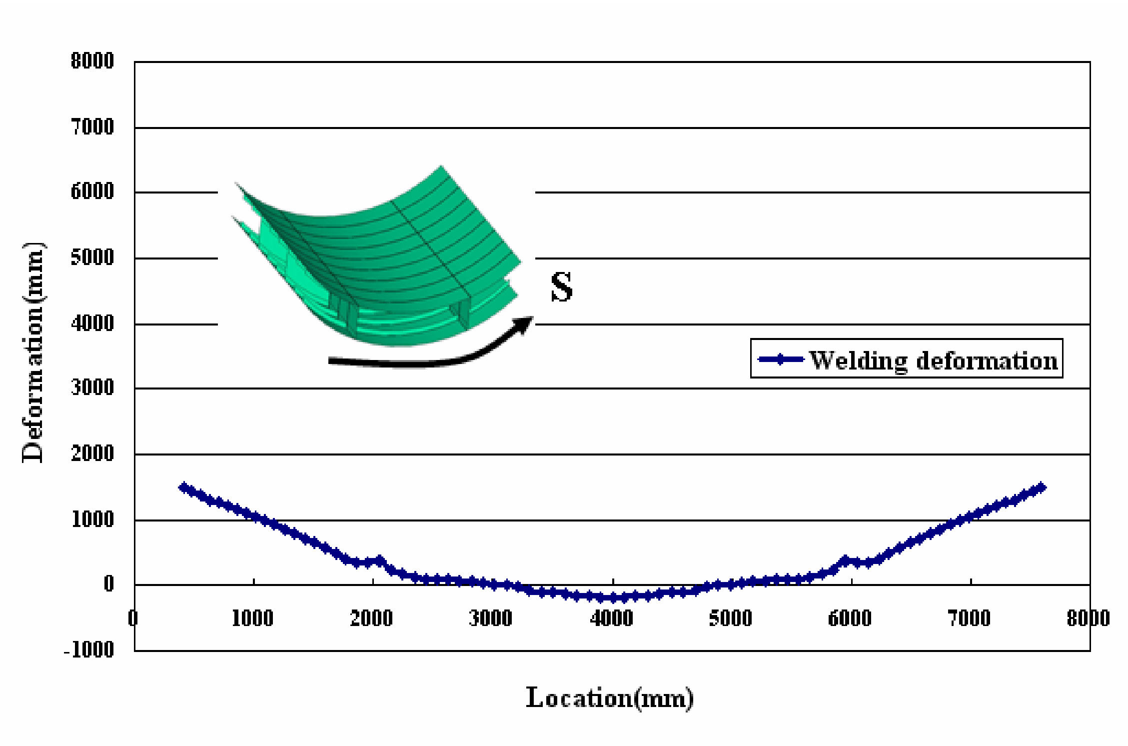

Fig. 119 Welding deformation in longitudinal direction of inner bottom

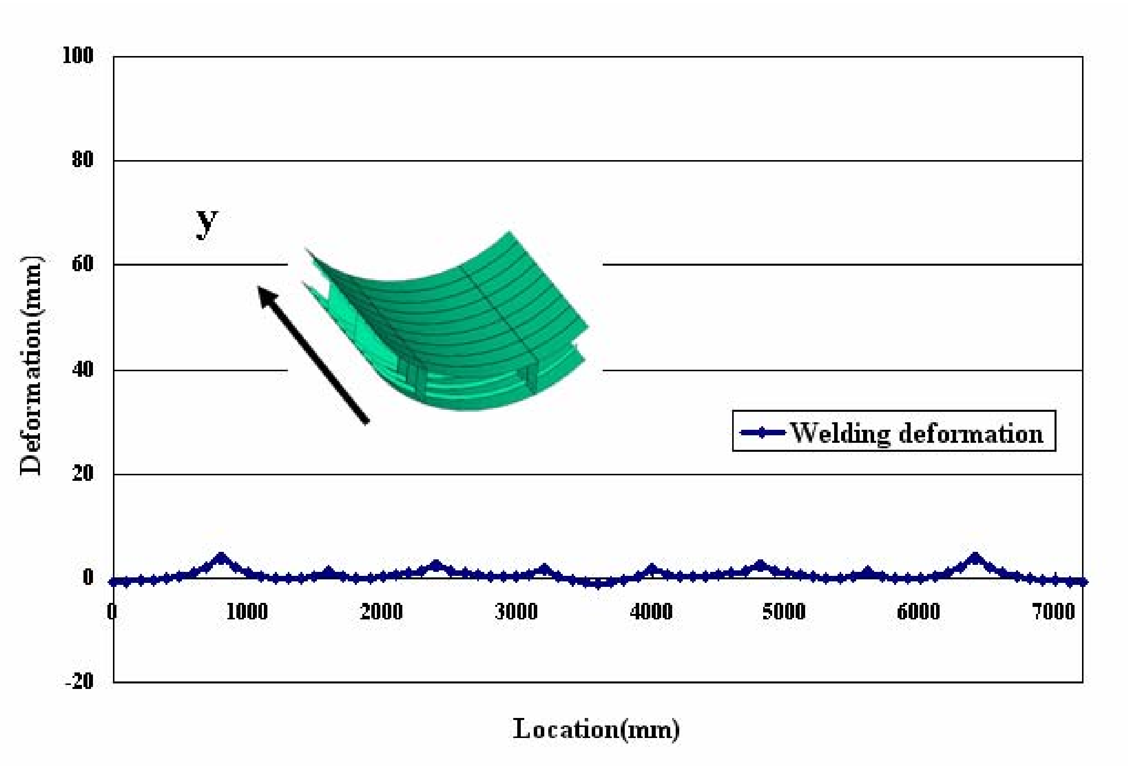

Fig. 120 Welding deformation in transversal direction of inner bottom

The welding deformations in longitudinal direction and transverse direction of surface and inner bottom plate are shown in Fig 117 - 120. The welding deformation in transverse direction of the surface bottom plate is convex between the longitudinal stiffeners, and the welding deformation in transverse direction of the inner bottom plate is concave between the longitudinal stiffeners.

The welding deformation in longitudinal direction of two bottom plate is not simple like the transverse cases. Because the buckling deformation occurs along the longitudinal direction, the welding deformation between the transverse webs has shapes of waves. It is thought that the buckling occurs because of an effect of the rigidity of the curved bottom plate. Because of the buckling, it is thought that the maximum welding deformation has a small value considering the block dimension.

The CPU running time is shown in Table. 5. The CPU running time proves the efficiency of the equivalent load method.

Table. 5 Comparison of computation time

	ELM	EPA
Analysis time (Experimental model)	3~4(min)	1.5~2(day)
Analysis time (Curved double hull block)	30(min)	impossible
Pentium Ⅳ: CPU 3.20GHz, 2.00GB RAM, Microsoft Windows XP		

11. Conclusions

In this research, welding deformation analysis using equivalent load method based on inherent strain is developed for prediction welding deformation of various hull block shapes including curved hull block. Developed welding deformation analysis can consider the various modes of welding deformation such as longitudinal/transverse shrinkage and longitudinal/transversal bending simultaneously. The analysis can reflect reasonably the change of structural stiffness by considering the welding sequence according to fabrication stages. Most of all, the efficiency of calculation time and cost is guaranteed considering the complexity of block shape by the developed analysis. The main conclusions of this research are summarized as follow:

(1) The welding region, where inherent strain occurs, is idealized as a bar-spring model. The inherent strain is determined by the thermal elasto-plastic analysis of bar-spring model which has two variables; highest temperature and the degree of restraint. Therefore, by the heat transfer analysis and the calculation of the degree of restraint, the distribution of inherent strain around the HAZ was calculated.

(2) The highest temperature is an important factor with the degree of restraint for calculating the inherent strain. For calculating the highest temperature, 2-D heat transfer analysis was performed. Actually, a phenomenon of heat transfer is a 3-dimensional phenomenon, but for the case with the long welding line like a ship hull block, it can be assume that the temperature transition of the welding edge area and the heat transfer to another stiffener is neglected. The 2-D heat transfer analysis, therefore, represented the welding heat transfer well.

(3) The degree of restraint is one of the important factors for calculating the inherent strain. The unit load method is used to calculate the degree of restraint. By the experiment, exact degree of restraint of curved plate is calculated at a free state. To reflect the change of structural stiffness according to the fabrication stages, two unit load elastic analysis, a free state and a restrained state, was performed.

(4) The inherent strain which is given by the 2-D heat transfer analysis and the unit load analysis was used to calculate the equivalent loads. The equivalent loads (axial force and moment) are calculated by integration of the inherent strain. The elastic analysis was performed to predict welding deformation by applying the equivalent loads.

(5) The welding experiment of the curved stiffened plate with different curvature and welding sequence was performed. The welding deformations by the equivalent load method, thermal elasto-plastic analysis and experiment are compared to prove the accuracy of the equivalent load method. The welding deformation by the equivalent load method has better agreement to the welding experiment compare with the welding deformation by the thermal elasto-plastic analysis. The equivalent load method is more precise and more effective than the elasto-plastic analysis..

(6) An efficiency of the equivalent load method is proved by predicting a welding deformation of curved double bottom block. Since it only requires experimental data of simple specimen, the equivalent load method can be utilized in the estimation of welding deformation of curved blocks which has more complex shapes.

(7) The most important merit by the equivalent load method is the efficiency to calculate the welding deformation. As shown in Table 5, the CPU running time proves the efficiency of the equivalent load method.

The welding deformation analysis by the equivalent load method can be applied to the design stage, so it can be utilized to decide exact margin. Furthermore, it is useful to minimize the welding deformation by controlling the welding condition and the welding sequence.

12. Acknowledgements

The authors would like to express our sincere gratitudes to Mr. Glenn M. Ashe, American Bureau of Shipping and all of the members of the Project Technical Committee for their supports. We also would like to thank Dr. Myoung Soo Han and Mr. Hyun Wook Kim, Deawoo Shipbuilding and Marine Engineering, Co., Ltd, for their supports to provide the facilities and conveniences for the welding distortion experiments in Okpo shipyard.

13. References

(1) Watanabe, M. and Satoh, K. (1965) “Welding mechanics and its applications.” Asakura Publication, pp. 367-411

(2) Masubuchi, K. (1980) “Analysis of welded structures.”Pergamon Press, pp. 239-243

(3) Tekriwal, P. (1989) “Three-dimensional transient thermo-elasto-plastic modeling of gas metal arc welding using the finite element method.” U. of Illinois at Urbana-Champaign, Urbana, Ill., USA

(4) Ueda, Y. and Ma, N.X. (1995) “Measuring Methods of Three-Dimensional Residual Stresses with Aid of Distribution Function of Inherent Strains(Report3).” Trans. of Japanese Welding Research Institute, 24(2), pp. 123-130

(5) Jang, C.D. and Seo, S.I. (1996) “A study on the automatic fabrication of welded built-up beams.” Trans. of the Society of Naval Architects of Korea, 33(1), pp. 206-213

(6) Jang, C.D., Seo, S.I. and Ko, D.E. (1997) “A Study on the Prediction of Deformations of Plates Due to Line Heating Using a Simplified Thermal Elasto-Plastic Analysis” Journal of Ship Production, Vol.13, No.1, pp.22-27

(7) Kim, S.I., Han, J.M., Cho, Y.K., Kang, J.K. and Lee, J.Y. (1997) “A study on the accuracy control of block assembly in shipbuilding.” ICCAS ’97, pp. 367-381

(8) Murakawa, H., Luo, Y. and Ueda, Y. (1997) “Prediction of welding deformation and residual stress by elastic FEM based on inherent strain” J. of the society of naval architects of Japan, 180, pp. 739-751

(9) Jang, C.D., Moon, S.C. (1998) “An Algorithm to Determine Heating Lines for Plate Forming by Line Heating Method” Journal of Ship Production, Vol.14, No.4, pp.238-245

(10) Jang, C.D. and Lee, C.H. (1999) “Prediction of Welding Deformation of Stiffened Plates using inherent Strain Method” Proceedings of the Thirteenth Asian Technical Exchange and Advisory Meeting on Marine Structures, pp. 485-492

(11) Seo, S.I. and Jang, C.D. (1999) “A study on the prediction of deformations of welded ship structures.” Journal of Ship Production, 15(2), pp. 73-81

(12) Jang, C.D., Moon, S.C. and Ko, D.E. (2000) “Acquisition of Line Heating Information for Automatic Plate Forming” Proc. Ship Structure Symposium, SSC, SNAME

(13) Seo, S.I., Yang, Y.H. and Jang, C.D. (2001) "Development of a New Finite-Element Analysis of Deformation of Plate Due to Line Heating" Journal of Ship Production, Vol. 17, No. 1, pp. 1-7

(14) Jang, C.D., Kim, H.K. and Song, H.C. (2002) "Optimum Structural Design of the High Speed Surface Effect Ships built of Composite Materials" Journal of Marine Technology, Vol. 38, No. 4

(15) Jang, C.D., Lee, C.H. and Ko, D.E. (2002) “Prediction of welding deformations of stiffened panels” Journal of Engineering for the Maritime Environment, Vol. 216, No. M2, pp. 133-143

(16) Jang, C.D., Ha, Y.S., and Ko, D.E. (2003) "An Improved Inherent Strain Analysis for the

Prediction of Plate Deformations Induced by Line Heating Considering Phase Transformation of Steel" Proc. of 13th ISOPE

(17) Jang, C.D. and Lee, C.H. (2003) "Prediction of Welding Deformations of Ship Hull Blocks" Journal of Ship and Ocean Technology, Vol. 7, No. 4, pp. 41-49

(18) Jang, C.D., Ryu, H.S. and Lee, C.H. (2004) "Prediction and Control of Welding Deformations in Stiffened Hull Blocks using Inherent Strain Approach" Proc. of 14th ISOPE, Vol. IV, pp.159-165

(19) Jang, C.D., Kim, T.H., Ko, D.E., Thomas Lamb and Ha, Y.S. (2005) "Prediction of steel plate deformation due to triangle heating using the inherent strain method." Journal of Marine Technology, Vol. 10, No. 4

(20) Jang, C.D., Ha, Y.S. and Kim, Y.T. (2006) “Determination of optimal heating conditions in line heating process with weaving motions.” Proc. Of 16th ISOPE, pp. 182~186

(21) Jang, C.D., Nomoto, T., Ko, D.E., Ryu, H.S. and Ha, Y.S. (2006) “Simulation of post welding distortion control of stiffened hull blocks by line heating.” Journal of Ship Research, Vol. 50, No. 3, pp. 268~277

PROJECT TECHNICAL COMMITTEE MEMBERS

The following persons were members of the committee that represented the Ship Structure Committee to the Contractor as resident subject matter experts. As such they performed technical review of the initial proposals to select the contractor, advised the contractor in cognizant matters pertaining to the contract of which the agencies were aware, performed technical review of the work in progress and edited the final report.

Chairman

Members
Contracting Officer's Technical Representative:

Marine Board Liaison:

Executive Director Ship Structure Committee:

Ship Structure Committee Liaison Members

Liaison Members

American Iron and Steel Institute	Mr. Alexander Wilson
American Society for Testing & Materials	Captain Charles Piersall (Ret.)
American Society of Naval Engineers	Captain Dennis K. Kruse (USN Ret.)
American Welding Society	Mr. Richard Frank
Bath Iron Works	Mr. Steve Tarpy
Canada Ctr for Minerals & Energy Technology	Dr. William R. Tyson
Colorado School of Mines	Dr. Stephen Liu
Edison Welding Institute	Mr. Rich Green
International Maritime Organization	Mr. Igor M. Ponomarev
Int'l Ship and Offshore Structure Congress	Dr. Jack Spencer
INTERTANKO	Mr. Dragos Rauta
Massachusetts Institute of Technology	
Memorial University of Newfoundland	Dr. M. R. Haddara
National Cargo Bureau	Captain Jim McNamara
Office of Naval Research	Dr. Yapa Rajapaksie
Oil Companies International Maritime Forum	Mr. Phillip Murphy
Tanker Structure Cooperative Forum	
Technical University of Nova Scotia	Dr. C. Hsiung
United States Coast Guard Academy	Commander Kurt Colella
United States Merchant Marine Academy	Dr. C. B. Kim
United States Naval Academy	Dr. Ramswar Bhattacharyya
University of British Columbia	Dr. S. Calisal
University of California Berkeley	Dr. Robert Bea
University of Houston - Composites Eng & Appl.	Dr. Jerry Williams
University of Maryland	Dr. Bilal Ayyub
University of Michigan	Dr. Michael Bernitsas
University of Waterloo	Dr. J. Roorda
Virginia Polytechnic and State Institute	Dr. Alan Brown
Webb Institute	Prof. Roger Compton
Welding Research Council	Dr. Martin Prager
Worchester Polytechnic Institute	Dr. Nick Dembsey
Samsung Heavy Industries, Inc.	Dr. Satish Kumar

RECENT SHIP STRUCTURE COMMITTEE PUBLICATIONS

Ship Structure Committee Publications on the Web - All reports from SSC 1 to current are available to be downloaded from the Ship Structure Committee Web Site at URL: http://www.shipstructure.org

SSC 445 – SSC 393 are available on the SSC CD-ROM Library. Visit the National Technical Information Service (NTIS) Web Site for ordering hard copies of all SSC research reports at URL: http://www.ntis.gov

SSC Report Number	Report Bibliography
SSC 452	Aluminum Structure Design and Fabrication Guide, Sielski R. 2007
SSC 451	Mechanical Collapse Testing On Aluminum Stiffened Panels For Marine Applications Paik, J.K. 2007
SSC 450	Ship Structure Committee: Effectiveness Survey, Buck R. Phillips, M.L., Jones L.M, Jr. 2007
SSC 449	Hydrodynamic Pressures and Impact Loads for High Speed Catamaran/SES, Vorus W. 2007
SSC 448	Fracture Mechanics Characterization of Aluminum Alloys for Marine Structural Applications, Donald J.K., Blair A. 2007
SSC 447	Fatigue and Fracture Behavior of Fusion and Friction Stir Welded Aluminum Components, Kramer R. 2007
SSC 446	Comparative Study of Naval and Commercial Ship Structure Design Standards, Kendrick, A., Daley C. 2007
SSC 450	Ship Structure Committee: Effectiveness Survey
SSC 449	Hydrodynamic Pressures and Impact Loads for High Speed Catamaran / SES
SSC 448	Fracture Mechanics Characterization of Aluminum Alloys for Marine Structural Applications
SSC 447	Fatigue and Fracture Behavior of Fusion and Friction Stir Welded Aluminum Components
SSC 446	Comparative Study of Naval and Commercial Ship Structure Design Standards
SSC 445	Structural Survivability of Modern Liners, Iversen R. 2005
SSC 444	In-Service Non-Destructive Estimation of the Remaining Fatigue Life of Welded Joints, Dexter R.J., Swanson K.M., Shield C.K. 2005